MODULATION OF PRESYNAPTIC ION CHANNELS

A DISSERTATION

SUBMITTED TO THE PROGRAM IN NEUROSCIENCES

AND THE COMMITTEE ON GRADUATE STUDIES

OF STANFORD UNIVERSITY

IN PARTIAL FULFILLMENT OF THE REQUIREMENTS

FOR THE DEGREE OF

DOCTOR OF PHILOSOPHY

Jeremy Ballard Bergsman

February 2000

© Copyright by Jeremy Bergsman 2000

All Rights Reserved

I certify that I have read this dissertation and that in my opinion it is fully adequate, in scope and quality, as a dissertation for the degree of Doctor of Philosophy.

_____

Richard W. Tsien Principal Advisor

I certify that I have read this dissertation and that in my opinion it is fully adequate, in scope and quality, as a dissertation for the degree of Doctor of Philosophy.

_____

Richard H. Scheller

I certify that I have read this dissertation and that in my opinion it is fully adequate, in scope and quality, as a dissertation for the degree of Doctor of Philosophy.

_____

Thomas L. Schwarz

Approved for the University Committee on Graduate Studies:

_____

Abstract

Understanding the neuronal presynaptic terminal is a major goal of neuroscience. The nerve terminal performs the final output of a neuron's computation and contributes to multiple forms of synaptic plasticity, important for development, learning, and memory. One interesting aspect of nerve terminal biology concerns how it may function when activity levels are high, taxing its homeostatic mechanisms. Herein are described two separate lines of investigation into compensatory mechanisms which may be invoked by the nerve terminal during periods of high activity.

When the presynaptic membrane protein syntaxin is co-expressed in *Xenopus* oocytes with N- or P/Q-type Ca^{2+} channels, it promotes their inactivation. (Bezprozvanny et al., 1995; Wiser et al., 1996; Wiser et al., 1999; Bezprozvanny et al., 2000; Degtiar et al., 2000) These findings have led to the hypothesis that syntaxin might influence Ca^{2+} channel function in presynaptic endings, in a reversal of the conventional flow of information from Ca^{2+} channels to the release machinery. Accordingly, we have examined the effects of enzymatic cleavage of syntaxin or other SNARE proteins on Ca^{2+} influx in isolated mammalian nerve terminals (synaptosomes). Botulinum neurotoxin type C1 (BoNtC1), which cleaves syntaxin near its transmembrane segment, was applied to rat neocortical synaptosomes at concentrations that completely blocked neurotransmitter release. This treatment altered the pattern of Ca^{2+} entry monitored with fura-2. Whereas the initial Ca^{2+} rise induced by membrane depolarization with K^+-rich solution was unchanged, late Ca^{2+} entry was strongly augmented by syntaxin cleavage. Similar results were obtained when Ca^{2+} influx arose from repetitive firing induced by the K^+-channel blocker 4-aminopyridine. Cleavage of VAMP with BoNtD or SNAP-25 with BoNtE failed to produce a significant change in Ca^{2+} entry. The BoNtC1-induced alteration in Ca^{2+} signaling was specific to voltage-gated Ca^{2+} channels, not Ca^{2+} extrusion or buffering, and it involved N-, P/Q- and R-type channels, the high voltage-activated channels

most intimately associated with presynaptic release machinery. The modulatory effect of syntaxin was not immediately manifest when synaptosomes had been K^+-predepolarized in the absence of external Ca^{2+}, but developed with a delay following admission of Ca^{2+}, suggesting that vesicular turnover may be necessary to make syntaxin available for its stabilizing effect on Ca^{2+} channel inactivation. The requirement for both Ca^{2+} channel inactivation and significant vesicle turnover suggests that this is a compensatory mechanism used by the nerve terminal during periods of high activity.

Models of the synaptic cleft predict that $[Ca^{2+}]_o$ decreases significantly during the course of an action potential (Smith, 1992; Vassilev et al., 1997; Egelman and Montague, 1998; Egelman and Montague, 1999). Recordings in the mammalian brain and single avian synapses have demonstrated decreases in $[Ca^{2+}]_o$ of between 0.6 and 1.5 mM (Nicholson et al., 1977; Nicholson et al., 1978; Borst and Sakmann, 1999; Stanley, 2000) which would decrease Ca^{2+} entry into the nerve terminal and reduce release probability of that synapse. We have made electrical recordings from synaptosomes and have found that a major component of the membrane current is supported by a novel non-specific cation channel and that this channel is activated by decreases in $[Ca^{2+}]_o$ and membrane depolarization. The responsiveness to $[Ca^{2+}]_o$ is mediated by a distinct receptor that is sensitive to Ca^{2+}, Mg^{2+}, Gd^{3+} and spermidine. These results indicate that the non-specific cation channel may act to counter the fall in release probability produced by physiological decreases in $[Ca^{2+}]_o$ at the synaptic cleft by broadening subsequent action potentials and countering the decreased electrochemical gradient for Ca^{2+}.

Acknowledgments

This dissertation is dedicated to my wife, Natalie Martina, my son, Raymond Martina, and my parents, Anne and Joel Bergsman. All these people have challenged, encouraged, and supported me in my life as well as in this endeavor, albeit in different ways.

Table Of Contents

List of Illustrations

1 Syntaxin Modulation of Calcium Channels in Cortical Synaptosomes as Revealed by Botulinum Toxin C1

1.1 Attribution and Acknowledgments

The material in this chapter derives from two sources as follows. (1) The General Introduction, Results, and Discussion are substantially similar to a manuscript I wrote with Dr. Richard Tsien, which has been submitted for publication in the *Journal of Neuroscience*. I performed all of the experiments. Dr. Tsien and I shared the task of writing the manuscript. The immediate inspiration for this line of experiments was Dr. Tsien and Dr. Ilya Bezprozvanny's work (Bezprozvanny et al., 1995). I thank Dr. David G. Nicholls who generously hosted me in his lab for a week to learn about synaptosome preparation and the glutamate release assay originally developed there. In addition the following people provided helpful discussions: I.B. Bezprozvanny, V.E. Degtiar, G.S. Pitt, R.H. Scheller, and S.M. Smith. (2) The Introduction to Voltage Gated Calcium Channels is substantially similar to a review I wrote with Dr. Tsien and Dr. David Wheeler for publication in 2000 by Springer Verlag in volume 147 of The Handbook of Experimental Pharmacology, *Pharmacology of Ionic Channel Function: Activators and Inhibitors*, edited by Dr. Makato Endo. The Functional Roles subsection is reorganized but similar to a previous review written by Dr. Wheeler and Dr. Tsien (Tsien and Wheeler, 1999). I wrote most of the remaining material, with some parts being from the previous review. Dr. Tsien assisted with polishing of the final prose.

1.2 General Introduction

Voltage-gated Ca^{2+} channels convert the action potential depolarization into a Ca^{2+} signal that in turn triggers vesicular neurotransmitter release. The triggering event is remarkably rapid and effective; its efficient achievement requires that Ca^{2+} channels and

the fusion machinery be held together in close proximity (Llinás et al., 1981). Indeed, Ca^{2+} channels have the capability of directly binding to SNARE proteins, putative components of the vesicular fusion complex (Sheng et al., 1994; Rettig et al., 1996; Charvin et al., 1997). These include a vesicular (v-)SNARE, VAMP (Vesicle-Associated Membrane Protein, also known as synaptobrevin), another vesicular protein—synaptotagmin—as well as syntaxin and SNAP-25, two target membrane (t-)SNAREs. The interactions with the v- and t-SNARES are most clear for the α_1 subunits of N- and P/Q-type channels, the types of voltage-gated Ca^{2+} channels (VGCCs) which are most important for fast neurotransmitter release at nerve terminals in the mammalian CNS [but see papers from the Atlas group (Wiser et al., 1996; Wiser et al., 1999) for a proposed interaction with L-type channels]. When isolated from rat forebrain, a majority of N- and P/Q-type channels appear associated with SNARE proteins (el Far et al., 1995; Martin-Moutot et al., 1996; Pupier et al., 1997; Vance et al., 1999). Disruption of the channel-SNARE protein interaction reduces the efficiency of excitation-secretion coupling (Mochida et al., 1995; Mochida et al., 1996; O'Connor et al., 1997; Rettig et al., 1997; Trudeau et al., 1998). The channel-SNARE protein interaction may be susceptible to regulation, since it displays Ca^{2+}-dependence (Sheng et al., 1996; Kim and Catterall, 1997; Sheng et al., 1997) and can be prevented by channel phosphorylation with PKC or CaMKII (Yokoyama et al., 1997).

The existence of physical interactions between Ca^{2+} channels and SNARE proteins raises an intriguing possibility: in addition to the mechanism whereby Ca^{2+} influx triggers secretion, originally proposed by Katz and Miledi (Katz and Miledi, 1965) and Douglas (Douglas, 1968), can the secretory machinery also exert an influence on Ca^{2+} influx? The idea of such a counterflow of information was suggested independently for two different proteins: cysteine string proteins, which were proposed to signal the presence of a docked vesicle to the Ca^{2+} channel (Mastrogiacomo et al., 1994), and syntaxin, whose overex-

pression was found to reduce Ca^{2+} influx in *Aplysia* neurons (Smirnova et al., 1995). Subsequently, heterologous co-expression of syntaxin, SNAP-25 or synaptotagmin with either N- or P/Q- type (and in some cases, L- type) VGCCs in *Xenopus* oocytes was shown to affect channel activity (Bezprozvanny et al., 1995; Wiser et al., 1996; Wiser et al., 1999; Bezprozvanny et al., 2000; Degtiar et al., 2000). Effects of co-expression of SNAP-25 and a specific isoform of $Ca_V2.1$ have also been seen in HEK 293 cells (Zhong et al., 1999). Syntaxin was also found to be required for G-protein modulation of Ca^{2+} channels in calyciform presynaptic terminals in chick ciliary ganglia (Stanley and Mirotznik, 1997). In addition to these effects on Ca^{2+} channels, syntaxin also appears to modulate the activity of other membrane transport proteins, including the CFTR chloride channel (Naren et al., 1997; Naren et al., 1998) was well as transporters for norepinephrine (Apparsundaram et al., 1998) and GABA (Beckman et al., 1998) (see Discussion).

These exciting observations prompted us to ask whether such interactions occur in functional mammalian nerve terminals, as they do in the oocyte expression system. Synaptosomes are an acute preparation of mechanically isolated nerve terminals which behave very similarly to nerve terminals *in vivo*. They maintain at rest a negative membrane potential (Blaustein and Goldring, 1975) and a low level of internal Ca^{2+} (Blaustein et al., 1980), and support Ca^{2+} entry through voltage-gated Ca^{2+} channels upon depolarization (Blaustein, 1975), which in turn induces neurotransmitter release (Nicholls and Sihra, 1986). Synaptosomes offer the possibility of measuring Ca^{2+} influx and glutamate release in the same system. Thus, much is known about their complement of Ca^{2+} channels and their contribution to triggering transmitter release (Turner et al., 1993; Turner et al., 1995; Vázquez and Sánchez-Prieto, 1997). To investigate the regulation of Ca^{2+} influx by specific SNARE proteins, we have measured Ca^{2+} changes and glutamate release fluorimetrically, and tested effects of various clostridial neurotoxins, proteases which selectively cleave SNARE proteins (Montecucco and Schiavo, 1995). The results

provided evidence that syntaxin exerts a significant influence on Ca^{2+} influx through N-, P/Q- and R-type channels in mammalian nerve terminals.

1.3 Introduction to Voltage-gated Ca^{2+} Channels

1.3.1 Generic Properties of Voltage-gated Ca^{2+} Channels

Voltage-gated Ca^{2+} channels are members of a superfamily of voltage-gated ion channels which also includes Na^+ channels and K^+ channels. Ca^{2+} channels transduce membrane potential changes to intracellular Ca^{2+}-signals in a wide variety of cell types, including nerve, endocrine, and muscle cells. Many types of Ca^{2+} channels have been characterized by pharmacological and biophysical criteria in various cell types. More recently, molecular cloning has revealed a wealth of genes encoding the subunits of native channels. Following a brief introduction to the basic properties and subunit composition of Ca^{2+} channels, we will proceed to an overview of their classification, molecular composition, and specialization for various functional roles. Ca^{2+} channels are subject to modulation by a variety of means, only one of which will be described below (Results). Likewise details about structure-function are left to other authors and we will confine our structural comments here to those that pertain to classification of the channels. In addition we will not touch on several other important aspects of regulation of $[Ca^{2+}]_i$, such as Ca^{2+} channels not gated by depolarization (Putney, 1997), Ca^{2+} sequestration and extrusion, and neuropathological conditions such as stroke, epilepsy, and migraine, some involving mutations of the Ca^{2+} channels themselves.

1.3.1.1 Basic functional properties

Our present-day understanding of Ca^{2+} channels began with their electrophysiological isolation and description. *Gating* describes the opening and closing of channels. Typically, Ca^{2+} channels open (or *activate*) within one or a few milliseconds after the membrane is depolarized from rest, and close (*deactivate*) within a fraction of a millisecond

following repolarization. Activation of Ca^{2+} channels is steeply voltage-dependent: channels open more quickly and with higher likelihood with larger depolarizations. *Inactivation*, the closing of channels during maintained or repeated depolarizations, strongly influences the cytosolic Ca^{2+} signal that arises from cellular electrical activity. While inactivation is a general property of Ca^{2+} channels, the speed of entry into and recovery from inactivation varies widely.

In addition to gating we consider two properties concerning the conduction of Ca^{2+} through the channel. *Selectivity* of voltage-gated Ca^{2+} channels for Ca^{2+} ions is remarkably high, so that Ca^{2+} is the main charge carrier even when Ca^{2+} is greatly outnumbered by other ions, as under normal physiological conditions. *Permeation* of Ca^{2+} through a single open Ca^{2+} channel can achieve rates of millions of ions per second when the electrochemical gradient is large. At driving forces reached physiologically, the flux rate is more modest, but sufficient to cause a large increase in $[Ca^{2+}]_i$ (>1 μM) in a very localized domain (~1 μm) near the mouth of the open channel.

1.3.1.2 Subunit composition

The powerful functional capabilities of Ca^{2+} channels are rooted in their molecular architecture. Voltage-gated Ca^{2+} channels contain at their core a protein known as α_1, which is a large (200-260 kDa) transmembrane protein that contains the channel pore, the voltage-sensor and the gating machinery. Most, or possibly all, channel types additionally contain subunits known as β, α_2, δ and γ (Figure 1-1), that come together with the α_1 subunit to form a large macromolecular complex. The first examples of each of these subunits were originally isolated from skeletal muscle transverse tubules by biochemical techniques more than a decade ago (Catterall and Curtis, 1987; Campbell et al., 1988; Catterall et al., 1988; Glossmann and Striessnig, 1990). Each subunit has since been cloned in several forms.

Because the α_1 subunit appears to be able to form a functional Ca^{2+} channel on its own, the other subunits are sometimes referred to as auxiliary or ancillary subunits although they may dramatically affect channel gating, modulation, pharmacology, and expression. In the last few years our understanding of the relationship between the α_1 subunits and the native channel classes has become increasingly clear. While the α_1 subunit is the major determinant of channel properties, the high level of promiscuity in the association of the α_1 subunit with the various forms of the auxiliary subunits, combined with alternative splicing, can likely produce an incredible diversity of properties.

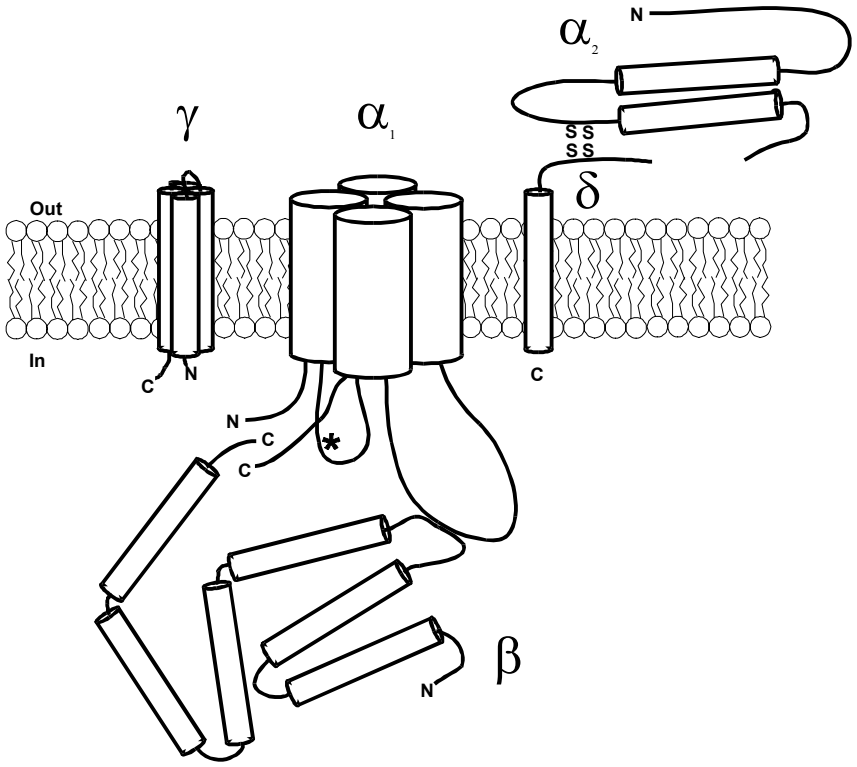

Figure 1-1. Structural Organization of Voltage-gated Ca^{2+} Channels

The subunits comprising a generic voltage-gated Ca^{2+} channel. *Small cylinders* represent α helices, *large cylinders* in the α_1 subunit represent 6 α helices. *Asterisk* marks the II-III loop of the α_1 subunit.

1.3.1.2.1 α_1

Much of the diversity of Ca^{2+} channel types seems to arise from the expression of multiple forms of the α_1 subunit, isolated by molecular cloning (e.g., Tanabe et al., 1987; Mikami et al., 1989; Mori et al., 1991; Starr et al., 1991; Dubel et al., 1992; Williams et al., 1992a; Williams et al., 1992b; Soong et al., 1993; Fisher et al., 1997; Cribbs et al.,

1998; Perez-Reyes et al., 1998; Lee et al., 1999). Details of the various α_1 subunits will be examined thoroughly below.

1.3.1.2.2 β

All high voltage activated Ca^{2+} channels (see below) in their native state appear to contain β subunits—peripheral membrane proteins associated with the cytoplasmic aspect of the surface membrane with an apparent molecular weight of ~55-60 kDa (Glossmann et al., 1987; Takahashi et al., 1987). The β subunit of Ca^{2+} channels is not homologous to the β1 and β2 subunits of Na^+ channels, which contain putative trans-membrane spanning domains and are significantly glycosylated (Isom et al., 1994). β subunits serve several important and intriguing functions: 1) They play a key role in the proper targeting of the complex of Ca^{2+} channel subunits, 2) they are subject to regulation by protein kinases, and 3) they act as modulators of the gating and pharmacological properties of α_1 subunits. In the present work we concern ourselves only with the last function. For more information on the other functions see recent reviews (Hofmann et al., 1994; Isom et al., 1994; De Waard et al., 1996; Walker and De Waard, 1998).

Four different types of β subunit are known to exist in mammals and are now known as β_1-β_4 (Birnbaumer et al., 1994). Diversity of these proteins is increased by alternative splicing (designated by lower case letters, β_{2a}, β_{2b} etc.). In general, β subunits are not found in one organ or tissue exclusively. Whereas β_1 transcripts are expressed primarily in skeletal muscle, they also appear in brain. β_2 is predominantly expressed in heart, aorta and brain, while β_3 is most abundant in brain but also present in aorta, trachea, lung, heart and skeletal muscle. β_4 mRNA is expressed almost exclusively in neuronal tissues, with the highest levels being found in the cerebellum. Because each of the β subunits appears able to partner with each of the α_1 subunits, β subunit heterogeneity may contribute to the diversity of Ca^{2+} channels in a multiplicative manner, however it seems unlikely that

β subunit differences are responsible for the differences between the major classes delineated below (L-, N-, P/Q-type, etc.).

1.3.1.2.3 α_2/δ

The $\alpha_2\delta$ subunit (175 kDa) is a dimer, consisting of glycosylated α_2 and δ proteins linked together by disulfide bonds, derived by posttranslational processing of a single parent polypeptide (Ellis et al., 1988; De Jongh et al., 1990; Williams et al., 1992b; Klugbauer et al., 1999). This pair of subunits has been shown to affect channel gating. The δ subunit is a transmembrane protein anchor and α_2 is entirely extracellular (Jay et al., 1991; Hofmann et al., 1994). Three α_2/δ genes have been isolated: α_2/δ-1 and α_2/δ-2 have wide tissue distribution while α_2/δ-3 is brain specific (Angelotti and Hofmann, 1996; Klugbauer et al., 1999). As with other Ca^{2+} channel subunits, α_2/δ diversity is increased by alternative splicing. The diversity of the α_2/δ genes has only recently begun to be characterized, and less is known about this subunit's effect on channel properties than that of the β subunit.

1.3.1.2.4 γ

A fifth subunit, known as γ (25-38 kDa), (Bosse et al., 1990; Jay et al., 1990; Eberst et al., 1997; Letts et al., 1998; Black and Lennon, 1999), has 4 transmembrane domains. Like the α_2/δ subunits, the γ subunit is now starting to receive widespread attention and little is known about its effect on channel properties, although it has been shown to promote inactivation (Eberst et al., 1997; Letts et al., 1998).

1.3.2 Classification of Native Ca^{2+} Channels According to Biophysical, Pharmacological, and Molecular Biological Properties

Multiple types of voltage-gated Ca^{2+} channels were first distinguished by voltage- and time-dependence of channel gating, single channel conductance and pharmacology (e.g., Carbone and Lux, 1984; Nowycky et al., 1985). One physiologically relevant characteristic which varies considerably among the different Ca^{2+} channel types is the

degree of depolarization required to cause significant opening. Based on this criterion, voltage-gated Ca^{2+} channels are sometimes divided into two groups, low voltage-activated (LVA) and high voltage-activated (HVA). Use of all the criteria listed above has led to a more specific classification of native Ca^{2+} channels as T-, L- N-, P/Q- and R-type (Tsien et al., 1987; Llinás et al., 1992; Randall and Tsien, 1995).

While this classification makes good sense in view of the varied biophysical properties and functional roles of the channel types in different organ systems, the relationship of these classes to the various cloned subunits has only recently been clarified. The recent findings from molecular cloning of Ca^{2+} channel subunits have greatly increased our understanding of Ca^{2+} channel diversity. This has allowed new perspective on the familial relationships between various channel types and a more precise characterization of the pharmacological properties of individual channel types.

1.3.2.1 Molecular biological nomenclature

Nine different Ca^{2+} channel α_1 subunit genes have been distinguished in mammalian brain and one in skeletal muscle and have been labeled classes A through I and S (Snutch et al., 1990; Snutch and Reiner, 1992; Birnbaumer et al., 1994). α_{1S} refers to the original Ca^{2+} channel clone from skeletal muscle, first isolated by the group of the late Shosaku Numa (Tanabe et al., 1987) and the letters A-I refer to subsequently cloned channels. Based on sequence homology, the ten α_1 subunits can be assigned to various branches of a family tree as reviewed in Figure 1-2. This sequence homology seems to follow channel properties and functional roles quite well. Following our newfound structural and functional understanding of the Ca^{2+} channels a new naming scheme similar to that used for voltage-gated K^+ channels has been proposed (W.A. Catterall, et al., personal communication). In the following discussion we will adopt this scheme in which *v*oltage-gated *Ca*$^{2+}$ channels are designated $Ca_V S.Tx$, where *S* and *T* are numbers which refer to the subfamily and type respectively, and *x* is a letter which corresponds to any splice vari-

ants. The α_1 subunits are named correspondingly as α_1S.Tx. The numbers and letters are assigned in order of discovery, thus α_{1S} becomes $\alpha_1$1.1 and so on.

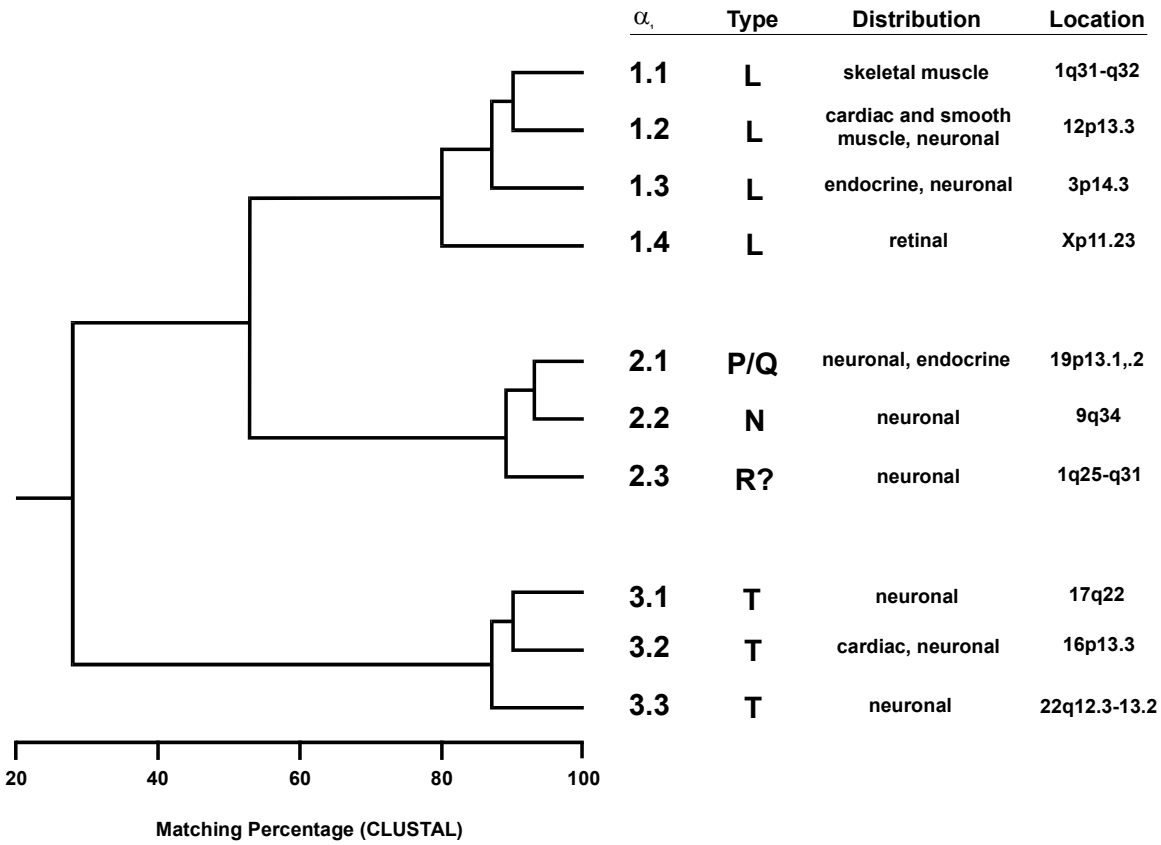

Figure 1-2. Ca^{2+} Channel α_1 Subunit Family Tree

Sequences of membrane spanning and P loop regions were aligned and matching percentages determined using CLUSTAL. Corresponding current type supported by each α_1 subunit is given, as well as tissue distribution and chromosome location of the human gene. Sequence data provided by Dr. Perez-Reyes, Department of Pharmacology, University of Virginia.

1.3.2.2 Ca_V1/L-type Ca^{2+} channels

L-type channels are generally categorized with the HVA group of channels, along with N-, P/Q-, and R-type channels. However, it is important to note that L-type channels may exhibit LVA properties under certain circumstances (Avery and Johnston, 1996). L-type channels in vertebrate sensory neurons and heart cells were initially labeled as a *l*arge Ba^{2+} conductance contributing to a *l*ong-lasting current, with characteristic sensitivity to DHPs such as nifedipine or Bay K 8444 (Bean, 1985; Nilius et al., 1985; Nowycky et al., 1985). Members of this group were subsequently identified in other excitable cells

such as vascular smooth muscle, uterus, and pancreatic β cells. Later, the designation of L-type was extended to refer to all channels with strong sensitivity to DHPs, including those found in skeletal muscle (Hofmann et al., 1988), even though clear-cut biophysical distinctions between skeletal and cardiac L-type channels were already known (Rosenberg et al., 1986). Thus, the category of L-type channels contains individual subtypes of considerable diversity. For example, three subtypes of L-type channel appear to co-exist in cerebellar granule neurons, two subtypes that resemble those found in heart and a third that shows prominent voltage-dependent potentiation (Forti and Pietrobon, 1993).

Three major families of α_1 subunits clearly emerge on the basis of sequence homology. The first subfamily ($\alpha_1 1$) consists of 4 α_1 members. Along with the $\alpha_1 1.1$ (α_{1S}) subunit from skeletal muscle, these include subunits first derived from heart muscle [$\alpha_1 1.2$ (α_{1C})] (Mikami et al., 1989), neuroendocrine tissue [$\alpha_1 1.3$ (α_{1D})] (Williams et al., 1992b), and retina [$\alpha_1 1.4$ (α_{1F})] (Fisher et al., 1997; Bech-Hansen et al., 1998; Strom et al., 1998). These cDNAs encode HVA channels classified as "L-type" because they are responsive to DHPs. The existence of four α_1 subunits, each capable of supporting L-type channel activity, provides an obvious starting point for attempts at understanding how L-type Ca^{2+} channel diversity might be generated from specific molecular structures. However, little information is yet available to link functionally distinct forms of L-type channel activity (e.g., Forti and Pietrobon, 1993; Kavalali and Plummer, 1994) to individual α_1 isoforms. While the $\alpha_1 1.1$ subunit appears to be largely excluded from neurons according to Northern analysis and electrophysiological criteria, no sharp distinction has been made between currents generated by $\alpha_1 1.2$ and $\alpha_1 1.3$. Single channel recordings of expressed $\alpha_1 1.3$ channels are lacking and analysis of the functional impact of various β subunits on $\alpha_1 1.2$ and $\alpha_1 1.3$ is not extensive.

Most of the attention to date has been focused on splice variations of $\alpha_1$1.2. These have a marked impact on channel behavior in several cases, producing 1) differences in sensitivity to DHPs in $\alpha_1$1.2 variants found in cardiac or smooth muscle (Welling et al., 1993), 2) differences in the voltage-dependence of DHP binding (Soldatov et al., 1995) and 3) differences in susceptibility to cyclic AMP-dependent phosphorylation (Hell et al., 1993b). Further analysis will be greatly facilitated by knowledge of the genomic structure of the human $\alpha_1$1.2 gene, which spans an estimated 150 kb of the human genome and is composed of 44 invariant and 6 alternative exons (Soldatov, 1994). The L-type channel in chick hair cells incorporates an $\alpha_1$1.3 subunit that differs from the $\alpha_1$1.3 subunit in brain due to expression of distinct exons at three locations (Kollmar et al., 1997). It will be interesting to see if additional splice variations can account for L-type channel activity found at the resting potential of hippocampal neurons, possibly important for setting the resting $[Ca^{2+}]_i$ (Avery and Johnston, 1996).

1.3.2.3 Ca_V2

The second α_1 subfamily consists of cDNAs which, when expressed, result in HVA channels which lack the characteristic DHP-response of L-type channels. These clones [$\alpha_1$2.1 (α_{1A}) (Mori et al., 1991), $\alpha_1$2.2 (α_{1B})(Dubel et al., 1992) and $\alpha_1$2.3 (α_{1E}) (Soong et al., 1993)] were derived from nervous tissue. Individual genes within this subfamily show ~89% identity with each other in the membrane spanning and pore forming regions but only ~53% or less with members of the $\alpha_1$1 subfamily.

1.3.2.3.1 $Ca_V2.2$/N-type Ca^{2+} channels

The most extensively characterized non-L-type Ca^{2+} channel was named N-type since it appeared to be largely specific to *n*eurons as opposed to muscle cells and was clearly *n*either T- nor L-type (Nowycky et al., 1985). It requires relatively negative resting potentials to be available for opening, somewhat like T-type, but is high voltage-activated, like L-type. This Ca^{2+} channel is potently and specifically blocked by a peptide

toxin derived from the venom of the marine snail, *Conus geographus*, ω-conotoxin GVIA (ω-CTx-GVIA). The N-type channel is found primarily in presynaptic nerve terminals and neuronal dendrites in addition to cell bodies (Westenbroek et al., 1992). The N-type current can be assigned with a fairly high degree of certainty to $Ca_V2.2$ (α_{1B}), which, when expressed, conducts ω-CTx-GVIA-sensitive currents with characteristics that match those of native N-type channels (Dubel et al., 1992; Williams et al., 1992a; Fujita et al., 1993).

As discussed earlier, an important source of channel heterogeneity is the association of α_1 subunits with different ancillary subunits. A good example of this is provided by the N-type Ca^{2+} channel in brain. Biochemical analysis has shown that the $\alpha_1 2.2$ subunit associates with three different isoforms of β subunit in rabbit brain (Scott et al., 1996). Antibodies against individual β subunits were each able to immunoprecipitate ω-CTx-GVIA binding activity (a marker of $Ca_V2.2$), while immunoprecipitation of $\alpha_1 2.2$ showed its association with β_{1b}, β_3 and β_4.

Different isoforms of the N-type Ca^{2+} channel subunit $\alpha_1 2.2$ have been isolated from rat sympathetic ganglia and brain by Lin *et al.* (1997). Alternative splicing determines the presence or absence of small inserts in the S3-S4 regions of domains III and IV (SFMG and ET respectively). Different combinations of inserts in these putative extracellular loop regions are dominant in central (+SFMG, ΔET) versus peripheral (ΔSFMG, +ET) nervous tissue. Most interestingly, the gating kinetics of ΔET-containing clones (as found in the central form) are significantly faster than the +ET form (Lin et al., 1999). This work provides a clear example of how alternative splicing contributes to diverse functional properties.

1.3.2.3.2 $Ca_V2.1$/P- and Q-type Ca^{2+} channels

Currents carried by P-type channels were originally recorded from cell bodies of cerebellar *P*urkinje cells (Llinás et al., 1989; Llinás et al., 1992). These channels are not

blocked by DHPs or ω-CTx-GVIA, but are exquisitely sensitive to block by ω-Aga-IVA or ω-Aga-IVB, components of the venom of the funnel-web spider, *Agelenopsis aperta* (Mintz et al., 1992a; Mintz et al., 1992b), with an IC_{50} of <1 nM for ω-Aga-IVA (Mintz and Bean, 1993). These channels support a current that hardly inactivates during depolarizations lasting for several seconds. They are seen in virtual isolation from other voltage-gated Ca^{2+} channels in cerebellar Purkinje neuron cell bodies, but also contribute substantially to somatic currents in many other central neurons (Mintz et al., 1992a).

Initial observations of current supported by $\alpha_1 2.1$ (α_{1A}) suggested that it corresponded to the P-type channel (Llinás et al., 1992), consistent with the strong expression of this subunit in cerebellar Purkinje cells (Mori et al., 1991; Mintz et al., 1992b; Stea et al., 1994). Closer comparison of the properties of $Ca_V 2.1$ expressed in *Xenopus* oocytes and those of P-type channels in Purkinje cells, however, revealed clear differences. P-type channels activate at relatively negative potentials and support a sustained, non-inactivating current during depolarizing pulses longer than 1 s (Llinás et al., 1992; Usowicz et al., 1992), whereas $\alpha_1 2.1$ subunits expressed in *Xenopus* oocytes activate at less negative potentials and exhibit marked inactivation within 100 ms (Sather et al., 1993). Furthermore, the IC_{50} for ω-Aga-IVA block of $Ca_V 2.1$ expressed in oocytes (Sather et al., 1993; Stea et al., 1994) or baby hamster kidney cells (Niidome et al., 1994) is 100-200 nM. A current with these properties was characterized in the cell bodies of cerebellar granule neurons and named Q-type (Zhang et al., 1993; Randall and Tsien, 1995) since it differed from the previously defined P-type current (which was also present in the granule neurons).

Subsequently channels of intermediate type have been found in several preparations (Tottene et al., 1996; Forsythe et al., 1998; Mermelstein et al., 1999), indicating that instead of two discrete channel types, P and Q may represent points on a spectrum of channel properties. Additionally, evidence has been mounting that both channels are

encoded by the same α_1 subunit (Gillard et al., 1997; Piedras-Rentería and Tsien, 1998; Pinto et al., 1998; Jun et al., 1999), and it has been shown that differences in inactivation and toxin affinity, the basis for distinctions between these two types, can be explained in part by splice variants or subunit composition (Liu et al., 1996; Bourinet et al., 1999; Mermelstein et al., 1999). With these facts in mind, the designation P-type or P/Q-type would be appropriate to indicate current through $Ca_V2.1$ or ω-Aga-IVA/B- or ω-CTx-MVIIC-sensitive current, regardless of inactivation characteristics. P/Q-type channels have a similar distribution to N-type channels.

1.3.2.3.3 $Ca_V2.3$/R-type Ca^{2+} channels

R-type Ca^{2+} channel currents were identified in cerebellar granule cells as a current that *r*emained in the presence of nimodipine, ω-CTx-GVIA, and ω-Aga-IVA, inhibitors of the L-, N-, and P/Q-type channels respectively (Ellinor et al., 1993; Zhang et al., 1993; Randall and Tsien, 1995). R-type currents have since been found in several other central nerve terminals (Meder et al., 1997; Namkung et al., 1998; Newcomb et al., 1998; Wu et al., 1998). This predominantly HVA current decays rapidly and is at least partially responsive to low doses of Ni^{2+} and, in some preparations, SNX-482, a toxin derived from tarantula venom (Newcomb et al., 1998). Less is known about the molecular basis of R-type currents than for any of the other channel types. Of all the known α_1 subunits, $\alpha_1$2.3 (α_1E) comes the closest. Expressed $Ca_V2.3$ currents display certain attributes of R-type channels: they are readily blocked by Ni^{2+} (Soong et al., 1993; Wakamori et al., 1994; Williams et al., 1994) and the spider toxin ω-Aga-IIIA (Randall and Tsien, 1998; Rock et al., 1998), and display a single channel conductance of ~12-14 pS in 100 mM Ca^{2+}, Ba^{2+}, or Sr^{2+} (Schneider et al., 1994; Wakamori et al., 1994; Bourinet et al., 1996; Tottene et al., 1996; Tottene et al., 1999). In addition $Ca_V2.3$ antisense treatment has been shown to reduce native R-type current (Piedras-Rentería and Tsien, 1998). Some studies have found reasons to question assignment of R-type currents to $Ca_V2.3$ (Soong et

al., 1993; Bourinet et al., 1996; Tottene et al., 1996; Piedras-Renteria et al., 1997; Meir and Dolphin, 1998), however some of these may be explained by diversity in R-type currents caused by splice variants and/or auxiliary subunit differences as seen for P- vs. Q-type channels. Support for the possibility of R-type diversity comes from studies that show that SNX-482, a synthetic peptide neurotoxin, blocks R-type currents in some cell types but spares them in others (Newcomb et al., 1998) and differences in Ni^{2+} block and activation voltage in R-type current in the same cell type (Tottene et al., 1996).

1.3.2.4 Ca_V3/T-type Ca^{2+} channels

LVA Ca^{2+} channels are exemplified by T-type channels, so-named because they carry *t*iny unitary Ba^{2+} currents (6-8 pS with ~100 mM Ba^{2+} or Ca^{2+} as charge carrier) that occur soon after the depolarizing step, giving rise to a *t*ransient average current (Carbone and Lux, 1984; Nilius et al., 1985; Nowycky et al., 1985). Another defining characteristic of classical T-type channels is their slow deactivation following a sudden repolarization (Matteson and Armstrong, 1986). T-type channel current records also exhibit a distinctive kinetic fingerprint: the superimposed current responses cross over each other in a pattern not found with other rapidly inactivating Ca^{2+} channels such as R-type (Randall and Tsien, 1998). The kinetic properties are dominated by a strikingly voltage-dependent delay between the depolarizing step and the channel's first opening (Droogmans and Nilius, 1989). In addition to these properties, T-type channels have a unique pharmacological profile, characterized by only mild sensitivity to 1,4-dihydropyridines (DHPs), such as nifedipine or nimodipine (Cohen and McCarthy, 1987), but acute sensitivity to mibefradil (Ertel and Ertel, 1997). A newly identified antagonist, kurtoxin, has recently been shown to affect $Ca_V3.1$ (Chuang et al., 1998). Kurtoxin is an α-scorpion toxin which also affects voltage-gated sodium channels and is currently the most specific antagonist with respect to T-type *versus* other Ca^{2+} channels. Within the overall category of T-type Ca^{2+} channel, further diversity has been found, particularly with respect to

kinetic characteristics and pharmacology (Akaike et al., 1989; Kostyuk and Shirokov, 1989; Huguenard and Prince, 1992). Various subtypes of T-type Ca^{2+} channel may co-exist in the same cell type and show rates of inactivation differing by as much as five-fold, while sharing similar voltage-dependence of inactivation (Huguenard and Prince, 1992). T-type channels are found in a wide variety of central and peripheral neurons.

The Ca_V3 subfamily of T-type channels is more distantly related to the two HVA subfamilies Ca_V1 and Ca_V2 than the latter two are to each other (Figure 1-2). Three genes in Ca_V3 have recently been identified, $Ca_V3.1$ (α_{1G}), $Ca_V3.2$ (α_{1H}), and $Ca_V3.3$ (α_{1I}) (Cribbs et al., 1998; Perez-Reyes et al., 1998; Lee et al., 1999). These genes encode LVA T-type channels when expressed without auxiliary subunits (Cribbs et al., 1998; Perez-Reyes et al., 1998; Lacinová et al., 1999; Lee et al., 1999). This is consistent with findings that native T-type currents are not dependent on auxiliary subunits (Lambert et al., 1997; Leuranguer et al., 1998), however there is a report that coexpression of $\alpha_2\delta$ can increase expression of native T-type current (Wyatt et al., 1998).

1.3.2.5 Note on pharmacology

Pharmacology is the most widely used criterion when distinguishing various types of Ca^{2+} currents. It should therefore be noted that antagonists discussed above are not perfectly selective. The P/Q-type blockers ω-Aga-IVA/B and ω-CTx-MVIIC all partially antagonize N-type channels at higher doses (Mintz I. M. & S. Sidach, The Society for Neuroscience abstract, 24:1021, 1998) (Hillyard et al., 1992; Grantham et al., 1994; Jun et al., 1999) and ω-Aga-IVA has been shown to have some effect on expressed $Ca_V2.3$ channels (Soong et al., 1993; Williams et al., 1994). In addition to the lack of complete specificity of these toxins, it should also be noted that there are occasional reports of currents that display pharmacological properties that do not fit any of the above categories. These include currents which can be blocked by either ω-CTx-GVIA or moderate doses of ω-Aga-IVA in rat supraoptic neurons (Fisher and Bourque, 1995) and chicken

forebrain synaptosomes (Lundy et al., 1994) and a current reversibly blocked by ω-CTx-GVIA (Mermelstein and Surmeier, 1997).

1.3.2.6 Evolutionary conservation of Ca^{2+} channel families

The evolutionary divergence of Ca_V1 and Ca_V2 Ca^{2+} channels occurred relatively early, as would be expected from the fairly low sequence homology between genes encoding channels from the two subfamilies (Figure 1-2). This deduction can be corroborated by an examination of the distribution of Ca^{2+} channel types in organisms spread across many phyla. Both subfamilies of HVA channels are present in vertebrate species ranging from marine rays (Horne et al., 1993) to humans (Williams et al., 1992a; Williams et al., 1992b), and in many cases both are expressed within the same cells (e.g., Randall and Tsien, 1995). Amongst invertebrates, both channel types have been observed in molluscs (Edmonds et al., 1990), insects (Grabner et al., 1994; Smith et al., 1996), and nematodes (Schafer and Kenyon, 1995). Given the widespread distribution of L- and non-L-type HVA Ca^{2+} channels across the animal kingdom their bifurcation must have occurred quite early during the speciation of Animalia. Presumably LVA and HVA channels diverged even earlier. A possible descendent of an ancestral HVA channel which resembles L-type channels has been cloned from jellyfish (Jeziorski et al., 1998). A "T-like" channel has been observed in paramecium (e.g. Ehrlich et al., 1988). LVA and HVA currents have been identified in cockroaches (Grolleau and Lapied, 1996) and leech (Lu et al., 1997). Whether the various LVA currents are carried by channels with a molecular structure similar to Ca_V3 is not known.

1.3.3 Functional Roles of Ca^{2+} Channels

1.3.3.1 Introduction/Subcellular localization

The diversity of voltage-gated Ca^{2+} channels is indicative of the variety of functional roles they are called upon to serve. With the exception of $\alpha_1$1.1, which appears highly localized to skeletal muscle, α_1 subunits are broadly distributed across the spectrum of

exocytotic cells. At the level of individual cells, however, the different channel types often show distinct patterns of localization to different parts of the cell.

Ca^{2+} channels of the Ca_V1 subfamily are widely distributed in muscle, nerve and endocrine cells. Their unique biophysical properties and subcellular localization put them in a good position to act as transducers linking membrane depolarization to intracellular signaling. In the brain, for example, Ca_V1 channels are found in the cell bodies and proximal dendrites of hippocampal pyramidal cells (Westenbroek et al., 1990). $\alpha_1$1.2-containing channels were concentrated in clusters at the base of major dendrites, while $Ca_V1.3$ channels were more generally distributed across the surface of cell bodies and proximal dendrites (Hell et al., 1993a).

The Ca_V2 subfamily of Ca^{2+} channels is widely distributed both pre- and postsynaptically in the central and peripheral nervous systems. In most regions of the brain, antibodies against $\alpha_1$2.2 bind primarily on dendrites and nerve terminals (Westenbroek et al., 1992) whereas $\alpha_1$2.1 subunits are concentrated in presynaptic terminals and are present at lower density in the surface membrane of dendrites of most major classes of neurons (Westenbroek et al., 1995). $Ca_V2.3$ epitopes are found mostly on cell bodies, and in some cases in dendrites, of a broad range of central neurons (Yokoyama et al., 1995). Thus, these classes of Ca^{2+} channels seem to be well positioned to support both presynaptic Ca^{2+} influx that triggers neurotransmitter release and postsynaptic Ca^{2+} entry that helps shape the response downstream to that release.

Little is known about the subcellular distribution of the recently cloned Ca_V3 subfamily of Ca^{2+} channels. The only systematic study so far (Talley et al., 1999) contains no information regarding subcellular distribution of these proteins. In many cell types T-type currents seem to be found primarily in the dendrites as compared to somata (Karst et al., 1993; Markram and Sakmann, 1994; Magee et al., 1995; Magee and Johnston, 1995;

Kavalali et al., 1997; Mouginot et al., 1997; but see Schultz et al., 1999). This is consistent with theories about their functional roles (see below).

1.3.3.2 Excitation-contraction coupling

L-type Ca^{2+} channels play a central role in excitation-contraction coupling in skeletal, cardiac and smooth muscle, although other channel types may play a supporting role in some of these cells (Zhou and January, 1998). In skeletal muscle, L-type Ca^{2+} channels contain the $\alpha_1$1.1, β_{1a}, γ_1, and $\alpha_2\delta$-1 subunits and are largely localized to the transverse tubule system. Ca^{2+} entry through the L-type channel is not required for skeletal muscle contraction (reviewed in Miller and Freedman, 1984), in contrast to cardiac muscle, where Ca^{2+} entry is essential for contractility (Näbauer et al., 1989). Interestingly, blockade of L-type channels in skeletal muscle by organic Ca^{2+} antagonists completely inhibits contraction (Eisenberg et al., 1983). The explanation of these findings centers on gating charge movement in the T-tubule membrane, which was known to be essential for intracellular Ca^{2+} release (Schneider and Chandler, 1973). DHPs eliminate charge movement, thereby blocking skeletal muscle contraction (Ríos and Brum, 1987). The implication of these findings was that DHP-sensitive L-type Ca^{2+} channels act as voltage sensors to link T-tubule depolarization to intracellular Ca^{2+} release.

This hypothesis was tested in elegant experiments by Tanabe, Numa, Beam and their colleagues. The cloning of the DHP receptor protein from skeletal muscle led immediately to its identification as a voltage-gated channel (Tanabe et al., 1987). Later, expression of the cloned DHP receptor in dysgenic skeletal muscle myotubes showed that it could restore electrically evoked contractility in these formerly non-responsive cells (Tanabe et al., 1988), along with L-type Ca^{2+} current (Tanabe et al., 1988; Garcia et al., 1994) and gating charge movement (Adams et al., 1990). While the skeletal DHP receptor allowed contraction even in the absence of extracellular Ca^{2+}, the cardiac L-type Ca^{2+} channel restored contractility only if Ca^{2+} entry occurred (Tanabe et al., 1990). The

structural basis of the skeletal-type excitation-contraction coupling was investigated with molecular chimeras. By inserting pieces of the $\alpha_1$1.1 gene into an $\alpha_1$1.2 background, Tanabe *et al.* (1990) showed that the key domain was the intracellular loop joining repeats II and III of $\alpha_1$1.1 (see asterisk in figure 1). More recently, other groups have shown that purified II-III loop fragments can directly activate the ryanodine receptor (Lu et al., 1994; el-Hayek et al., 1995) and that this region may contain phosphorylation sites for the regulation of excitation-contraction coupling (Lu et al., 1995).

1.3.3.3 Rhythmic activity

1.3.3.3.1 Pacemaker

In cardiac cells, T-type Ca^{2+} channels are generally present at much lower density than L-type channels, if at all. However, T-type channels supply a major fraction of the current recorded in cells from the sinoatrial node, the natural source of cardiac rhythms, and thus provide a significant contribution to the inward current that drives the last stages of the pacemaker depolarization (Hagiwara et al., 1988; Lei et al., 1998).

1.3.3.3.2 Other

T-type channels also support oscillatory activity and repetitive activity in the thalamus (Jahnsen and Llinás, 1984; McCormick and Bal, 1997). Along with an apamin-sensitive Ca^{2+}-activated K current, T-type channels in the nucleus reticularis generate rhythmic action potential bursts. In thalamocortical neurons the overlapping activation and inactivation curves of T-type currents support rebound burst firing in which a hyperpolarization is followed by a Ca^{2+} spike results in the generation of several action potentials. Interestingly, expression of T-type channels in smooth muscle fluctuates in synchrony with the cell cycle (Kuga et al., 1996), and may be associated with cell proliferation (Schmitt et al., 1995).

1.3.3.4 Excitation-secretion coupling

1.3.3.4.1 Generic properties

The most commonly studied role of Ca^{2+} is its ability to trigger neurotransmitter release. The importance of Ca^{2+} ions in the release of neurotransmitter has been appreciated for more than 60 years (Feng, 1936). Seminal work by Douglas (1963) and Katz (1969) and their colleagues demonstrated that Ca^{2+} ions exert their influence at the nerve terminal where they control the amount of neurotransmitter that is released. The action of Ca^{2+} ions in the regulation of neurotransmission was shown to be cooperative, requiring about four Ca^{2+} ions to bind to their receptor in order to trigger release (Dodge and Rahamimoff, 1967). The importance of Ca^{2+} action in the nerve terminal was further supported by the observation that injection of Ca^{2+} into the terminal triggered the release of transmitter at the squid giant synapse (Miledi, 1973). Subsequently, the Ca^{2+}-sensitive protein, aequorin, was used to show that presynaptic $[Ca^{2+}]_i$ increases during neurotransmission (Llinás and Nicholson, 1975).

Studies using simultaneous voltage clamp of the presynaptic terminal and postsynaptic axon of the squid giant synapse provided direct measurements of the Ca^{2+} currents in the presynaptic membrane that trigger the release of neurotransmitter (Llinás et al., 1981; Augustine et al., 1985). Ongoing issues include the identification of presynaptic Ca^{2+} channels and clarification of the functional consequences of their diversity (for other recent reviews, see Olivera et al., 1994; Dunlap et al., 1995; Reuter, 1996).

Ca^{2+} channels from the Ca_V2 subfamily are the primary types responsible for excitation-secretion coupling. Interestingly just as the II-III loop of the Ca_V1 channel interacts with the Ca^{2+} channel's effector for contraction, the II-III loop of the Ca_V2 channel interacts with its effector: the secretory apparatus (Sheng et al., 1994) (asterisk in figure 1). The specific type of channel involved in secretion from various cell types is discussed in greater detail below.

While the vast majority of studies of neurotransmitter release have failed to identify a role for L-type Ca^{2+} channels (Dunlap et al., 1995), this subtype has been implicated in a few specialized forms of exocytosis. For example, activation of L-type channels is required for zona pellucida-induced exocytosis from the acrosome of mammalian sperm (Florman et al., 1992). L-type channels also seem to play a role in mediating hormone release from endocrine cells. Inhibition of L-type Ca^{2+} channels reduces insulin secretion from pancreatic β cells (Ashcroft et al., 1994; Bokvist et al., 1995), oxytocin and vasopressin release from the neurohypophysis (Lemos and Nowycky, 1989), luteinizing hormone-releasing hormone release from the bovine infundibulum (Dippel et al., 1995) and catecholamine release from adrenal chromaffin cells (Lopez et al., 1994). L-type channels also seem to play an important role in supporting release of GABA from retinal bipolar cells (Maguire et al., 1989; Duarte et al., 1992), as well as dynorphin release from dendritic domains of hippocampal neurons (Simmons et al., 1995). In some cases L-type channels may function to release excitatory amino acid transmitters, in response to particular patterns of activity (Bonci et al., 1998), in cells that exhibit graded potentials (Schmitz and Witkovsky, 1997) during extended depolarizations with high K^+ or under the experimental influence of the DHP agonist Bay K 8644 (e.g., see Sabria et al., 1995).

In addition to admitting the Ca^{2+} which directly triggers neurotransmitter release, Ca^{2+} channels regulate and are regulated by the state of the nerve terminal. Ca^{2+} entry though the same channels which trigger transmitter release, and most likely through other presynaptic channels more distant from the release site (possibly including L-type channels) affects the background level of Ca^{2+} in the terminal, which regulates endocytosis, release probability, various dynamic parameters of the vesicle pool, as well as the channels themselves (reviewed in Neher, 1998). Ca^{2+} channels also receive direct feedback about the state of the release machinery (see Results).

1.3.3.4.2 Peripheral

At the neuromuscular junction, the release of neurotransmitter is generally mediated by a single Ca^{2+} channel type, although there is variation in the type that predominates from species to species. Invertebrate motor end plates utilize primarily P/Q-type channels. In crayfish, for example, inhibitory and excitatory transmitter release onto the claw opener muscle was completely abolished by ω-Aga-IVA, while ω-CTx-GVIA and nifedipine were both ineffective (Araque et al., 1994). In locusts and houseflies, motor end plate potentials are blocked by type I and II Agatoxins, which inhibit P/Q-type channels, but not by type III Agatoxins, which potently block both L- and N-type channels (Bindokas et al., 1991). In non-mammalian vertebrates, unlike invertebrates, neurotransmitter release at the neuromuscular junction is completely blocked by ω-CTx-GVIA. This is true for frogs (Kerr and Yoshikami, 1984; Katz et al., 1995), lizards (Lindgren and Moore, 1989) and chicks (De Luca et al., 1991; Gray et al., 1992). In mammals on the other hand, ω-CTx-GVIA does not seem to have any effect on the evoked release of acetylcholine at the neuromuscular junction (Sano et al., 1987; Wessler et al., 1990; De Luca et al., 1991; Protti et al., 1991; Bowersox et al., 1995). In contrast, block of P/Q-type Ca^{2+} channels by ω-CTx-MVIIC, ω-Aga-IVA or FTx completely abolishes transmission in mice (Protti and Uchitel, 1993; Bowersox et al., 1995; Hong and Chang, 1995) and humans (Protti et al., 1996). In all of these species, neuromuscular transmission seems to rely on a single type of channel from the Ca_V2 subfamily.

In general, sympathetic neurons contain both L- and N-type Ca^{2+} channels but not P/Q-type channels (Hirning et al., 1988; Mintz et al., 1992a; Zhu and Ikeda, 1993) (but see Namkung et al., 1998). However, only N-type Ca^{2+} channels seem to be important for the release of norepinephrine, inasmuch as ω-CTx-GVIA blocks NE secretion (Hirning et al., 1988; Fabi et al., 1993) but DHPs do not (Perney et al., 1986; Hirning et al., 1988; Koh and Hille, 1996). Along similar lines, N- but not L-type Ca^{2+} channels in sympa-

thetic nerve terminals are susceptible to modulation of Ca^{2+} current via autoreceptors for NE or neuropeptide Y (Toth et al., 1993). Thus, sympathetic nerve endings are like motor nerve terminals in relying on a single predominant type of Ca^{2+} channel, in this case N-type, despite the sizable contribution of L-type channels to the global Ca^{2+} current. Reliance on N-type channels cannot be generalized to all autonomic terminals since P/Q-type channels play a prominent role in transmitter release in rodent urinary bladder (Frew and Lundy, 1995; Waterman, 1996) and also participate in triggering release of exocytosis from mouse sympathetic and parasympathetic nerve terminals (Waterman, 1997; Waterman et al., 1997)

1.3.3.4.3 Central

At central synapses, unlike synapses in the periphery, neurotransmitter release often involves more than one Ca^{2+} channel type. Central neurons appear to be richly endowed with Ca^{2+} channels, with many as five or six different types of channels in an individual nerve cell (Mintz et al., 1992a; Randall and Tsien, 1995). Several recent papers have reported that neurotransmission at specific synapses in the CNS depends upon the concerted actions of more than one type of Ca^{2+} channel (Luebke et al., 1993; Takahashi and Momiyama, 1993; Castillo et al., 1994; Regehr and Mintz, 1994; Wheeler et al., 1994; Mintz et al., 1995). The relative importance of N-, P/Q-, and R-type Ca^{2+} channels can vary from one synapse to another. Studies of synapses in hippocampal and cerebellar slices suggest that the vast majority of single release sites are in close proximity to a mixed population of Ca^{2+} channels that jointly contribute to the local Ca^{2+} transient that triggers vesicular fusion (e.g., Mintz et al., 1995; but see also Reuter, 1995; Poncer et al., 1997; Reid et al., 1997). The synergistic effect of multiple Ca^{2+} channels arises because of limitations on the Ca^{2+} flux through individual channels under physiological conditions. Indeed, the reliance on multiple types of Ca^{2+} channels was not absolute but could be relieved by increasing the Ca^{2+} influx per channel, either by prolonging the presynap-

tic action potential or by increasing $[Ca^{2+}]_o$ (Wheeler et al., 1996). The reliance on more than a single Ca^{2+} channel type may offer the advantage of precise control over Ca^{2+} influx and transmitter release by allowing for differential modulation (Tsien et al., 1988; Mogul et al., 1993; Swartz et al., 1993; Mynlieff and Beam, 1994).

1.3.3.5 Postsynaptic Ca^{2+} influx

1.3.3.5.1 Dendritic information processing

Much of the electrical and biochemical signal processing in central neurons takes place within their dendritic trees. Ca^{2+} entry through voltage-gated channels is critical for many of these events. The idea that voltage-gated Ca^{2+} channels may contribute to electrogenesis in dendrites first arose in the interpretation of intracellular recordings from hippocampal pyramidal neurons (Spencer and Kandel, 1961). Initial intradendritic voltage recordings were conducted on the dendritic arbors of cerebellar Purkinje neurons (Llinás and Nicholson, 1971; Llinás and Hess, 1976; Llinás and Sugimori, 1980) and apical dendrites of hippocampal pyramidal neurons (Wong et al., 1979). The ability of dendrites to support Ca^{2+}-dependent action potential firing was reinforced by experiments where apical dendrites of pyramidal neurons were surgically isolated from their cell bodies in a hippocampal slice preparation (Benardo et al., 1982; Masukawa and Prince, 1984). These experiments revealed a variety of Ca^{2+}-dependent active responses in the dendrites of central neurons that could be elicited by excitatory postsynaptic potentials or injection of depolarizing current pulses.

Recent studies of the electrical properties of dendrites have been facilitated by the ability to visualize dendrites in brain slices, thus rendering dendrites accessible to patch electrodes (Stuart et al., 1993). These studies revealed that back-propagating Na^+-dependent action potentials can activate dendritic Ca^{2+} channels, thereby causing substantial increases in intradendritic free Ca^{2+} (Jaffe et al., 1992; Stuart and Sakmann, 1994; Markram et al., 1995; Schiller et al., 1995; Spruston et al., 1995). Subthreshold excitatory postsynaptic potentials can also open Ca^{2+} channels and result in more

postsynaptic potentials can also open Ca^{2+} channels and result in more localized changes in intradendritic Ca^{2+} concentration (Markram and Sakmann, 1994; Yuste et al., 1994; Magee et al., 1995). T-type Ca^{2+} channels play a prominent role in dendritic Ca^{2+} signaling in hippocampal and cortical neurons (Magee et al., 1995), presumably due to their ability to open at relatively negative membrane potentials.

The presence of multiple types of voltage-gated Ca^{2+} channels on dendrites has been demonstrated by several techniques, including Ca^{2+} imaging (Markram et al., 1995; Watanabe et al., 1998), dendrite-attached patch clamp recordings (Usowicz et al., 1992; Magee and Johnston, 1995) and immunocytochemistry (Westenbroek et al., 1990; Westenbroek et al., 1992; Hell et al., 1993a; Westenbroek et al., 1995; Yokoyama et al., 1995). Recordings from isolated dendritic segments of acutely dissociated hippocampal neurons indicated that T-, N-, P/Q- and R-type channels all contribute to the overall Ca^{2+} current in dendrites, with T-type current particularly enhanced when compared to somata (Kavalali et al., 1997).

1.3.3.6 Excitation-expression coupling and changes in gene expression

A number of extracellular factors that influence cell growth and activity depolarize the membranes of their target cells (Hill and Treisman, 1995). Membrane depolarization opens voltage-gated Ca^{2+} channels and the resulting influx of Ca^{2+} can trigger gene transcription (for a review, see Morgan and Curran, 1989). L-type Ca^{2+} channels are thought to play a role in this cascade because agonists of these channels can induce expression of several protooncogenes in the absence of other stimuli (Morgan and Curran, 1988). Indeed the mode and location of Ca^{2+} entry may be important to how the Ca^{2+} signal is interpreted by the cell (Ghosh et al., 1994; Rosen and Greenberg, 1994). Some recent studies have shed light on the cascade of events that follows influx of Ca^{2+} through L-type channels.

An example of a signal-transduction cascade where Ca^{2+} entry is important involves the cAMP and Ca^{2+} response element (CRE), and its nuclear binding protein (CREB) (Montminy and Bilezikjian, 1987; Hoeffler et al., 1988). The interaction of CREB with the CRE is facilitated when CREB is phosphorylated on serine-133 (Gonzalez and Montminy, 1989). The phosphorylation of CREB is catalyzed by several kinases including Ca^{2+}-calmodulin kinases II and IV, cAMP-dependent protein kinase (Greenberg et al., 1992), and others. Thus, rises in $[Ca^{2+}]_i$ can act either directly, via Ca^{2+}-calmodulin and its dependent kinases, or indirectly, by stimulating Ca^{2+}-calmodulin-sensitive adenylate cyclase leading to increased cAMP levels. Recent work has shown that Ca^{2+} entry through L-type channels can trigger CREB phosphorylation (Yoshida et al., 1995; Deisseroth et al., 1998; Rajadhyaksha et al., 1999), and that the Ca^{2+} probably binds to a target molecule within 1 μm of the point of entry (Deisseroth et al., 1996).

In addition to Ca^{2+}, Zn^{2+} influx is interesting because it regulates a wide variety of enzymes and DNA binding proteins, provides an important developmental signal, and may be involved in excitotoxicity and responses to trauma (for a review, see Smart et al., 1994). Interestingly, L-type Ca^{2+} channels can support Zn^{2+} influx into heart cells, where it can induce transcription of genes driven by a metallothionein promoter (Atar et al., 1995). Morphological studies have revealed that Zn^{2+} is highly enriched in a number of nerve fiber pathways, especially in boutons where it appears to be contained within vesicles (Smart et al., 1994). Furthermore, Zn^{2+} can be released from brain tissue during electrical or chemical stimulation (Assaf and Chung, 1984; Howell et al., 1984; Charton et al., 1985). Given that Zn^{2+} can be released by synaptic activity, and can enter cells via voltage-dependent Ca^{2+} channels, it seems likely that Zn^{2+} may play an important role in excitation-expression coupling.

1.3.4 Concluding Remarks

Understanding of the diversity of voltage-gated Ca^{2+} channels has greatly increased over the last decade or so as a result of several synergistic approaches. The identification of multiple types of Ca^{2+} channels on the basis of biophysical and pharmacological criteria has been complemented by studies of the biochemistry and molecular biology of their underlying subunit components. The most recent advances have been made in understanding the basis of P/Q-, R- and T-type Ca^{2+} channel activity. Considerable progress has also been made in clarifying molecular mechanisms of the structural features that distinguish individual types of Ca^{2+} channels and enable them to perform specialized functional roles or to respond to type-selective drugs. The largest area of uncertainty concerns the three-dimensional structures of Ca^{2+} channels and the structural basis of differences among channel subtypes.

1.4 Results

1.4.1 Cleaving Syntaxin with Botulinum Toxin C1 Increases Calcium Influx

To determine whether syntaxin influences Ca^{2+} channels in nerve terminals, we looked for an effect of botulinum neurotoxin C1 (BoNtC1), which cleaves syntaxin, on Ca^{2+} entry in rat cortical synaptosomes (Figure 1-3A). Ca^{2+} entry was evoked by successive application of 1 mM $CaCl_2$ and 60 mM KCl, 3.5 s apart to fura-2-loaded synaptosomes. The synaptosomes were preincubated in nominally 0 Ca^{2+} external solution, an important experimental feature for the results that follow (see Methods). Since N- and P/Q-type channels are the main putative targets of syntaxin action (Bezprozvanny et al., 1995), experiments were performed in the presence of 10 μM nimodipine to block L-type channels unless otherwise specified. Figure 1-3A compares depolarization-dependent fluorescence signals recorded from synaptosomes that had been pretreated with BoNtC1 with signals taken from control synaptosomes, not treated with toxin. Traces from three

separate runs are shown in each case, and the signals have been corrected for the depolarization-independent signal caused by addition of Ca^{2+} without K^+ (Figure 1-4A). As a result of depolarization-induced opening of Ca^{2+} channels, the control traces rose rapidly to a peak before progressively decaying over the next 60 s. The Ca^{2+} signals from three parallel runs with BoNtC1-treated synaptosomes showed an early rise nearly identical to the control traces, but decayed much more slowly and to a lesser extent. Thus, the impact of the toxin pretreatment grew progressively larger over the course of the depolarization. This effect was not observed when synaptosomes were pretreated with heat-inactivated BoNtC1 (Figure 1-3B): in this case, no significant alteration of the depolarization-induced Ca^{2+} transients was observed ($p>0.4$). In separate experiments, we verified that pretreatment with the heat-inactivated toxin failed to cleave syntaxin or to block Ca^{2+}-dependent glutamate release, effects clearly evident with BoNtC1 (data not shown).

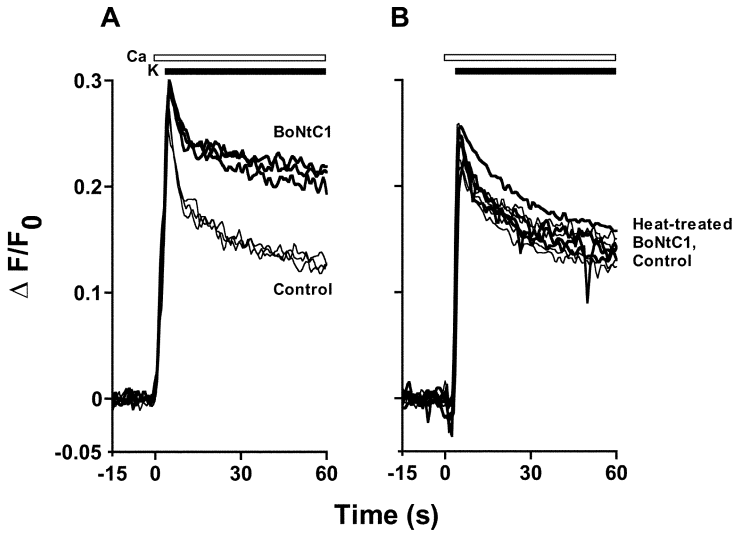

Figure 1-3. BoNtC1 Treatment Increases Ca^{2+} Influx

(A) Fura-2-loaded synaptosomes were either mock treated ("Control") or pretreated with 66 nM BoNtC1 ("BoNtC1") for 45 min at 37°C. At time t = 0 external free Ca^{2+} was raised to 1 mM. At t = 3.5 s external K^+ was raised to 60 mM. *Horizontal bars* mark times of additions. Ordinate indicates the fractional decrease in fluorescence relative to baseline, signifying elevated Ca^{2+}. 10 μM nimodipine was present throughout to block L-type Ca^{2+} channels. Data have been corrected for the depolarization-independent signal (see Methods). Three runs from one synaptosome preparation are depicted under each condition. In all subsequent Figures in this chapter thick traces denote toxin-treated synaptosomes and thin traces denote mock-treated synaptosomes. (B) Same conditions as in (A) except BoNtC1 was incubated for 45 min at 95°C before application to synaptosomes. Data show 4 runs for each condition (2 runs from each of 2 synaptosome preparations).

1.4.2 The Effect of BoNtC1 Is Specific to Depolarization-Induced Ca^{2+} Entry

We carried out additional control experiments to find out whether BoNtC1 acted on pathways for Ca^{2+} equilibration, distinct from voltage-dependent Ca^{2+} channels. Figure 1-4A illustrates the depolarization-independent Ca^{2+} rise that was produced by exposing the synaptosomal preparation to 1 mM $CaCl_2$ without subsequent addition of 60 mM KCl. Parallel experiments showed that this fluorescence signal arose from Ca^{2+} uptake into a compartment distinct from functional synaptosomes (see Methods). The uptake process was unresponsive to inhibitors of known Ca^{2+} transport pathways and was not associated with any detectable glutamate release (Figure 1-4A, inset). As shown in Figure 1-4A, the depolarization-independent Ca^{2+} rise was not significantly affected by BoNtC1 ($p>0.4$). Corrections have been made for the depolarization-independent Ca^{2+} rise in all other Figures (see Methods for details).

Another series of experiments tested for an effect of syntaxin cleavage on the performance of Ca^{2+} buffering and extrusion mechanisms. These are undoubtedly recruited once intrasynaptosomal Ca^{2+} has been elevated by voltage-gated Ca^{2+} entry. Figure 1-4B shows the protocol we used to focus on Ca^{2+} restorative processes. At different intervals following the introduction of KCl to depolarize the synaptosomes (3.5 s or 25 s), sufficient EGTA was added to the cuvette to return $[Ca^{2+}]_o$ to a level below 10 nM. In the virtual absence of external Ca^{2+}, Ca^{2+} entry through voltage-dependent channels must cease, leaving only processes of Ca^{2+} buffering and extrusion. As expected, the averaged fluorescence signal after EGTA addition (traces labeled 'EGTA') declined much more rapidly than the signal that included the contribution of continuing Ca^{2+} channel influx ('no EGTA'). This indicated that Ca^{2+} influx into the synaptosomes continued over the entire course of the prolonged depolarization, as previously reported (McMahon and Nicholls, 1991).

As shown in Fig.1-4C, pretreating the synaptosomes with BoNtC1 had no effect on the Ca^{2+} signal recorded following EGTA addition. Thus, cleavage of syntaxin did not affect the Ca^{2+} buffering and extrusion that followed the initial Ca^{2+} rise. An incremental effect of BoNtC1 pretreatment was only seen when depolarization-induced Ca^{2+} entry was allowed to continue.

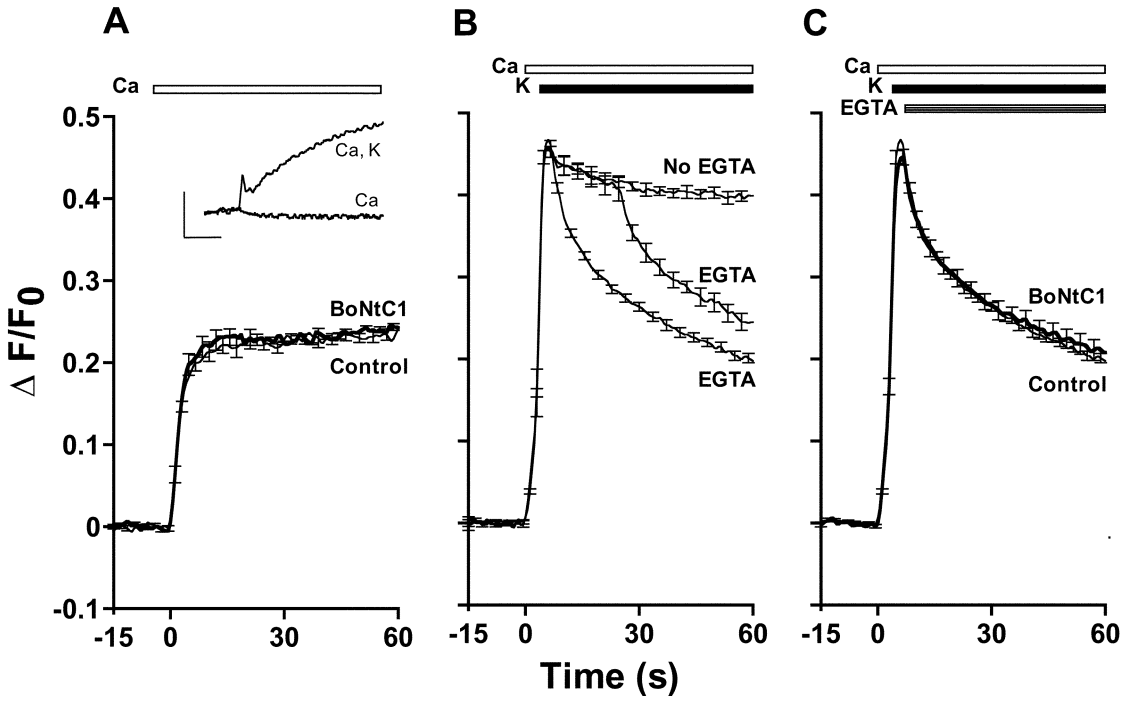

Figure 1-4 Analysis of Ca^{2+} Channel-Independent Ca^{2+} Fluxes

(A) Effect of BoNtC1 on response to elevating external Ca^{2+}. Ca^{2+} was added to fura-2-loaded synaptosomes at t = 0 s without elevation of external K^+. Traces are averages of ≥5 runs from 2 synaptosome preparations. (Inset) Ca^{2+}-dependent glutamate release caused by raising Ca^{2+} only ("Ca") compared with release caused by raising Ca^{2+} at t = 0 followed by elevated K^+ at t = 3.5 s ("Ca, K"). Both release signals were corrected for Ca^{2+}-independent release and for enzyme lag (Methods). Vertical scale bar, 10 nMol glutamate / mg synaptosomal protein; horizontal scale bar, 100 s. (B) Distinction between Ca^{2+} influx and Ca^{2+} buffering and extrusion. Control fura-2-loaded synaptosomes. Ca^{2+} and K^+ were elevated at t = 0 and t = 3.5 s respectively. In the lower traces ("EGTA"), EGTA was elevated at either t = 7 s (lowest trace) or 25 s (middle trace). EGTA elevation lowered external free Ca^{2+} to less than 10 nM. EGTA was not elevated in the upper trace ("No EGTA"). Means ± SEM of ≥4 runs from ≥2 synaptosome preparations. (C) Effect of BoNtC1 on Ca^{2+} buffering and extrusion. Ca^{2+} and K^+ were elevated at t = 0 and t = 3.5 s respectively and EGTA was elevated at t = 7 s, reducing external free Ca^{2+} to less than 10 nM. Means ± SEM of ≥8 runs from ≥4 synaptosome preparations. 10 μM nimodipine was present in all experiments shown in this Figure. No correction for depolarization-independent Ca^{2+} signal in any of the panels (in contrast to other Figures).

1.4.3 The BoNtC1-Induced Increase in Ca^{2+} Influx Does not Result from Block of Glutamate Release

We considered the idea that BoNtC1 treatment might increase Ca^{2+} influx by blocking neurotransmitter release, thereby relieving Ca^{2+} channels from feedback inhibition via presynaptic receptors. This possibility gains plausibility with knowledge that glutamatergic nerve terminals greatly outnumber presynaptic terminals containing other neurotransmitters, (e.g. Verhage et al., 1991; McMahon et al., 1992; Verhage et al., 1995) and activation of metabotropic glutamate receptors (mGluRs) is known to down-regulate non-L-type Ca^{2+} channels. Accordingly, we tested whether the BoNtC1 effect persisted when Ca^{2+} influx was evoked in the presence of a group III mGluR agonist (30 μM L-AP4) or a general mGluR antagonist (0.75 or 1.5 mM +MCPG) . Neither agent caused a significant change in the magnitude or time course of the BoNtC1 effect (data not shown). If anything, +MCPG slightly decreased Ca^{2+} influx, in the opposite direction from what would be expected from feedback via mGluR receptors. Additional evidence against secondary effects of blocking neurotransmitter release was derived from experiments with other clostridial neurotoxins (see below).

1.4.4 Modification of Voltage-Gated Ca^{2+} Influx Is Specific to BoNtC1

It was of interest to compare the effect of BoNtC1 with that of other clostridial neurotoxins. Figure 1-5A shows pooled results for the effect of BoNtC1, obtained from 5 independent synaptosome preparations (13 BoNtC1 trials and 10 control trials). The averaged data show once again that the toxin pretreatment did not alter the magnitude of the Ca^{2+} increase over the first few seconds but produced a highly significant increase in late Ca^{2+} influx ($p<0.001$).

A potential complication in experiments with BoNtC1 is the possibility of contamination of the toxin preparation with a related molecule, BoNtC3, an ADP ribosyltransferase, that might be isolated from the same organism in trace amounts. This cannot be completely excluded even though according to the manufacturer, Wako Chemicals, the commercially available preparation of BoNtC1 toxin appeared as a single band upon

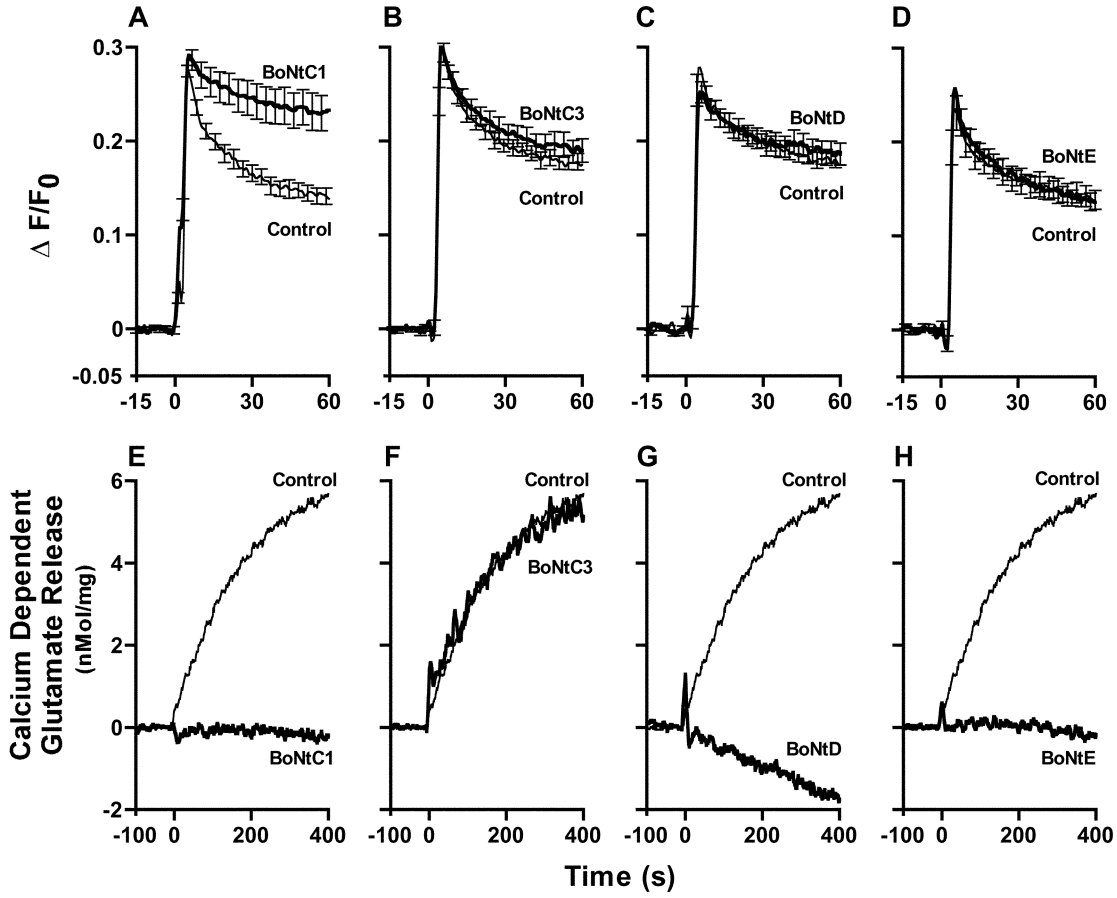

Figure 1-5. Differential Effect of Various Clostridial Neurotoxins on Ca^{2+} Influx

Synaptosomes were treated with various clostridial toxins and tested for altered Ca^{2+} influx. Ca^{2+} and K^+ were elevated at t = 0 and t = 3.5 s respectively. 10 μM nimodipine was present throughout all experiments shown in this figure. (A) Effect of pretreatment with BoNtC1 (66 nM), mean ± SEM of ≥10 runs from 5 synaptosome preparations, including the data shown in Figure 1-3A. (B) Effect of pretreatment with BoNtC3 (1.67 μg/mL), mean ± SEM of 6 runs from 2 synaptosome preparations; (C) Effect of pretreatment with BoNtD (110 nM), mean ± SEM of ≥6 runs from 2 synaptosome preparations; (D) Effect of pretreatment with BoNtE (110 nM), mean ± SEM of 6 runs from 2 synaptosome preparations. (E-H) Ca^{2+}-dependent glutamate release after treatment with the same toxins as in (A-D), respectively. Release was corrected for Ca^{2+}-independent release and for the enzyme lag (Methods) and was expressed as nmol glutamate per mg of synaptosomal protein. Note difference in time scale from (A-D). Negative Ca^{2+}-dependent release in (G) results from BoNtD block of Ca^{2+}-independent release as well as Ca^{2+}-dependent release, a consistent finding.

disc-PAGE. Accordingly, we tested BoNtC3 at a dose that would allow for up to 5% contamination of the BoNtC1 preparation. Even at this relatively high concentration, BoNtC3 produced no significant effect on the intracellular Ca^{2+} transient (Figure 1-5B) ($p>0.3$), and no detectable effect on Ca^{2+}-dependent glutamate release (Figure 1-5F).

1.4.5 Cleavage of VAMP or SNAP-25 Does not Affect Calcium Influx

Syntaxin is but one of several SNARE proteins known to be involved in vesicle docking and fusion in presynaptic terminals. Other SNARE proteins include SNAP-25 and VAMP. Since SNAP-25 and VAMP have been found to engage in direct binding interactions with voltage-gated Ca^{2+} channels (el Far et al., 1995; Rettig et al., 1996; Sheng et al., 1996; Kim and Catterall, 1997), it was of considerable interest to test for possible modulatory effects on Ca^{2+} channel activity. Accordingly, we asked whether Ca^{2+} influx might be modified by cleaving VAMP with botulinum toxin D or SNAP-25 with botulinum toxin E (Niemann et al., 1994). (Unfortunately, no neurotoxin is available to cleave synaptotagmin.) Both of these toxins cleaved their expected targets as shown by their complete block of Ca^{2+}-dependent glutamate release (Figure 1-5G, H). However, the depolarization-induced Ca^{2+} transient was not affected by pretreatment of the synaptosomes with BoNtD (Figure 1-5C, $p>0.5$), nor by BoNtE pretreatment (Figure 1-5D, $p>0.7$). Western analysis of toxin-treated synaptosomes showed only partial cleavage of syntaxin, SNAP-25, and VAMP (data not shown), in accord with previous reports (Schiavo et al., 1992; Blasi et al., 1993a; Blasi et al., 1993b; Schiavo et al., 1995; Williamson et al., 1996; Capogna et al., 1997; Raciborska et al., 1998). Various possibilities that might account for the partial cleavage are as follows. The SNARE proteins might be present in intact synaptosomes, but sequestered in a non-cycling pool that is uncleavable by BoNts. Alternatively, they may be trapped as heterotrimeric complexes resistant to BoNt cleavage (Hayashi et al., 1994) if they were in metabolically inactive synaptosomes where NSF would be inoperative. Finally, SNARE proteins may be present in lysed

synaptosomes and unsealed membrane fragments (e.g. Fried and Blaustein, 1978), which are unable to produce or retain the toxin light chain. The latter possibilities would not affect our conclusions since they involve structures that would not participate in either transmitter release or Ca^{2+} influx. Since we could not be certain about the basis for the incomplete cleavage we proceeded to examine the effects of more aggressive toxin treatment. Doses of BoNtD or BoNtE three-fold higher than those used to produce an effect with BoNtC1, applied for periods lasting over twice as long, still failed to produce an effect on Ca^{2+} influx (data not shown). The lack of effect of BoNtE is particularly notable, because it excludes the possibility that BoNtC1 might have acted merely through cleavage of SNAP-25 rather than syntaxin (Foran et al., 1996; Williamson et al., 1996; Capogna et al., 1997). The lack of effect of either BoNtD or BoNtE rules out the idea that BoNtC1's action is secondary to blockade of exocytosis (see above); if this were the case, each of the clostridial toxins that block neurotransmitter release would be expected to have similar effects, contrary to what was observed.

1.4.6 Identification of Ca^{2+} Channel Types Susceptible to Modulation by Syntaxin

The results presented so far (Figures 1-3→1-5) apply to all non L-type channels pooled together. To discriminate further among the individual channel types, further pharmacological dissection of Ca^{2+} influx was carried out using channel-specific toxins against a constant background of L-type blockade (Figure 1-6B-D). Figure 1-6B shows Ca^{2+} entry signals evoked in the presence of AgaIVB (1 μM), a potent blocker of P/Q-type channels which largely spares N-type channels (Adams et al., 1993; Teramoto et al., 1993 M. Cataldi personal communication) (see also sections 1.3.2.3.2 and 1.3.2.5). Under these conditions, the ability of BoNtC1 to modify Ca^{2+} influx remained significant ($p<0.05$), and was retained to at least the same degree (61% increase) as that found when the P/Q-type channels were full contributors to the Ca^{2+} signal (56% increase, Figure 1-

6A) (changes measured over the last 10 s of the 60 s exposure to high K^+). Likewise, the BoNtC1 effect persisted ($p<0.001$) when N-type channels were blocked with 0.5 μM GVIA (Figure 1-6C), although it was smaller than when N-type channels were not blocked (38% vs. 56%). Reports of significant R-type current in some rat central nerve terminals (Randall and Tsien, 1995; Meder et al., 1997; Newcomb et al., 1998; Wu et al.,

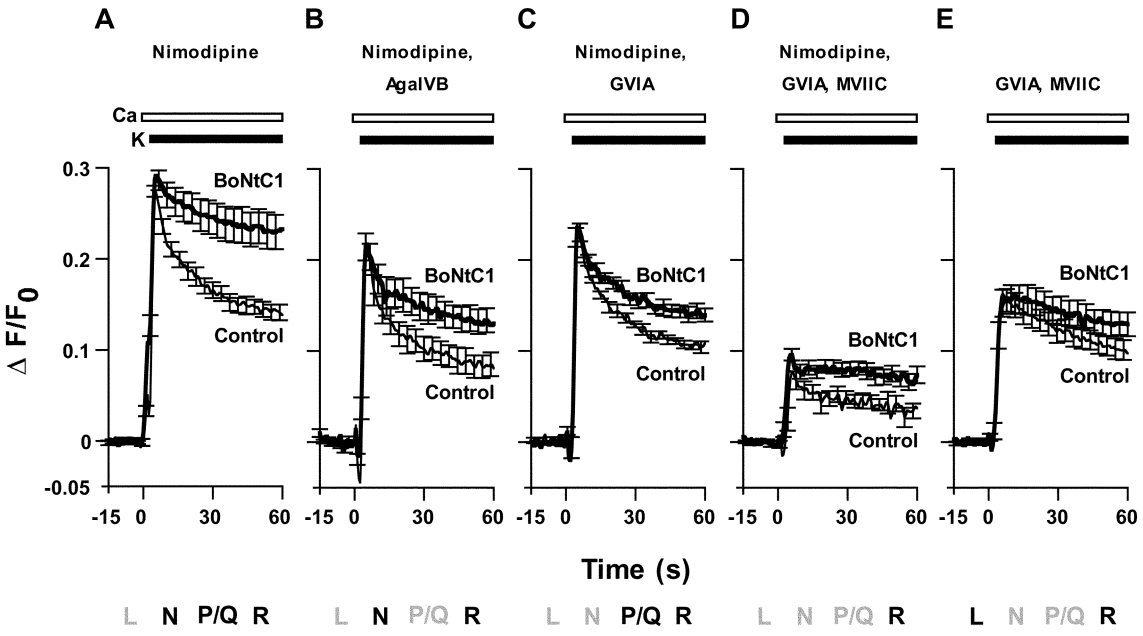

Figure 1-6. Effect of Syntaxin Cleavage on Various Ca^{2+} Channels

The effect of BoNtC1 treatment in the presence of various Ca^{2+} channel blockers. (A) 10 μM nimodipine. Mean ± SEM of ≥10 runs from 5 synaptosome preparations. (B) 10 μM nimodipine, 1 μM AgaIVB. Mean ± SEM of 6 runs from 2 synaptosome preparations. (C) 10 μM nimodipine, 0.5 μM GVIA. Mean ± SEM of 6 runs from 2 synaptosome preparations. (D) 10 μM nimodipine, 0.5 μM GVIA, and 1 μM MVIIC. Mean ± SEM of 6 runs from 2 synaptosome preparations. (E) 0.5 μM GVIA, and 1 μM MVIIC. Mean ± SEM of ≥9 runs from 3 synaptosome preparations. Due to optical effects of nimodipine, the magnitude of the signals in this panel are not directly comparable with those in other panels of this or other Figures. Note that panel A repeats the data shown in Figure 1-5A, for the sake of comparison to B-D.

1998) prompted us to test for effects of cleaving syntaxin on this type of Ca^{2+} influx. Figure 1-6D shows Ca^{2+} signals obtained with both N- and P/Q-type channels blocked under the combined influence of 0.5 μM GVIA + 1 μM ω-conotoxin MVIIC (once again under conditions of L-type channel blockade). The Ca^{2+} signal supported by the remaining R-type channels reached a peak only about one third as large as that produced by all non-L type channels together. Nevertheless, the BoNtC1 effect on this influx was rather

large (112% increase, $p<0.01$). Taken together, these results suggest that R-type channels, like other non-L-type channels, are capable of responding to syntaxin cleavage.

In addition to testing the effect of BoNtC1 on non L-type channels, we specifically looked for an effect of the toxin under conditions where L-type channels made a prominent contribution to the synaptosomal Ca^{2+} entry. Synaptosomes were exposed to GVIA (0.5 μM) and MVIIC (1 μM), which should block N-type and N-, P-, and Q-type channels respectively, sparing L- and R-type channels (Fig. 1-6D). The remaining Ca^{2+} influx stimulated by KCl depolarization was minimally affected by BoNtC1, resulting in a 30% increase which was not significantly different ($p>0.1$), due in part to larger variability in these experiments. It is possible that any impact of BoNtC1 under these conditions arose from the responsiveness of a minority fraction of unblocked R-type channels, although we cannot exclude an additional small effect of syntaxin on L-type channels themselves. The overall conclusion is that syntaxin cleavage affects N-type and R-type channels most prominently, exerts a milder effect on P/Q-type channels, and gives little or no effect on L-type channels.

1.4.7 BoNtC1 Reveals Syntaxin Effect on Ca^{2+} Influx Stimulated by 4-Aminopyridine

A critical series of experiments tested whether the influence of syntaxin extended to Ca^{2+} influx stimulated by methods other than direct K^+-depolarization. We used the K^+ channel inhibitor 4-aminopyridine (4-AP), which blocks certain voltage-gated K^+ channels and thereby causes spontaneous, TTX-sensitive repetitive firing in synaptosomes (Tibbs et al., 1989; Tibbs et al., 1996). Fig. 7 shows the Ca^{2+} signal evoked by stimulating synaptosomes with 2 mM 4-AP and the effect of BoNtC1. 4-AP produced a sustained rise in synaptosomal free Ca^{2+} concentration somewhat smaller than that evoked by high K^+ (Tibbs et al., 1989). Pretreatment with BoNtC1 caused a significant increase in the steady level of Ca^{2+} ($p<0.002$), very much like that found with high K^+ stimulation. On a

percentage basis, the BoNtC1-mediated increase was at least as large with 4-AP (63%) as it was with K^+ stimulation (56%). If anything, the incremental difference in the Ca^{2+} signal

in treated and untreated synaptosomes developed more rapidly with 4-AP stimulation, reaching its maximum value after ~15 s, whereas this difference continued to develop for at least 30 s with K^+ stimulation. The magnitude of the difference and the speed of its development may be accounted for by the kinetic properties of the syntaxin inhibition as studied with cloned N-type Ca^{2+} channels ($Ca_V2.2$) in *Xenopus* oocytes (Degtiar et al., 1999). In comparison to maintained depolarizations, repeated brief depolarizations (akin to the activity thought to be induced by 4-AP) are not only more efficient in inducing inactivation of Ca^{2+} channels (Patil et al., 1998) but also more effective in allowing syntaxin to exert its inactivation-promoting effect (see Discussion). An additional possibility is that 4-AP induced Ca^{2+} entry through a somewhat different mixture of Ca^{2+} channel types than that stimulated by K^+ elevation.

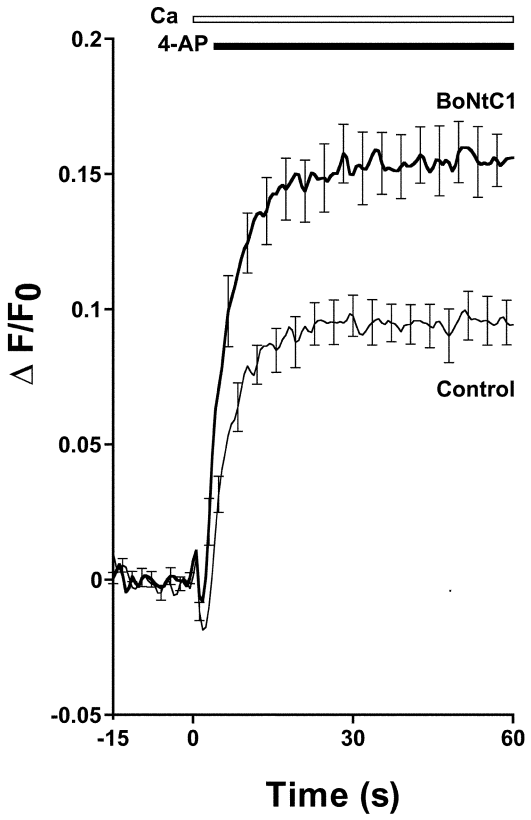

Figure 1-7. BoNtC1 Effect on Ca^{2+} Influx Induced by Repetitive Firing

At t = 0 external free Ca^{2+} was raised to 1 mM. At t = 3.5 s, 2 mM 4-aminopyridine was added as a depolarizing agent in lieu of 60 mM K^+. Mean ± SEM of 6 runs from 2 synaptosome preparations. 10 μM nimodipine present throughout.

1.4.8 Time Course of Syntaxin's Action

The absence of an immediate effect is noteworthy in light of our previous findings in *Xenopus* oocytes (Bezprozvanny et al., 1995; Degtiar et al., 2000). These results showed that free syntaxin decreased the availability of N- and P/Q-type Ca^{2+} channels over a wide range of membrane potentials, probably spanning the resting potential of the synaptosomes. Thus, if syntaxin were free to interact with Ca^{2+} channels, we would have expected a decrease in Ca^{2+} influx immediately after K^+-depolarization, very like that seen in oocyte recordings of Ca^{2+} channel current. In contrast, there is a striking absence of any immediate effect with either high K^+ or 4AP stimulation. We considered three possible explanations of the delayed effect. In one scenario, cleavage of syntaxin by previously internalized BoNtC1 light chain would await activation of the release machinery. This interpretation seems highly unlikely in light of our finding that glutamate release is completely blocked by the standard toxin pretreatment, with no hint of a brief burst of release followed by no release as would be expected for delayed cleavage by toxin. In a second scenario, synaptosomal Ca^{2+} channels would undergo voltage-dependent inactiva-

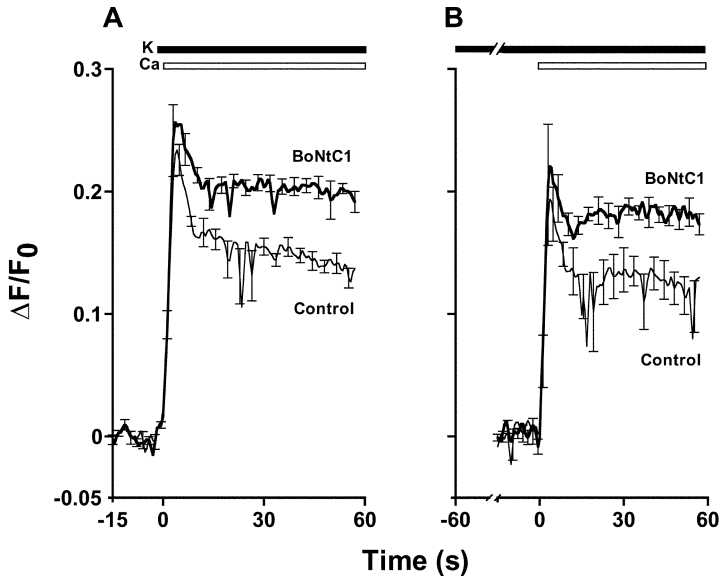

Figure 1-8. BoNtC1 Effect on Ca^{2+} Influx Following a Predepolarization

Synaptosomes were predepolarized by elevating K^+ before elevating Ca^{2+} in the presence of 10 μM Nimodipine. (A) K^+ was elevated at t = -3.5 s and Ca^{2+} was elevated at t = 0 s. Mean ± SEM of 6 runs from 2 synaptosome preparations. (B) K^+ was elevated at t = -60 s and Ca^{2+} was elevated at t = 0 s. Average ± SEM of ≥4 runs from the same 2 synaptosome preparations as in (A). Note *Axis Break* between t = -60 s and t = -15 s.

tion at relatively depolarized potentials, so that syntaxin stabilization of inactivation would only be asserted after external K^+ had been elevated. Finally, it seemed possible that the syntaxin in synaptic terminals would not be free at first to modulate the Ca^{2+} channels, but would only become capable of channel modulation as a consequence of the progressive vesicular turnover that follows depolarization-induced Ca^{2+} entry (Bezprozvanny et al., 2000). To distinguish between these latter two possibilities, we applied a strong predepolarization in the absence of Ca^{2+}, to increase the degree of channel inactivation before assaying Ca^{2+} entry. Synaptosomes were exposed to 60 mM K^+, low Ca^{2+} solution for either 3.5 s (Figure 1-8A) or 60 s (Figure 1-8B) before admission of Ca^{2+}. This procedure would maximize the chances of detecting an immediate effect of syntaxin if the first scenario were applicable. As expected, predepolarization significantly attenuated the initial rise in Ca^{2+}. There was a 14% drop in peak Ca^{2+} level with the 60 s predepolarization relative to that evoked following the 3.5 s predepolarization (and probably an even greater decrease relative to Ca^{2+} transients evoked without any predepolarization, e.g. Figure 1-5A). However, following either 3.5 or 60 s predepolarizations, there was still no significant difference between the initial Ca^{2+} signals with and without BoNtC1 pretreatment. The modulatory effect of syntaxin developed with a delay, just as in the experiments where no predepolarization was imposed. This experiment excluded the second scenario, but left open the possibility that syntaxin's modulatory action was not asserted until some event downstream of Ca^{2+} entry had taken place, vesicular turnover being a likely possibility.

1.5 Discussion

Our experiments have provided the first evidence that that a SNARE protein can influence Ca^{2+} influx in vertebrate nerve terminals. Treatment of synaptosomes with BoNtC1 to cleave syntaxin caused an increase in Ca^{2+} entry due to a lessened shutting off of Ca^{2+} channels, not an enhancement of Ca^{2+} extrusion. The increase in Ca^{2+} influx

required syntaxin cleavage: neither BoNtD cleavage of VAMP nor BoNtE cleavage of SNAP-25 had any detectable effect, although all the toxins were confirmed as active by monitoring the cleavage of SNARE protein targets and the blockade of glutamate release. Because synaptosomes contain N-, P/Q-, R-, and L-type channels that are distinguished pharmacologically, we were able to estimate the extent to which each of these channel types was modulated. This effect appeared to be greatest on the activity of N- and R-type channels, smaller on P/Q-type channels, and was not detectable in the case of L-type channels.

1.5.1 Requirement for Calcium-Free Incubation

The effect of BoNtC1 was only seen if the synaptosomes were preincubated in nominally zero Ca^{2+} solution, presumably because this preserved a low initial level of $[Ca^{2+}]_i$ (see Methods). We considered the possibility that the initial $[Ca^{2+}]_i$ might influence the activity of protein kinases that can in principle interfere with the interaction between syntaxin and the α_1 subunit of the Ca^{2+} channel (Yokoyama et al., 1997). However, when we tested effects of 10 μM KN62, an inhibitor of CaMKII, or 2 μM staurosporine, a relatively broad spectrum kinase inhibitor that blocks the action of PKC, we were unable to rescue the BoNtC1 effect in the face of preincubation in Ca^{2+}-containing external solution. Thus, it remains unclear how the basal Ca^{2+} level regulates syntaxin's effects on Ca^{2+} channels. The explanation may be important in understanding the physiological significance of the syntaxin modulation.

1.5.2 Comparison with Previous Results in Other Systems

The influence of syntaxin on Ca^{2+} influx in nerve terminals was similar to that found for Ca^{2+} channel currents in syntaxin-expressing oocytes. The specificity of syntaxin for certain types of high voltage-activated channels and not others is in good agreement with that found with cloned Ca^{2+} channel subunits in oocytes (Bezprozvanny et al., 1995) but see (Wiser et al., 1996; Wiser et al., 1999). If anything, P/Q-type channels seemed less

responsive to BoTxC1 in synaptosomes than expected from the earlier oocyte data, but this may reflect splice variations in $Ca_V2.1$ (which in some cases prevent binding to and modulation by syntaxin (Zhong et al., 1999)) or differences in the composition of ancillary subunits. Syntaxin cleavage increased synaptosomal Ca^{2+} influx during repetitive firing stimulated by 4-AP at least as much as that during steady depolarizations evoked by high K^+, consistent with findings with trains of brief depolarizations in oocytes (Degtiar et al., 2000). However, there was one important respect in which the influence of syntaxin in nerve terminals differed significantly from that found in the oocyte expression system. In the synaptosomes, cleavage of syntaxin by BoNtC1 pretreatment made little difference during the first few seconds of stimulation, but only caused significantly increased Ca^{2+} entry upon prolonged stimulation (Figure 1-3). Thus, the syntaxin inhibition was not tonically enabled, but developed gradually with time. In contrast, Ca^{2+} channel currents in oocytes were diminished from the very beginning of a test depolarization due to decreased availability of Ca^{2+} channels (Bezprozvanny et al., 2000; Degtiar et al., 2000). For both N- and P/Q-type channels, the decrease in availability was found over a wide range of steady holding potentials, spanning the –55 to –60 mV resting potential expected for synaptosomes (Blaustein and Goldring, 1975). Thus, if the synaptosomes had behaved like the oocytes, one would have expected BoNtC1 to induce a significant difference in Ca^{2+} influx immediately following the elevation of external K^+.

The lack of a significant BoNtC1 effect on early Ca^{2+} entry in the synaptosomes is consistent with previous findings in other neuronal preparations where investigators have looked for an influence of syntaxin on Ca^{2+} channel currents. These systems include the squid giant synapse (Marsal et al., 1997; O'Connor et al., 1997; Sugimori et al., 1998), the presynaptic terminals of calyx synapses in chick ciliary ganglia (Stanley and Mirotznik, 1997), presynaptic terminals of *Xenopus* motoneurons (Rettig et al., 1997), and cell bodies of rat superior cervical ganglion neurons that have formed synaptic connec-

tions with each other (Mochida et al., 1995; Mochida et al., 1996). In each case, application of BoNtC1 to cleave syntaxin, or antibodies to inactivate it, failed to alter peak inward Ca^{2+} channel current, measured within milliseconds after application of a depolarizing voltage clamp step, in agreement with data presented here. Although voltage control and time resolution were much less precise in the synaptosome experiments, this did not pose a problem since the effect of syntaxin developed slowly and was not critically dependent on the test potential (Degtiar et al., 2000). Synaptosomes are well-suited for measurements of Ca^{2+} evoked by persistent or repetitive depolarizations, conditions that uncovered the syntaxin modulation most clearly. It would be interesting to see if stimulation with persistent or repetitive depolarizations might reveal syntaxin responsiveness of Ca^{2+} channels in presynaptic terminals amenable to electrophysiological analysis (e.g. Forsythe et al., 1998, see also Chapter 2).

1.5.3 Syntaxin Inhibition Depends Jointly on Channel Inactivation and Vesicular Turnover

Our working hypothesis is as follows. The time course of the Ca^{2+} signal in the BoNtC1-treated synaptosomes represents the simpler case where influx is limited only by intrinsic channel inactivation. In comparison to this the untreated synaptosomes (containing intact syntaxin) show an increasing inhibition of influx. The time course of this effect is primarily mediated by the need for the channels to inactivate before they can be locked in the inactivated state by syntaxin (Degtiar et al., 2000). However, as seen in Figure 1-8, even when channel inactivation is allowed to proceed before exposure to Ca^{2+}, there is a delay before the presence of syntaxin causes a diminished influx. We interpret this to be due to the need for Ca^{2+}-triggered turnover of SNARE complexes to occur before syntaxin can inhibit Ca^{2+} channels.

The progressive development of syntaxin inhibition in synaptosomes suggested that syntaxin trapping of Ca^{2+} channels must lag behind the depolarizing stimulus. While the

delay may be attributed in part to the kinetics of slow inactivation (Degtiar et al., 2000), our evidence suggests that it also depends on an event downstream of Ca^{2+} entry. The development of syntaxin-mediated channel inhibition was delayed until after admission of external Ca^{2+}, even in the wake of a preceding depolarization that had already promoted channel inactivation (Figure 1-8). We can be reasonably sure that internal Ca^{2+} *per se* is not required for syntaxin's modulatory action, since a striking modulation of Ba^{2+} currents was found in oocytes even after they had been injected with high concentrations of internal divalent cation buffer (Degtiar et al., 2000). The most likely possibility that remains is that the limiting factor is the availability of syntaxin itself. Since presynaptic terminals display an abundance of synaptic vesicles near their Ca^{2+} channels, syntaxin's availability may be controlled by some aspect of vesicle fusion or turnover. This idea gains support from the positioning of amino acids critical for syntaxin's effect, alanine240 and valine244 (Bezprozvanny et al., 2000), which appear to be buried within the core of the four-helix bundle of the SNARE complex (Sutton et al., 1998). So long as syntaxin were sequestered in the SNARE complex by interactions with SNAP-25 and VAMP, it would remain incapable of exerting its modulatory effect. If syntaxin were only made available for modulation after bouts of high activity, nerve terminals would be expected to differ from model systems where syntaxin was deliberately over-expressed (oocytes, Aplysia neurons).

In addition to providing a structural basis for the delay in the syntaxin-dependent Ca^{2+} channel inhibition, this hypothesis also supplies a rationale for our findings with BoNtD and E. Both of these toxins were found to block exocytosis, yet neither produced a significant change in the pattern of Ca^{2+} influx or inactivation (Figure 1-5C, D). The Ca^{2+} trajectory was similar to that found in the absence of toxin pretreatment, not like that seen after BoNtC1. One interpretation is that BoNtD and BoNtE prevent the fusion reaction but allow the release machinery to respond to rises in Ca^{2+} by advancing through

states in which syntaxin is available to interact with the Ca^{2+} channel (see for example Chen et al., 1999). Further structural studies of BoNtD- and BoNtE-treated SNARE complexes are needed to verify this explanation.

1.5.4 Comparison with Published Effects of Vesicular Depletion

Our working hypothesis predicts that presynaptic Ca^{2+} channel function might be significantly affected by depletion of synaptic vesicles. Indeed, such an effect has already been demonstrated in *shibire* mutants of *Drosophila,* which undergo a temperature sensitive block of endocytosis due to a defect in dynamin (Kosaka and Ikeda, 1983; Ramaswami et al., 1994). Ca^{2+} influx at the fly neuromuscular junction was completely blocked following vesicle depletion (Umbach et al., 1998), consistent with the idea that excess syntaxin had been made available to inhibit voltage-gated Ca^{2+} channels. It would be very interesting to see if similar results could be obtained with vesicular depletion in the synaptosomes. We have considered experiments utilizing α-latrotoxin or trachnilysin (Colasante et al., 1996) to deplete vesicles, but were discouraged by the fact that these toxins also render synaptosomes exceedingly leaky for Ca^{2+} (Finkelstein et al., 1976; Nicholls et al., 1982) (J. Molgó, personal communication).

1.5.5 Physiological Relevance

The steep power-law relationship between Ca^{2+} influx and neurotransmitter release (Dodge and Rahamimoff, 1967) ensures that even a modest modulation of Ca^{2+} channels could have a significant impact on synaptic transmission. In fact, the modulatory effect of syntaxin on synaptosomal Ca^{2+} influx can be substantial (up to 50%), so the consequences for synaptic transmission could be striking. What role would this modulation play in nerve terminals? Our experiments provided a starting point for assessing these possibilities. Based on the results illustrated in Figures 1-7 and 1-8, modulation of Ca^{2+} channels by syntaxin is an unlikely mechanism for short term synaptic refractoriness. On the other hand, syntaxin regulation of Ca^{2+} influx seems well-suited for control of synap-

tic strength over a span of tens of seconds or minutes, much the same time scale as that required for induction of long-term synaptic plasticity. Along these lines, the functional relevance of slow inactivation of presynaptic Ca^{2+} channels has been demonstrated at a calyx synapse in the brainstem, where conventional depolarizing pulses or trains of brief pulses caused a long-lasting inactivation of presynaptic P-type channels and substantial post-tetanic depression of transmission (Forsythe et al., 1998). The inactivation was dependent on divalent cation entry and required 1-2 min for full recovery, in accord with the modulatory effects described here. Whether syntaxin actually participates in this modulation remains to be seen. Meanwhile, we find it particularly interesting that channel gating and vesicular turnover may both be required to initiate the syntaxin stabilization of the inactivated state. The stabilization would be most powerful during and after bouts of high activity. In principle, such a mechanism might serve as a coincidence detector, to coordinate the trafficking of internal membranes and excitable membrane function.

1.6 Materials and Methods

1.6.1 Synaptosome preparation

Synaptosomes were prepared essentially as described (McMahon et al., 1992). Brains from two or three 6-8 week old Sprague-Dawley rats were homogenized in approximately 20 mL of ice cold 0.32M sucrose in a Potter-Elvehjem (Teflon-glass) tissue homogenizer driven at 400-500 RPM. This suspension was diluted to a final volume of about 20 mL per brain with more ice cold sucrose and centrifuged at 3000 g for 3 min at 4°C. Sufficient dilution of synaptosomes was important to prevent clumping. The supernatant was centrifuged at 14,600 g for 12 min at 4°C. The upper layers of the pellets formed were resuspended in approximately 2 mL ice-cold sucrose per brain used. Before use synaptosomes were washed by 1:2 dilution with Basal Buffer ("BB", in mM: NaCl 140, KCl 5, $MgCl_2$ 1, $NaHCO_3$ 5, HEPES pH 7.4 20, glucose 10, 0.2 μm filtered) and

resuspended in the medium of choice. A sample of each synaptosome preparation was washed and solubilized in 0.15% SDS for the determination of protein concentration using the BCA kit (Pierce, Rockford, IL) with BSA as a standard.

1.6.2 Features Common to All Experiments

All dye and clostridial toxin treatment was done in bulk for the day's experiments as described below. Dye loading preceded toxin treatment. After any dye loading and/or clostridial toxin treatment, synaptosomes were washed by pelleting and resuspension in the appropriate buffer. After the final treatment, synaptosomes were washed and resuspended at 2 mg/mL in BB. This suspension was aliquoted into single run amounts (2 mg for glutamate release and 1 mg for Ca^{2+} measurements) and stored on ice. Such aliquots were spun down and resuspended in 2 mL of pre-warmed experimental buffer and allowed to equilibrate to 36-37°C for 4 min in the continuously stirred, heated cuvette holder of the spectrofluorimeter immediately before each experiment. In all experiments, the cuvette contained 0.63 mM EGTA, along with any Ca^{2+} channel blockers or other drugs during the 4 min warming period. To produce the free Ca^{2+} levels indicated in the text, $CaCl_2$ was added in amounts calculated by the Maxchelator software version 6.50 using the Bers constants (Chris Patton, Stanford University, Pacific Grove, CA). Fluorescence measurements were made in a Perkin-Elmer (Norwalk, CT) LS50B spectrofluorimeter using the Perkin-Elmer FLDM software. Data were exported in ASCII format.

1.6.3 Calcium Indicator Loading

Synaptosomes to be used for Ca^{2+} measurements for a given day were suspended at 2 mg/mL in Loading Buffer ("LB", BB with 1.3 mM Ca^{2+} and 50 mg/mL BSA, 0.2 μm filtered). The synaptosomes were loaded with fura-2 AM dissolved in DMSO (or Mag-fura-2 AM in some experiments not shown) at a final concentration of 10 μM (final [DMSO] = 0.5%) for 45 min at 37°C.

1.6.4 Clostridial Toxin Treatment

Synaptosomes to be treated with clostridial toxins were suspended at 2 mg/mL in LB. Toxins were normally used at the following concentrations: BoNtC1 66 nM, BoNtD 110 nM, BoNtE 110 nM, BoNtC3 1.67 μg/mL. All lots of BoNtC1, BoNtD, and BoNtE used were tested and were found to completely block Ca^{2+}-dependent glutamate release at these concentrations. Toxin treatment was at 37°C for 45 min. In some experiments indicated in the text, BoNtD and E were used at 220 nM and treatment was for 120 min. Control synaptosomes in toxin experiments received mock treatments in parallel that differed only in that toxin was not added. In heat-treated toxin controls, toxin was diluted to twice its final concentration in BB and held at 95°C for 45 min. This was cooled and combined with synaptosomes at 4 mg/mL in LB (yielding the identical toxin and synaptosome concentrations used in the other experiments) and incubated at 37°C for 45 min.

1.6.5 Calcium Flux Measurement and Corrections

In control experiments we found that our dye-loaded synaptosomes contained dye in one or more compartments which were inaccessible even after treatment with digitonin (18 mg/mL) or ionomycin (100 μM), compared to treatment with SDS (0.1%), as well as one or more compartments which allowed voltage-independent Ca^{2+} fluxes (Figure 1-4A, and see below). This compartmentalization was very similar between fura-2 and mag-fura-2 and was not dependent on the dye concentration during loading (not shown). Our experiments indicated that the inaccessible dye was not in synaptosomal cytosol (Figure 1-4A inset, and see below). Some of this dye was Ca^{2+}-bound and some was Ca^{2+}-free since the direction of the fluorescence change upon SDS treatment following previous digitonin or ionomycin treatment was $[Ca^{2+}]_o$-dependent. The similar results with the indicators of different Ca^{2+} affinities suggested that the dye resided in at least two compartments and that each compartment had either very high or very low $[Ca^{2+}]$ relative to the indicators' affinities. Under these conditions application of the equation used by

Grynkiewicz et al. (Grynkiewicz et al., 1985) to calculate [Ca^{2+}] was inappropriate, since one of its assumptions is that all dye molecules are experiencing the same [Ca^{2+}]. Additionally, nerve terminals have very high concentrations of endogenous Ca^{2+} buffers (Fontana and Blaustein, 1993) that would skew the relationship between our parameter of interest, Ca^{2+} influx, and free [Ca^{2+}]. For these two reasons, we chose to employ relatively heavy fura-2 loading and to use the change in fluorescence normalized by the baseline fluorescence at the beginning of the experiment as a measure of accumulated Ca^{2+} influx (Neher and Augustine, 1992; Neher, 1995). Since this method only required measuring at one wavelength, it also had the benefit of allowing faster sampling rates. The principal concerns when not using ratiometric methods are dye photobleaching and changes in path length. We determined in control experiments that bleaching was not significant on the time scale of our experiments (not shown). Changes in path length are not of concern in a stirred cuvette.

We measured Ca^{2+} influx by monitoring the fluorescence at 505 nm from excitation at 382 nm, sampled once per 0.6 second. Background fluorescence from an equivalent sample of synaptosomes not loaded with dye was recorded at the beginning of each day's experiments and subtracted from all subsequent readings. When drugs which affected fluorescence readings, such as nimodipine, were used, background readings taken with the drug present were subtracted from the experimental results. Note that experiments with and without such compounds may not be compared quantitatively. Background fluorescence was typically less than 10% of the total signal. After background subtraction, each trace was normalized to the average fluorescence during its 15 s baseline. Fluorescence decreases at 382 nm, signifying increases in [Ca^{2+}], are plotted upwards in the Figures.

1.6.6 Characterization and Correction of the Depolarization-Independent Calcium Signal

We presumed that the depolarization-independent signal that resulted from the addition of Ca^{2+} alone seen in Figure 1-4A was Ca^{2+} equilibrating into some compartment that contained fura-2 but had its Ca^{2+} depleted during the 4 min incubation in EGTA. If this compartment was separate from the synaptosomal cytosolic compartment we wanted to subtract the change of fluorescence due to Ca^{2+} entering this compartment so as to reveal the true size of any change in the signal that resulted from influx through voltage-gated Ca^{2+} channels into synaptosomes. We therefore investigated the nature of this compartment.

In principle, a depolarization-independent signal might result from the binding of added Ca^{2+} to fura-2 which had leaked out of the synaptosomes or other structures into the incubation medium. This was not the case since 1) the signal was only about two-thirds saturated by the addition of 10 μM Ca^{2+} (which is ~50 times fura-2's K_d for Ca^{2+}) and 2) none of the signal returned quickly to baseline after the addition of sufficient EGTA to lower the free [Ca^{2+}] to <10 nM (unlike free fura-2, which released its bound Ca^{2+} within the few seconds mixing time of our equipment, data not shown). Therefore this fura-2 was trapped in some compartment that exchanges Ca^{2+} with the external medium with some resistance.

Because the entry of Ca^{2+} into the compartment containing this fura-2 was not depolarization dependent, we presumed that it does not represent flux through VGCCs into synaptosomes. To confirm this, we performed several control experiments with known blockers of VGCCs. The depolarization-independent Ca^{2+} signal was not significantly changed ($p>0.38$) when external Ca^{2+} was added in the combined presence of blockers of L-type (10 μM nimodipine), N-type (1 μM GVIA), and P/Q-type (1 μM ω-Agatoxin IVA

or 1 μM MVIIC) Ca^{2+} channels (not shown). This ruled out the possibility of a flux through VGCCs that were somehow open even in resting synaptosomes.

We next considered the possibility that the depolarization-independent Ca^{2+} signal might arise from Na^{+}/Ca^{2+} antiport. This was not the case since exposure to 50 μM Bepridil, an inhibitor of the Na^{+}/Ca^{2+} antiporter (Kleyman and Cragoe, 1988), did not affect the Ca^{2+} signal that resulted from the Ca^{2+} addition (not shown). We also tested the idea that the Ca^{2+} signal might arise from flux into or out of mitochondria or other Ca^{2+} stores: when the protocol was performed after preincubation (4 min) and in the continued presence of 1 μM thapsigargin (an inhibitor of a Ca^{2+} store Ca^{2+}-ATPase) or 3 μM FCCP (a protonophore that causes discharge of mitochondrial Ca^{2+} stores) the signal was unchanged compared to that in the absence of drug (not shown). (The experiments using FCCP were performed by exciting fluorescence at 340 nm instead of 382 nm as FCCP has a strong absorbance peak at the latter wavelength.) Finally, if the depolarization-independent signal resulted from Ca^{2+} binding to fura-2 in the synaptosomal cytosol, given the magnitude of the signal we would expect that such Ca^{2+} should have caused some neurotransmitter release. When we measured glutamate release due to Ca^{2+} addition without depolarization, no increase above the small background release rate was seen (Figure 1-4A inset).

Since the depolarization-independent signal resulted from Ca^{2+} binding to fura-2 in a pool that was separate from the one in which we were interested, we have subtracted the depolarization-independent signal from all traces shown except those in Figure 1-4. In order not to introduce noise from the subtraction, we subtracted smooth curves that were fit to the average depolarization-independent signals from each day's experiments. The curves had no theoretical significance and consisted of a flat baseline which changed to the sum of two exponentials plus a sloping line at the time of Ca^{2+} addition. Curves were fit by minimizing least square differences with Microsoft Excel 7.0a. Such a subtraction

in the fluorescence domain is valid when comparing fluorescence changes if and only if the subtracted fluorescence signal arises outside the dye pool of interest. Depolarization-independent signals were collected for each experimental condition, and were not found to be significantly different for any experimental condition tested. Approximately equal numbers of depolarization-independent and depolarization-dependent signals were measured each day in each condition.

1.6.7 Calcium-Free Incubation Required to See Syntaxin Effect

In our initial efforts, we failed to detect an effect of botulinum toxin C1 on Ca^{2+} influx in synaptosomes, despite complete inhibition of Ca^{2+}-dependent release (Bergsman and Tsien, 1996). We discovered that an effect of BoNtC1 was revealed if the resting $[Ca^{2+}]$ in the synaptosomes were lowered with a preincubation in a solution with a free Ca^{2+} concentration <10 nM. We confirmed that preincubation in Ca^{2+}-containing medium eliminated the syntaxin effect by varying the interval between Ca^{2+} and KCl addition between 3.5 s (the shortest we were able to perform) and 25 s. When Ca^{2+} was applied for 25 s before the stimulus, BoNtC1-treated synaptosomes displayed a Ca^{2+} rise that was not significantly different than that in control synaptosomes ($p>.25$).

1.6.8 Glutamate Release Measurement and Corrections

Glutamate release was monitored essentially as described (Nicholls et al., 1987). Released glutamate was detected as an increase in the fluorescence at 460 nm, with excitation at 340 nm, caused by the production of NADPH from $NADP^+$, coupled to the oxidation of the released glutamate to 2-oxoglutarate by glutamate dehydrogenase (GDH). Two mg of synaptosomes were suspended in 2 mL BB made up to 1 mM $NADP^+$. 100 units of GDH were added immediately before the start of data collection. A reading of the background fluorescence of the synaptosomes and any $NADP^+$/NADPH was taken at the start of each run and subtracted from subsequent measurements.

The data from glutamate release experiments were corrected for the lag of the enzyme in NADPH production by a program written for this purpose. The kinetics of the response of the system to a pulse of glutamate added at the end of each run were used to back-calculate the amount of unconverted glutamate for a given rate of NADPH production. This value was added to the raw NADPH data and the result was converted from fluorescence to amount of glutamate based on the amplitude of the response to the glutamate standard. Although the data were collected and displayed every 0.6 s, the correction algorithm filters the data to approximately 8 s resolution.

1.6.9 Statistics

Statistical differences were assayed on the average of the last 10 s of each trace using a two-tailed t-test assuming unequal variances. Calculations were performed with Microsoft Excel 7.0a using the data analysis add-in.

1.6.10 Materials

Clostridial toxins were from Wako USA (Richmond, VA). The VGCC blockers GVIA, AgaIVA and MVIIC were from Peptide Institute, Japan. AgaIVB was a generous gift from Michael Adams (University of California, Riverside). L-AP4 was from Tocris (Ballwin, MO). Nimodipine, (+)MCPG, and thapsigargin were from RBI (Natick, MA). Glutamate dehydrogenase, staurosporine, ionomycin, and $NADP^+$ were from Calbiochem (La Jolla, CA). Fura-2 AM and Magfura-2 AM were from Molecular Probes (Eugene, OR). Cuvettes were UV-grade acrylic and were from Denville Scientific (Metuchen, NJ). Western analysis was done according to standard protocols and detected with the ECL kit (Amersham, Buckinghamshire, England). Other reagents were from Fluka, Aldrich, or Sigma and were of at least ACS grade where applicable.

2 Extracellular Ca^{2+} Modulates a Novel Nonspecific Cation Channel

2.1 Attribution

This chapter describes work in progress. Stephen M. Smith and I contributed equally to the experiments which were performed in the laboratories of Dr. Richard Scheller and Dr. Richard Tsien. I did most of the writing, with feedback by Dr. Smith. Dr. Tsien also provided advice on the form of the figures. I prepared fixed synaptosomes on which Nafisa Ghori performed the electron microscopy.

2.2 Introduction

Many targets for Ca^{2+} as a second (intracellular) messenger are known, however Ca^{2+} is less frequently considered as an extracellular messenger. It is well established that extracellular $[Ca^{2+}]$ affects such neuronal functions as excitability via surface charge screening (Frankenhaeuser and Hodgkin, 1957) and synaptic transmission due to Ca^{2+} entering the nerve terminal during the action potential to trigger exocytosis (Katz and Miledi, 1965; Douglas, 1968). However, studies of these roles have generally considered $[Ca^{2+}]_o$ to be relatively static. Models of the synaptic cleft predict a more complicated scenario in which $[Ca^{2+}]_o$ decreases greatly during the course of an action potential (Smith, 1992; Vassilev et al., 1997; Egelman and Montague, 1998; Egelman and Montague, 1999). Recordings in the mammalian brain and single calyciform synapses in bird and rat have demonstrated falls of between 0.6 and 1.5 mM in $[Ca^{2+}]_o$ (Nicholson et al., 1977; Nicholson et al., 1978; Borst and Sakmann, 1999; Stanley, 2000) which would decrease Ca^{2+} entry into the nerve terminal and reduce release probability at that synapse.

The nerve terminal continues to be of special interest to neurobiologists as it is the site at which the electrical impulse of the action potential is transduced to a chemical

message. It is this chemical message that underlies cell-cell communication in the nervous system. One line of study has been to make direct measurements from nerve terminals. However because of the small size and inaccessibility of cortical nerve terminals, most attention has been focused on unusually large nerve terminals such as the squid giant synapse, the goldfish retinal bipolar cell, the chick ciliary ganglion, and the mammalian calyx of Held. In an attempt to study mammalian cortical nerve terminals another approach has been adopted—fusing together nerve terminals. While allowing the biophysical study of some ion channels, this preparation destroys the release machinery and other intracellular signaling pathways.

Using patch clamp techniques we have for the first time recorded from normal-sized mammalian central nerve terminals and shown that under certain conditions a major component of the membrane current is supported by a novel non-specific cation (NSC) channel which is activated by decreases in $[Ca^{2+}]_o$. The channel is activated by membrane depolarization and modulated by a separate receptor that is sensitive to Ca^{2+}, Mg^{2+}, Gd^{3+} and spermidine. These agents are also known to act at the Ca^{2+}-sensing receptor (CaR) which is responsible for regulating serum Ca^{2+} activity in vertebrates (Brown, 1991; Brown, 1999). The CaR is a G-protein-coupled receptor that was initially identified as the receptor present in parathyroid cells responsible for detecting decreased serum $[Ca^{2+}]$ and triggering secretion of parathyroid hormone which in turn increases serum $[Ca^{2+}]$. More recently it has been cloned from numerous mammalian tissues including the parathyroid, kidney, the calcitonin-secreting parafollicular cells (C-cells) of the thyroid, and brain (Brown et al., 1993; Garrett et al., 1995; Riccardi et al., 1995; Ruat et al., 1995), as well as from fish (Naito et al., 1998). Activation of the CaR in HEK-293 cells and the somata of neurons has previously been proposed to be coupled to activation of a nonspecific ion channel (Ye et al., 1996a; Ye et al., 1996b; Washburn et al., 1999). The pattern of CaR staining in brain is consistent with synaptic localization (Ruat et al., 1995)

although the function of these receptors has not been extensively investigated. Throughout this chapter the term "Ca^{2+} receptor" or "CaR" will refer exclusively to this molecule.

2.3 Results

2.3.1 Characterization of the Synaptosomes

Synaptosomal preparations are considered to be relatively pure preparations of nerve terminals (Whittaker, 1993). Our synaptosome preparations were able to release the

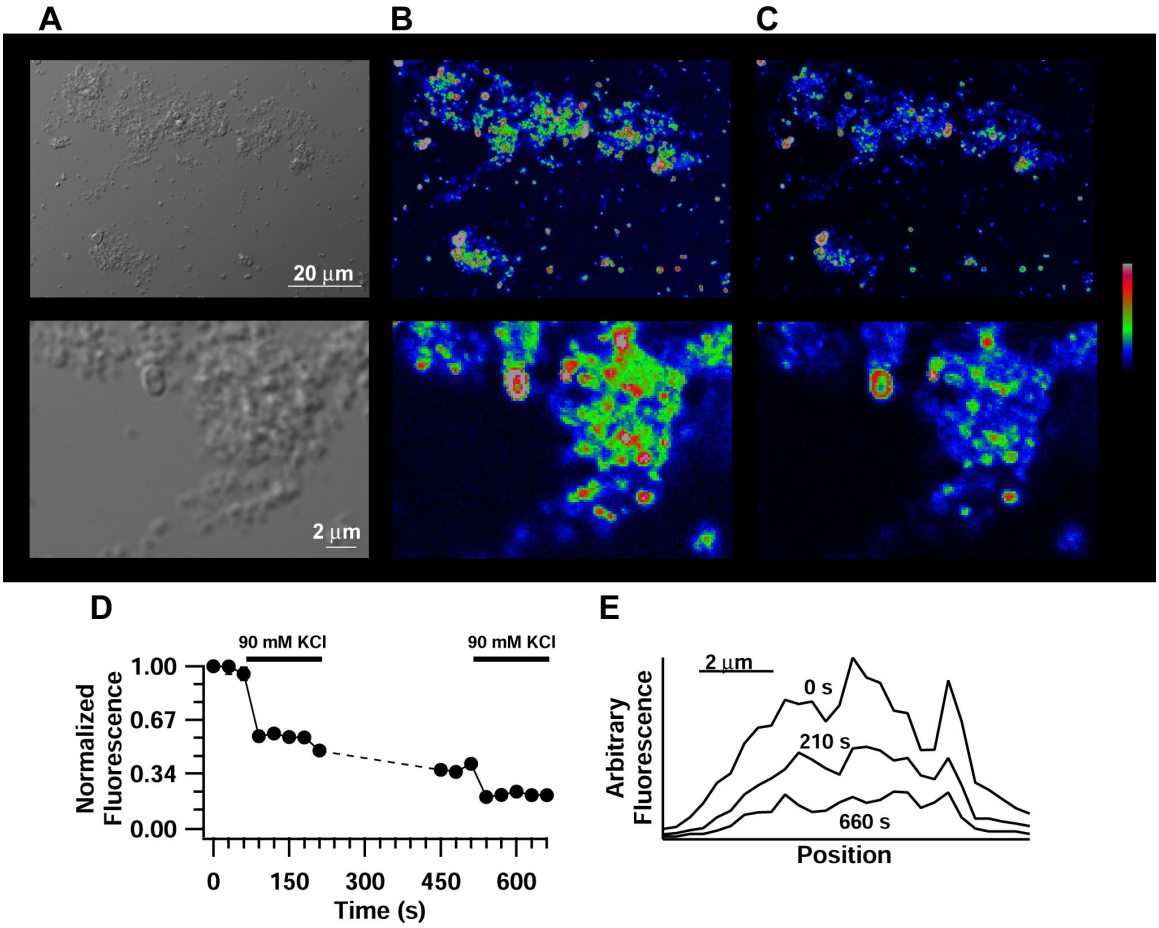

Figure 2-1. FM 1-43 Staining of Plated Synaptosomes

(A) DIC images of plated synaptosomes. Lower image is an expanded area of upper image. (B) Fluorescence image of the same fields as in (A) at t=0 shows FM 1-43 uptake after washing. Note *fluorescence scale bar* at far right. (C) Fluorescence image at t=210 s, after ~150 s of 90 mM KCl. (D) Time course of destaining. Two applications of 90 mM KCl were made at the times indicated by the *bars*, just after the third image in each series. Error bars depict +/- SEM and are generally smaller than the symbols. (E) Line plot showing uniformity of destaining in the X dimension at three time points. The peak represents an X-axis bisection of the large clump in the center of the lower panels of (A)-(C). The "line" was ~2 μM wide in the Y dimension.

neurotransmitter glutamate in a Ca^{2+} dependent manner when depolarized by high K^+ (e.g. Figure 1-5E). However, for the experiments in this chapter, isolated nerve terminals which are normally studied in suspension were allowed to settle on and adhere to glass coverslips to allow electrophysiological investigation. To confirm that this procedure did not select for nonsynaptosomal material we studied the ability of such "plated" material to undergo vesicle cycling. Figure 2-1A shows DIC images of a coverslip plated with synaptosomes. (The lower panel is an expanded region from the upper panel.) After loading with FM1-43, a fluorescent marker for cell membranes (Betz et al., 1996), and subsequent washing of non-endocytosed dye from the plasma membrane, the remaining fluorescence demonstrated endocytosed vesicles (Figure 2-1B, same fields as 2-1A). Much of this fluorescence was released upon stimulation with high potassium (Figure 2-1C), indicating that the material attached to the coverslip was capable of exocytosing the vesicles which had previously been stained with the FM1-43. The time course and extent of this destaining (Figure 2-1D) was typical of nerve terminals in other preparations, such as cultured neurons (Klingauf et al., 1998). The majority of the terminals affixed to the coverslip were destainable. This is clearly seen by comparing Figure 2-1 B and C and highlighted further in Figure 2-1E which plots the fluorescence along a line across a clump of plated material before and after destaining. Virtually all the material in the clump destains to a similar extent.

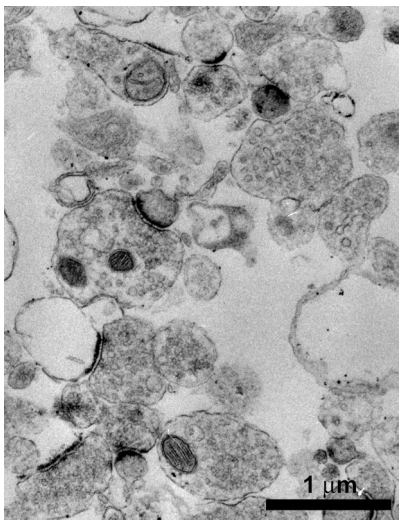

Figure 2-2. Electron Micrograph of Synaptosomes

Electron micrographs of synaptosomes (Figure 2-2) confirmed that this preparation consisted mainly of presynaptic elements, as judged by their size (0.5-1.5 µm) and intracellular contents (numerous 40-50 nm vesicles and mitochondria). Most contaminating material consisted of unsealed membrane frag-

ments. Together these results suggest that we may expect that most seals formed in this preparation would be on intact synaptosomes. Consistent with this conclusion, unintentional recordings from disrupted nerve terminals are low probability occurrences as reversal potentials of currents were not dependent on extracellular ion concentrations before experimental disruption of the nerve terminal's integrity.

2.3.2 Recordings of Large Conductance, Ca^{2+}-activated K^+ Channels

Recordings from single nerve terminals occasionally showed large single channel openings. Figure 2-3B shows such openings recorded in the inside-out configuration. The open probability of the channels in this patch depended on $[Ca^{2+}]_i$. Five consecutive records with 1 μM Ca^{2+} bathing the intracellular surface of the patch contained no

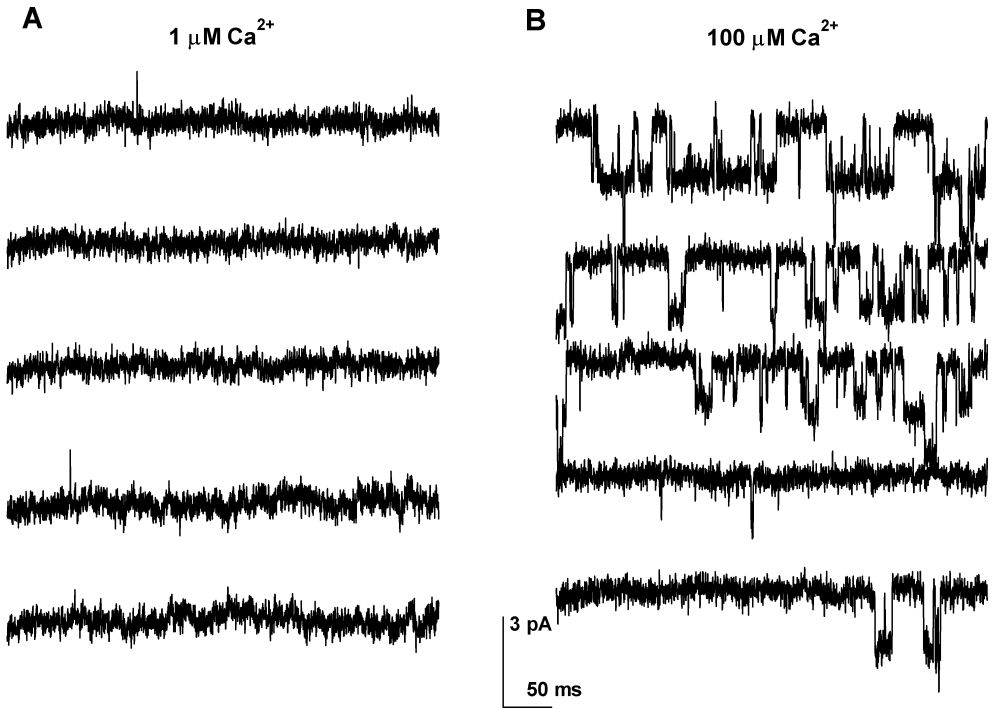

Figure 2-3. BK Channels Recorded in a Presynaptic Terminal

(A) and (B) Five consecutive sweeps from an inside-out recording in symmetrical 155 mM KCl. The pipette contained 2 mM Ca^{2+} and Mg^{2+} and the bath contained 0 Mg^{2+} and the indicated $[Ca^{2+}]$. The holding potential was -10 mV.

openings (Figure 2-3A) whereas five consecutive records in 100 μM Ca^{2+} showed numerous openings (Figure 2-3B). Single channel current-voltage relationships demonstrated a conductance of 80 pS and a reversal potential of 70 mV with 4 mM K^+ in the bath which shifted to 230 pS and 0 mV in symmetrical 155 mM K^+ (Figure 2-4), indicating that the openings represent a K^+ channel. All these characteristics are consistent with the BK channel, a large conductance Ca^{2+}-activated potassium channel (Vergara et al., 1998). BK channels are known to be present in presynaptic terminals (e.g. Sun et al., 1999) and therefore are expected in synaptosomes.

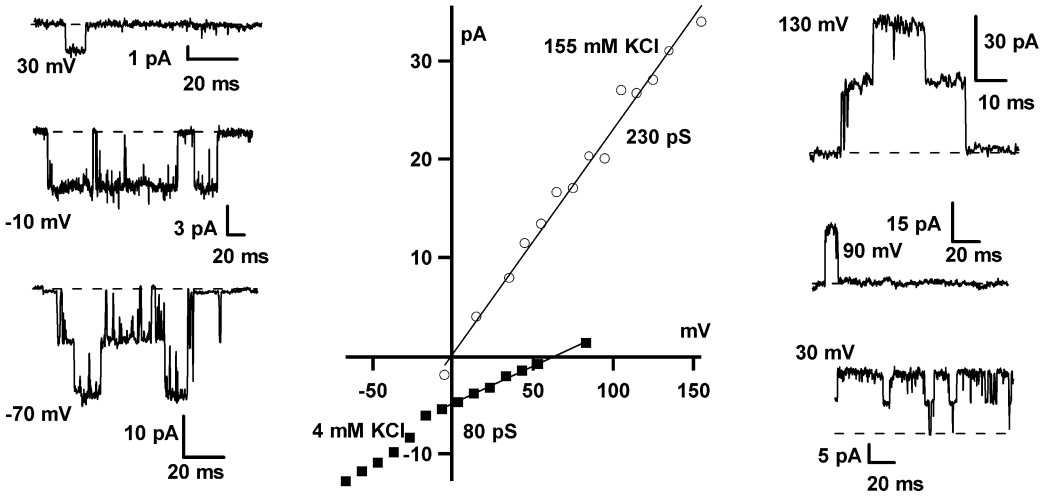

Figure 2-4. Current-Voltage Relationships of the Channels in Figure 2-3

The same patch from Figure 2-3 was exposed to 155 mM KCl or 4 mM KCl+150 mM NaCl in the presence of 100 μM Ca^{2+}. The graph represents measurements of single opening amplitudes at the indicated potentials, as well as the derived single channel conductances. Example traces at three different voltages in 4 mM KCl are shown at left and in 155 mM KCl at right. The closed state is indicated by a dotted line.

2.3.3 Decreased $[Divalent]_o$ Reveals a Slowly Activating Current

As discussed above, Ca^{2+} in the synaptic cleft is expected to decrease significantly during periods of activity. Accordingly we examined the effects of changing $[Ca^{2+}]_o$ (in the absence of $Mg^{2+}{}_o$, see below) on currents recorded from nerve terminals. Figure 2-5A shows currents recorded in the synaptosome-attached configuration. A strong depolariza-

tion in 6 mM extracellular Ca^{2+} activated no current. In contrast, when $[Ca^{2+}]_o$ was reduced to 600 or 60 μM the same depolarization activated a current which developed over the course of a few hundred milliseconds. This effect was rapidly reversible (not shown). Varying Mg^{2+} in the absence of Ca^{2+} had a similar effect (Figure 2-5B).

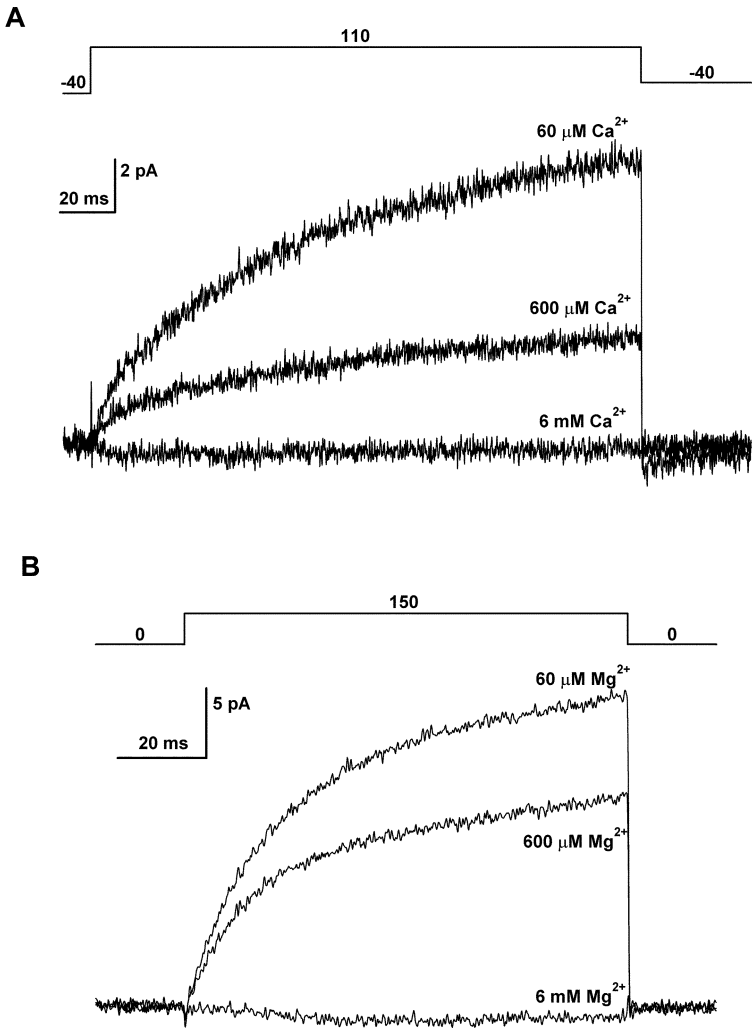

Figure 2-5. Removal of $[Divalent]_o$ Reveals a Slowly Activating Current

(A) A 150 mV depolarization from a holding potential of –40 mV (see voltage trace *top*) in various $[Ca^{2+}]_o$. $[Mg^{2+}]_o$ was nominally 0. (B) Similar to (A) except holding potential was 0 mV and Mg^{2+} was varied in the absence of Ca^{2+}.

The rate of appearance of this current after removal of Ca^{2+} was assessed by lowering $[Ca^{2+}]_o$ during a steady depolarization (Figure 2-6A). The current appeared a few seconds after removal of external Ca^{2+}. Solution exchange was complete within a few hundred ms (Figure 2-6B). The delayed onset of this effect and the activation of a current within the pipette by a change in $[Ca^{2+}]_o$ on the membrane outside the pipette are consistent with an extracellular Ca^{2+} sensor which generates a second messenger which in turn

modulates a channel (Figure 2-6C).

2.3.4 Voltage Characteristics of the Ca^{2+}-Modulated Current

We examined the voltage characteristics of these currents by depolarizing to a range of potentials in the inside-out configuration. The family of curves following depolarization from -40 mV to between -30 and 130 mV in 10 mV steps in low Ca^{2+} (Figure 2-7A) shows that the current amplitude increased with increasing depolarizations (Figure 2-7B). These currents did not inactivate appreciably at this time scale.

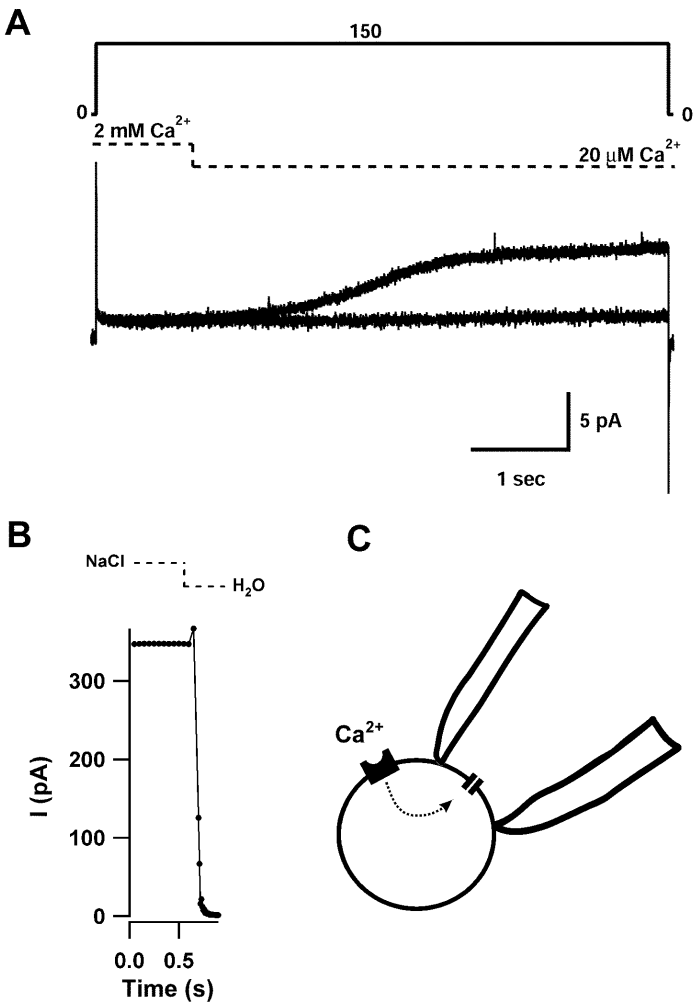

Figure 2-6. Rate of Appearance of Slowly Activating Current

(A) $[Ca^{2+}]_o$ was lowered by a stepper motor-positioned "sewer pipe" perfusion system during a continuous depolarization (voltage protocol is indicated by the *solid line*). Stepper movement is indicated by the *dotted line.* Upper trace: solution changed from 2 mM to 20 µM Ca^{2+}. $[Ca^{2+}]_o$ was not lowered during the lower trace. (B) Time course of solution change was estimated by recording current through a patch pipette and reducing the conductance of the perfusate. 100 mM NaCl was switched to H_2O as indicated by the *dotted line*. Voltage steps between 0 and 10 mV were made and the current change was plotted against time. The magnitude of current change decreased after a delay of ~ 100 ms, reaching steady state after another ~ 100 ms, indicating complete solution exchange after 200 ms. (C) Cartoon showing separation of the $[Ca^{2+}]_o$ sensor and the channel it inhibits.

Tail currents were evoked by a hyperpolarizing step to -80 mV following these depolarizations (Figure 2-7C). They deactivated monoexponentially with a time constant in this experiment of ~ 14 ms. Tail current amplitudes were used to

construct a conductance-voltage plot (Figure 2-7D). The conductance increased with depolarization, and was fit with a single Boltzman with a half maximal activation of 90 mV and a slope factor of –30 mV.

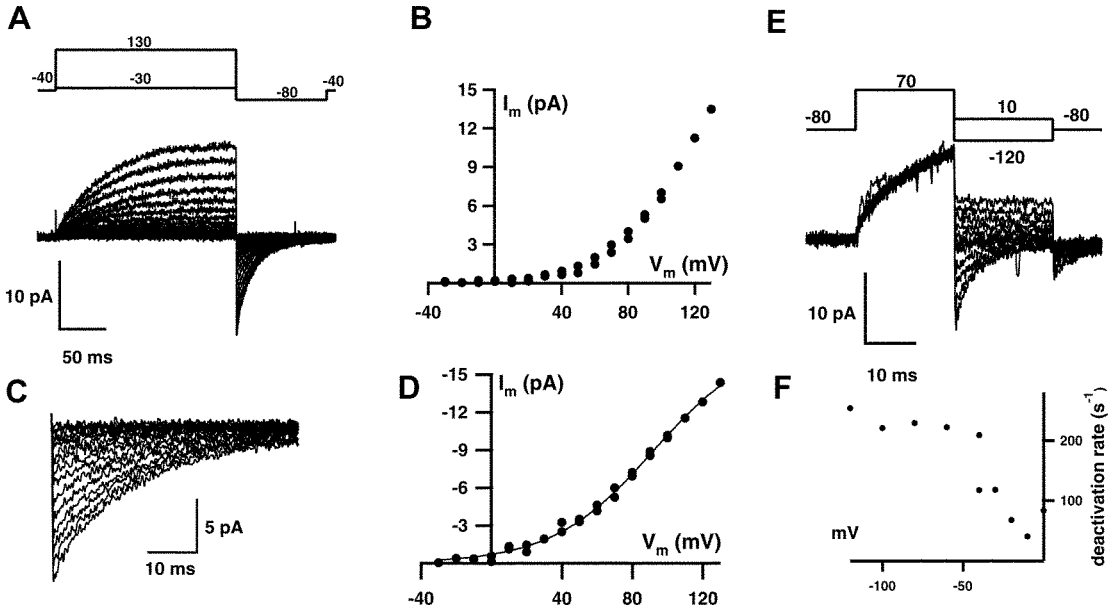

Figure 2-7. Voltage Characteristics of the Slowly Activating Current

(A)-(D) Analysis of an inside-out recording in symmetrical 150 mM NaCl with 2 mM Ca^{2+} and 0 Mg^{2+} in the pipette. Ca^{2+} was 60 μM and Mg^{2+} was 0 in the bath. (A) Family of curves activated by depolarizing steps from –40 mV to between –30 and 130 mV in 10 mV steps (*solid line* shows voltage protocol). (B) Peak amplitude of currents in (A) plotted against voltage. (C) Tail currents from (A) shown in expanded view. (D) Peak tail current as a function of voltage during depolarization. Smooth line is a Boltzman fit to the data.

(E) and (F) Deactivation kinetics recorded in the synaptosome-attached configuration in symmetrical 155 mM KCl. 2 mM Ca^{2+} and Mg^{2+} in the pipette, 1 μM Ca^{2+} and 0 Mg^{2+} in the bath. (E) Family of curves activated by depolarization to 70 mV and repolarization to between 10 and -120 mV (*solid line* shows voltage protocol). (F) Rate of deactivation determined by fitting tail currents with a single exponential plotted as a function of voltage during tail.

The effect of voltage on the deactivation kinetics as assessed by measuring the rate of decay of tails evoked at various potentials (Figure 2-7E). Little voltage dependence of deactivation was seen at voltages equal to or more negative than –50 mV (Figure 2-7F), which in this cell produced deactivation rates around 225 s^{-1}. The deactivation rate slowed considerably at voltages more positive than –40 mV.

2.3.5 Other Considerations

Next we wondered about the mechanism by which Ca^{2+} inhibited this current. To begin to study this we asked whether Ca^{2+} decreased the maximal extent of activation of the channel, as seen for some examples of second messenger channel modulation (e.g. muscarinic inhibition of M current, Hille, 1994), or affects the voltage range of activation, also seen in second messenger modulation (Hille, 1994), or as might be seen if Ca^{2+} were merely having an effect through surface charge screening. Synaptosome-attached patches were depolarized between –20 and 200 mV and subsequently hyperpolarized to –100 mV to generate tail currents in several external Ca^{2+} concentrations (Figure 2-8A).

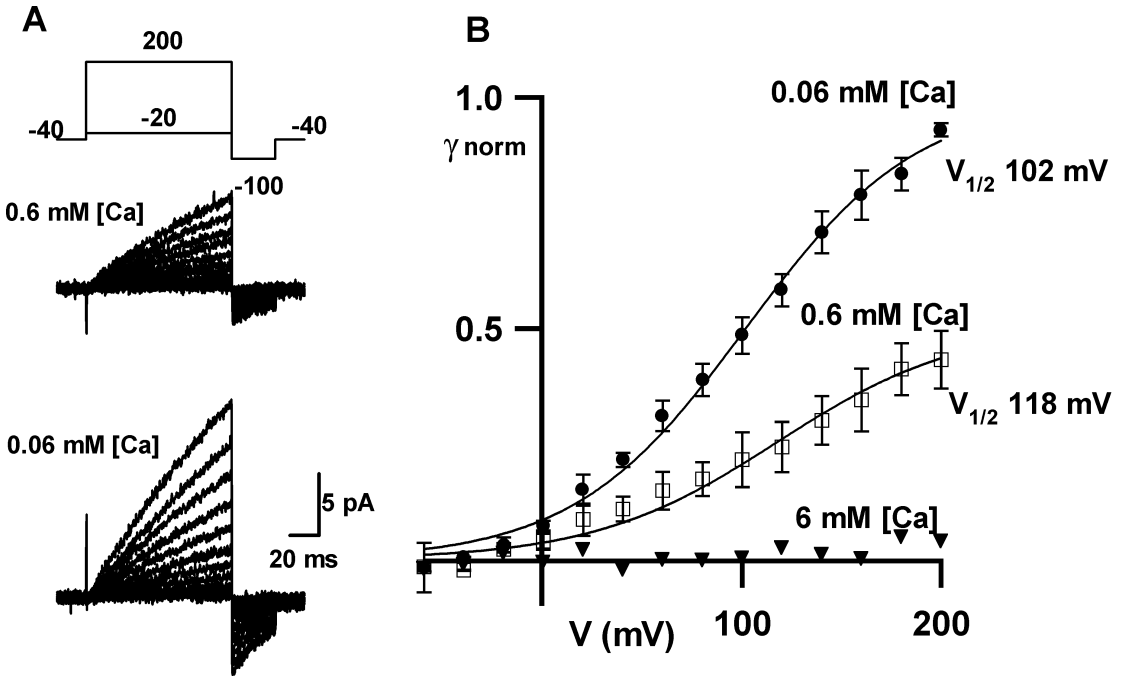

Figure 2-8. Interactions Between Ca^{2+} and Voltage in Activating Current

Synaptosome-attached recording in symmetrical 150 mM NaCl. Pipette contained 2 mM Ca^{2+} and Mg^{2+}. Bath contained nominally 0 Mg^{2+} and the indicated $[Ca^{2+}]$. (A) Example families of curves activated by depolarizing from –40 mV to between –20 and 200 mV (*solid line* shows voltage protocol) in two $[Ca^{2+}]_o$. (B) Compiled data from three such recordings, peak tail currents were measured and normalized in each condition before averaging and plotting as a function of depolarization voltage. Recordings were made in three values of $[Ca^{2+}]_o$: 6 mM (*triangles*), 600 μM (*open squares*), and 60 μM (*circles*). Smooth lines are Boltzman curves with the indicated voltage of half activation.

The resulting conductance-voltage relationships (Figure 2-8B) were fit with Boltzman curves to determine the voltage range of activation and maximal extent of activation. In 6 mM Ca^{2+} essentially no current is seen. Between 600 μM and 60 μM Ca^{2+} the conductance of this current doubled with only a small shift of the half maximal voltage of activation. The shift in the activation voltage was less than 20 mV, indicating that the effect of Ca^{2+} is on the extent of activation and not through surface charge effects and that there is little if any interaction between the voltage sensor of the channel and the modulation by Ca^{2+}_o.

We assessed whether the current activated by decreases in $[Ca^{2+}]_o$ was well isolated in two ways, both of which are based on the assumption that it is unlikely that two or more independent channel types will have the same kinetics of activation and inactivation and the same E_r. We compared the current activated by depolarization to 90 mV

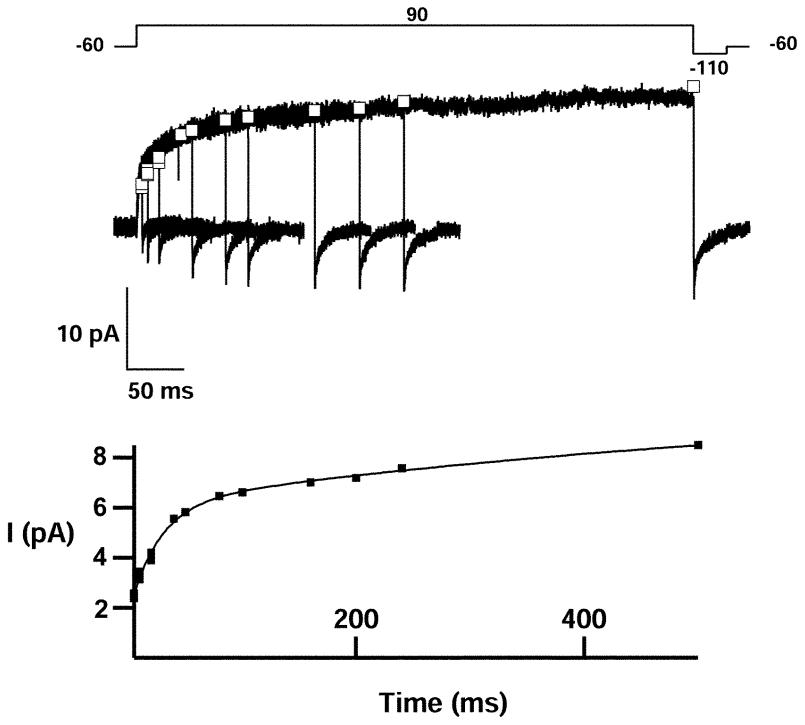

Figure 2-9. Envelope Current Analysis

Synaptosome-attached recording with 150 mM NaCl and 2 mM Ca^{2+} and Mg^{2+} in the pipette; 155 mM KCl, 1 μM Ca^{2+}, and nominally 0 Mg^{2+} in the bath. Patch was depolarized from a holding potential of –60 mV to 90 mV for a range of times (longest depolarization is shown in the voltage protocol depicted by the *solid line* in (A)). (A) *Traces* show currents evoked by the depolarizations. *Squares* are scaled tail current amplitudes from (B). Inverted tail current peak amplitudes are plotted against length of depolarization.

for various times with the isochronic tail current at -110 mV. When the tail current amplitudes were inverted and scaled (Figure 2-9B and squares in 2-9A) they aligned quite well with the current measured after an isochronic depolarization (continuous trace in Figure 2-9A).

Second we assessed whether the reversal potential of the activated current was dependent on the duration of activation. If the current seen were actually the combination of two different currents carried by different ions, the reversal potential would be a function of the ratio of the activated conductances, which again would be expected to change with time unless both currents had identical activation and inactivation kinetics. We measured

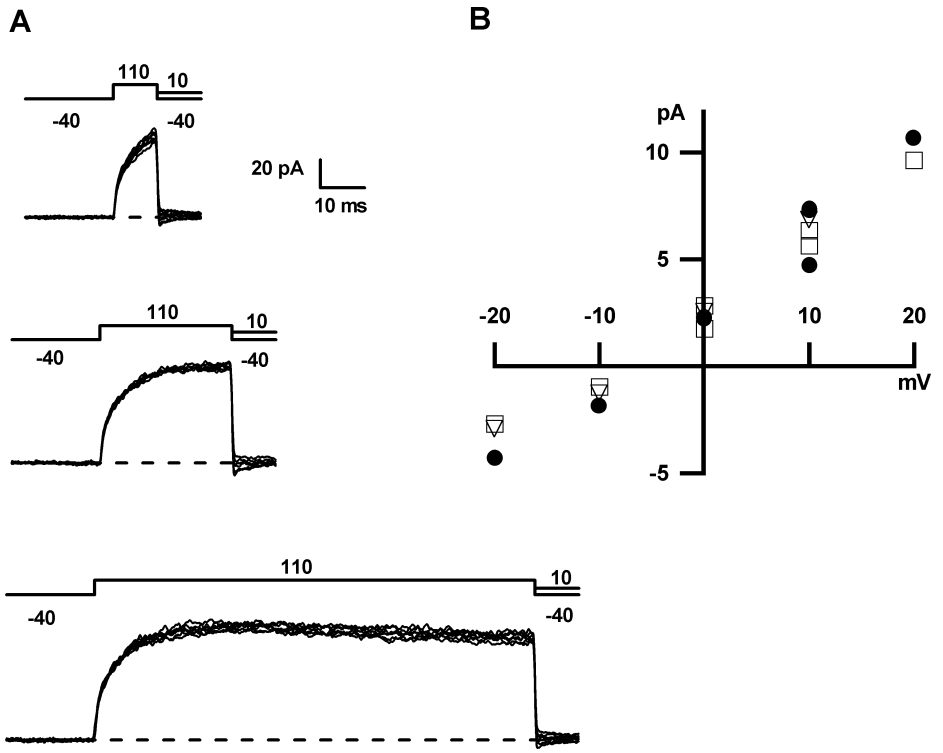

Figure 2-10. Reversal Potential as a Function of Activation

(A) Inside-out recording with 150 mM NaCl and 2 mM Ca^{2+} and Mg^{2+} in the pipette; 155 mM KCl, 1 μM Ca^{2+}, and nominally 0 Mg^{2+} in the bath. Patch was depolarized from a holding potential of –40 mV to 110 mV for 10, 30, or 100 ms and returned to a range of voltages to evoke tail currents (shown in the voltage protocols depicted by the *solid lines*). (B) Peak tail current amplitudes plotted as function of voltage. Data are from 10 ms (*open squares*), 30 ms (*open triangles*), and 100 ms (*filled circles*) depolarizations before the tail.

tail currents generated by steps to a range of potentials after 110 mV depolarizations which lasted 10, 30, or 100 ms (Figure 2-10A). In each case the reversal potential was near 0 mV (Figure 2-10B), again arguing against the presence of multiple channels underlying this current.

In some patches containing the Ca^{2+}-modulated current (Figure 2-11 lower trace) other currents were seen (Figure 2-11 upper trace). These single openings can be seen to have clear, rapid opening and closings arguing against the slower current resulting from some aspect of the synaptosome-attached recording configuration.

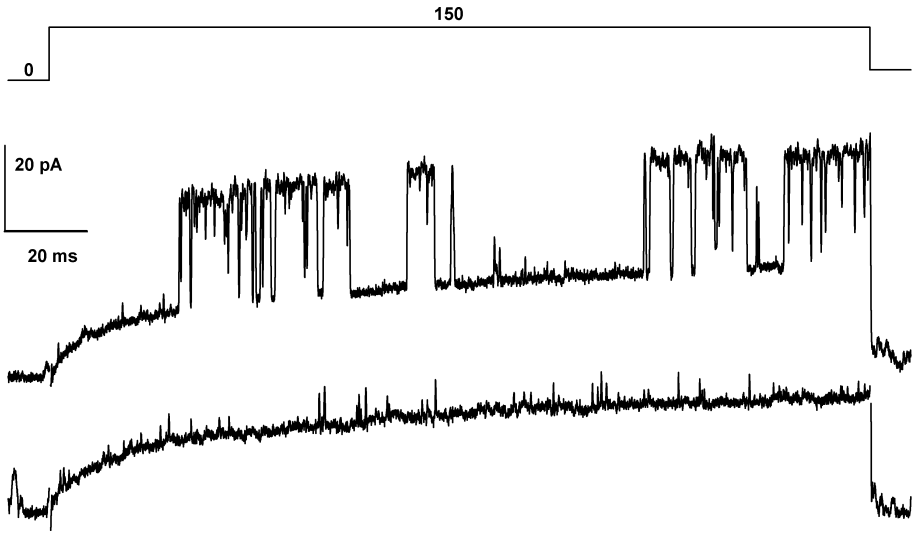

Figure 2-11. Ca^{2+}-modulated Current Co-localized with Large and Small Conductance Channels

Synaptosome-attached recording with 150 mM NaCl and 2 mM Ca^{2+} and Mg^{2+} in the pipette; 75 mM KCl + 150 mM sucrose, 10 μM Ca^{2+}, and nominally 0 Mg^{2+} in the bath. Patch was depolarized from a holding potential of 0 mV to 150 (as shown in the voltage protocol depicted by the *solid line*). Some traces showed large single channel openings in conjunction with the slowly activating, small single channel conductance current (*upper trace*) whereas others recorded within a time frame of a few seconds did not (*lower trace*).

2.3.6 Permeation Characteristics of the Ca^{2+}-Modulated Current

We studied the ionic basis of these currents by measuring the reversal potentials (E_r) in inside-out patches obtained from synaptosomes. Following strong depolarizations the

membrane potential was stepped to a range of voltages straddling the reversal potential (Figure 2-12A). The tail currents (shown expanded in Figure 2-12B) were measured 400-800 μs after the repolarization and plotted against voltage (Figure 2-12C). With 150 mM NaCl in the pipette and 155 mM KCl in the bath the currents reversed at –2 mV suggesting that this is a nonspecific cation or chloride channel. To differentiate between these possibilities the KCl was substituted by isotonic sucrose. This shifted E_r in the positive

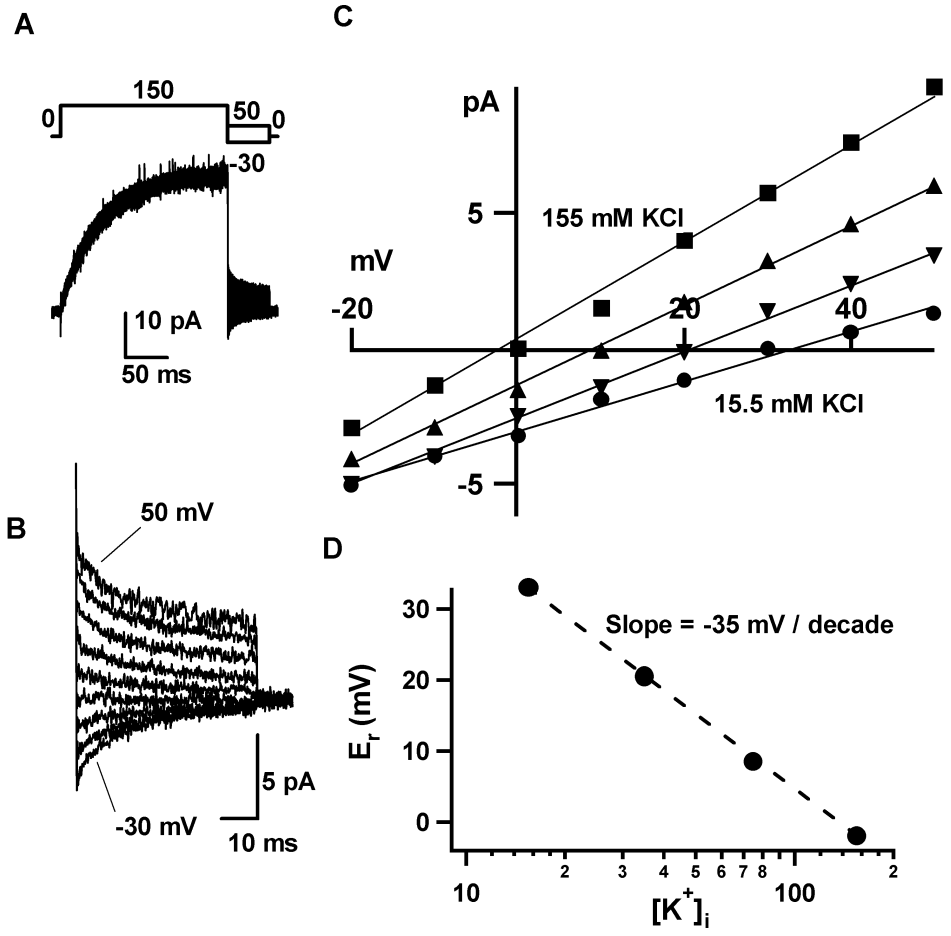

Figure 2-12. Reversal Potential as a Function of $[K^+]_i$

(A) Family of curves from an inside-out recording with 150 mM NaCl, 2 mM Ca^{2+} and Mg^{2+} in the pipette. The bath contained the indicated [KCl] made isotonic with sucrose, 10 μM Ca^{2+} and nominally 0 Mg^{2+}. Patch was depolarized from a holding potential of 0 mV to 150 and repolarized to various potentials to evoke tail currents (as shown in the voltage protocol depicted by the *solid line*). (B) Expanded tail currents from (A). (C) Tail current peak amplitude plotted against voltage for four values of $[KCl]_i$: 155 mM (*squares*), 75 mM (*upright triangles*), 35 mM (*inverted triangles*), and 15.5 mM (*circles*). *Straight lines* are linear fits to the data. (D) Averaged interpolated reversal potentials from the data in (C) and three other similar recordings plotted against $[KCl]_i$.

direction, consistent with a nonspecific cation (NSC) channel. The effect of $[K^+]_i$ on E_r is illustrated in (Figure 2-12D), where it can be seen that E_r shifts by –35 mV/decade. This is similar to another NSC channel, the nicotinic AChR (Lewis, 1979) but less than seen for many other ion channels.

Consequently we investigated the anion permeability of this channel. The lack of permeation by Cl^- was demonstrated in anion substitution experiments wherein large, presumably impermeant anions like gluconate or smaller anions like nitrate which are known to be highly permeant through some anion channels were substituted for Cl^-. The

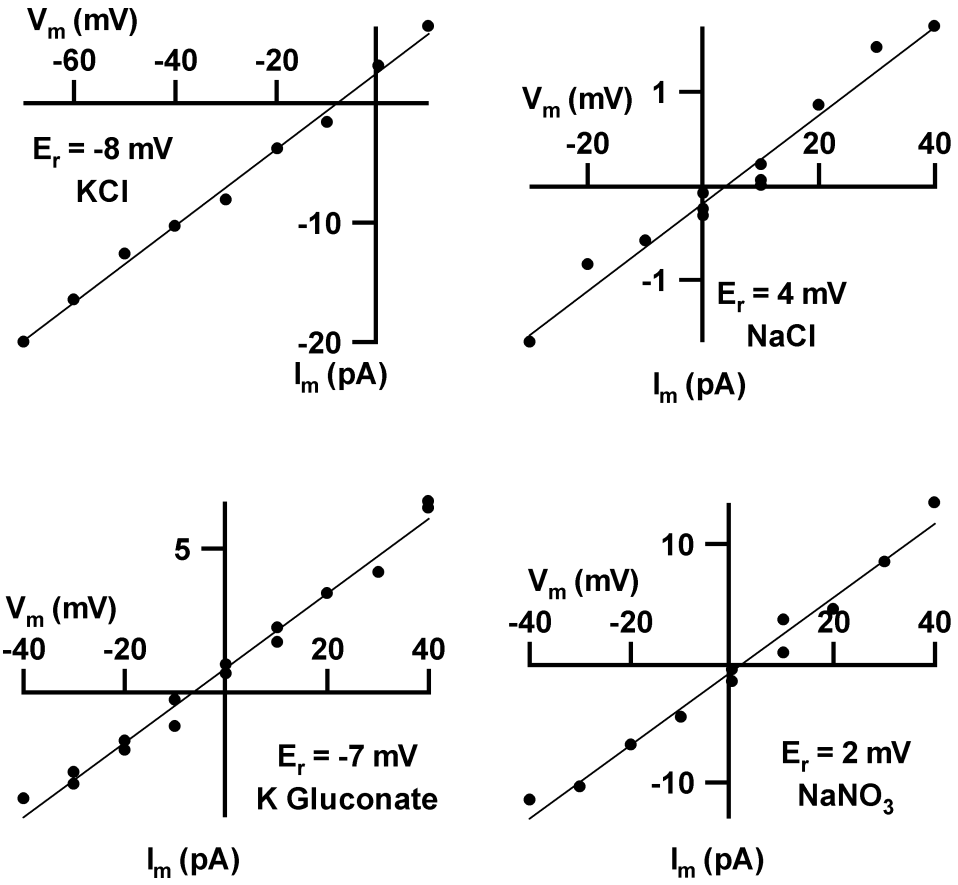

Figure 2-13. Reversal Potential is Unaffected by Reducing $[Cl^-]_o$.

Inside-out recording with 150 mM NaCl and 2 mM Ca^{2+} and Mg^{2+} in the pipette; 155 mM of the indicated salt in the bath (with low Ca^{2+} and Mg^{2+}). Data show peak amplitude of the tail current evoked at the indicated voltage after a depolarization to 110 mV. Interpolated reversal potential (E_r) is also shown.

substitution of gluconate changed the reversal potential of the tail currents by only 1 mV (Figure 2-13, compare "KCl" to "KGluconate") and substitution of nitrate changed E_r by 2 mV (compare NaCl to $NaNO_3$). The lack of significant change in E_r with these anions indicates that this is a cation channel.

Preliminary experiments examining Na^+ permeability resulted in a positive shift in E_r when NaCl was substituted by isotonic sucrose, consistent with this channel's being

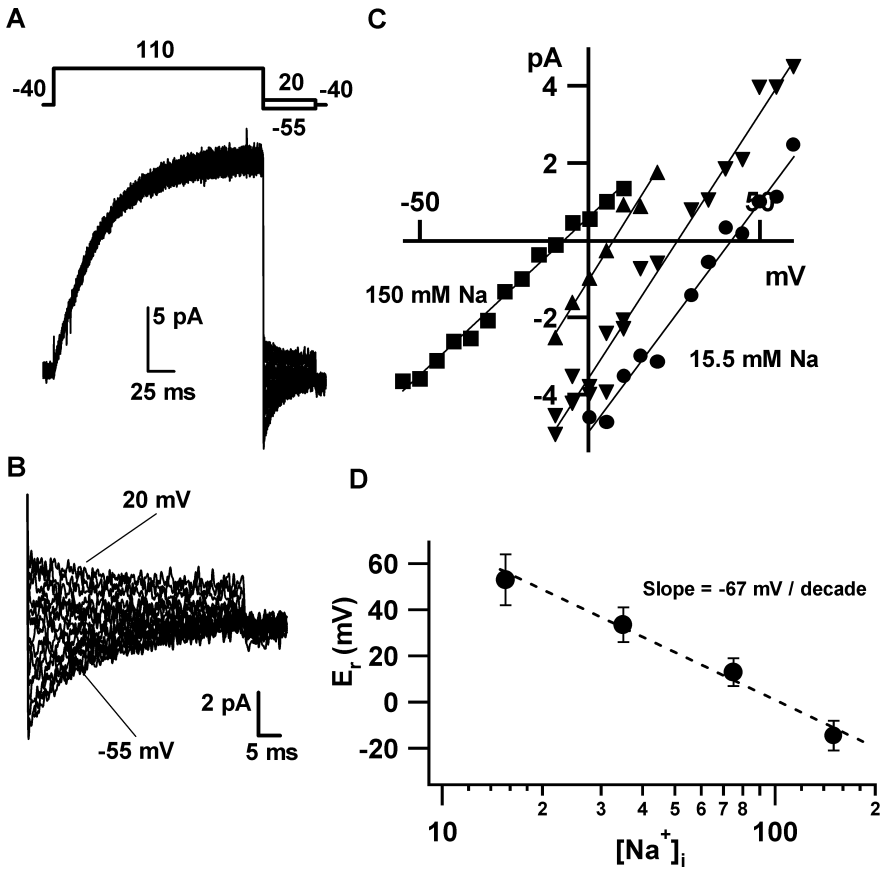

Figure 2-14. Reversal Potential as a Function of $[Na^+]_i$

(A) Family of curves from an inside-out recording with 150 mM NaCl, 2 mM Ca^{2+} nominally 0 Mg^{2+} in the pipette. The bath contained the indicated [NaCl] made isotonic with sucrose, 60 μM Ca^{2+} and nominally 0 Mg^{2+}. Patch was depolarized from a holding potential of -40 mV to 110 and repolarized to various potentials to evoke tail currents (as shown in the voltage protocol depicted by the *solid line*). (B) Expanded tail currents from (A). (C) Tail current amplitude plotted against voltage for four values of $[NaCl]_i$: 150 mM (*squares*), 75 mM (*upright triangles*), 35 mM (*inverted triangles*), and 15.5 mM (*circles*). *Straight lines* are linear fits to the data. (D) Averaged interpolated reversal potentials from the data in (C) and another similar recording plotted against $[NaCl]_i$.

permeable to Na^+ as well as K^+. The slope of E_r as a function of $[Na^+]_i$ was –67 mV/decade (Figure 2-14D). The reason for the discrepancy with the K^+ data is not clear but may reflect a small preference for K^+ over Na^+ (e.g. compare KCl to NaCl in Figure 2-13) or possibly the fact that the K^+ data were collected using a holding potential of 0 mV at which voltage the channel is slightly activated. Further experiments changing $[KCl]_i$ and $[NaCl]_i$ are warranted to resolve this question.

Many NSC channels are permeable to Ca^{2+} as well as monovalent cations. We began to assess the Ca^{2+} permeability of the channel by measuring E_r while varying $[Ca^{2+}]_o$. In preliminary experiments, when $[Ca^{2+}]_o$ was increased in inside-out recordings, E_r shifted in the hyperpolarizing direction (Figure 2-15), contrary to what would be expected for a Ca^{2+}-permeable channel. Such experiments with Ca^{2+} are difficult to interpret conclusively due to the inhibition of the current by Ca^{2+} but our data weigh against this channel's being permeable to Ca^{2+}. Again further experiments investigating the divalent permeability of this channel are warranted.

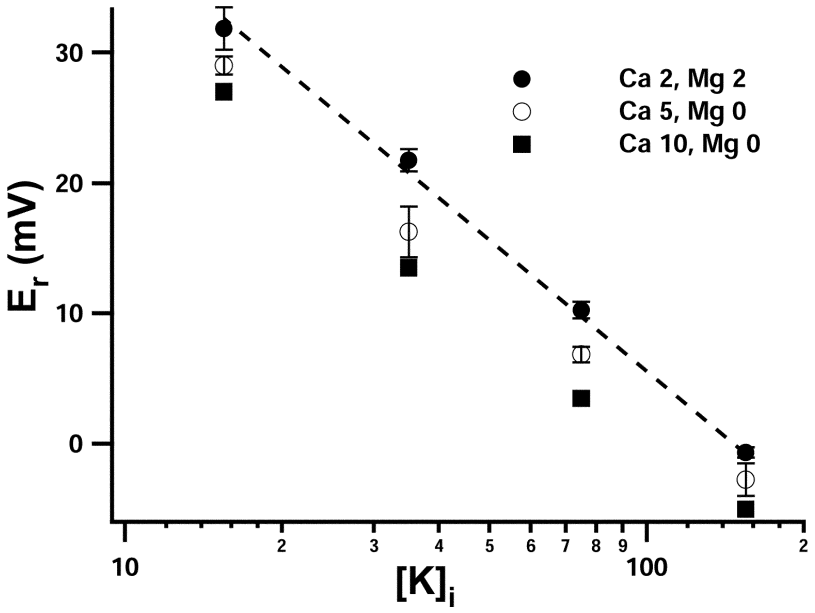

Figure 2-15. Reversal Potential as a Function of $[K^+]_i$ and $[Divalent]_o$

Filled circles are the data from Figure 2-12D. Similar experiments with different [divalent] in the pipette are shown on the same graph. *Open circles* show averages +/- SD of data from two recordings with 5 mM Ca^{2+} and 0 Mg^{2+} and *filled squares* show data from one recording with 10 mM Ca^{2+} and 0 Mg^{2+}.

2.3.7 Characterization of the Target of Divalent Cations

Changes in $[Ca^{2+}]_o$ modulating a NSC channel are reminiscent of an effect shown for the extracellular Ca^{2+} receptor (CaR) in hippocampal neurons and HEK-293 cells (Ye et al., 1996a; Ye et al., 1996b) and in the subfornical organ (Washburn et al., 1999). Accordingly we undertook experiments designed to compare the previously identified CaR to the sensor for Ca^{2+} responsible for modulating the NSC channel in nerve terminals. To do this we first quantified the effect of Ca^{2+} and Mg^{2+} on the modulation of the nerve terminal channel by measuring current amplitudes in the presence of a wide range of $[\text{divalent cation}]_o$. The dose-response curve for channel modulation by $[Ca^{2+}]_o$ showed that in the absence of other divalents a concentration of 300 μM Ca^{2+} resulted in 50% elimination of the current (Figure 2-16 open squares). This concentration of $[Ca^{2+}]_o$ is within the range estimated to occur physiologically at synapses undergoing activity (see

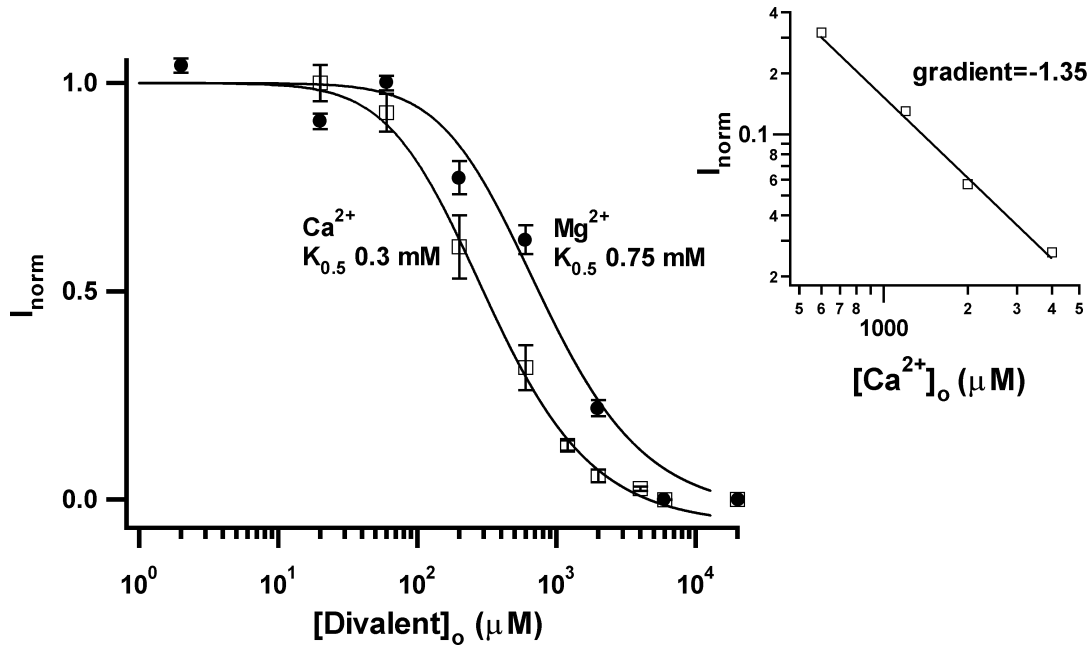

Figure 2-16. Dose-Response of $[Divalent]_o$.

Synaptosome-attached recordings were depolarized repeatedly in the presence of various $[Ca^{2+}]_o$ (*open squares*) or $[Mg^{2+}]_o$ (*filled circles*) in the absence of the other divalent cation. The responses were normalized to the value in 20 μM Ca^{2+} or 60 μM Mg^{2+} respectively and averaged. N for each point ranges between 2 and 11, error bars represent SEM. *Inset* log-log plot of the foot of the Ca^{2+} curve.

references above). The log-log plot of the foot of the curve showed a slope of –1.35 (Figure 2-16 inset). Mg^{2+} had an effect similar to Ca^{2+} but was less potent, with an EC_{50} of 750 μM. The effect of Ca^{2+} and Mg^{2+} with an ~3 fold preference for Ca^{2+} is similar to the action of these agents at the CaR although the EC_{50}s in the literature tend to be ~10 fold higher.

In addition to Ca^{2+} and Mg^{2+}, the CaR is also activated by Gd^{3+} (Brown et al., 1993), polycations such as spermidine (Quinn et al., 1997), and two phenylalkylamines, NPS R-467 and NPS R-568 (Hammerland et al., 1998); accordingly we tested such compounds

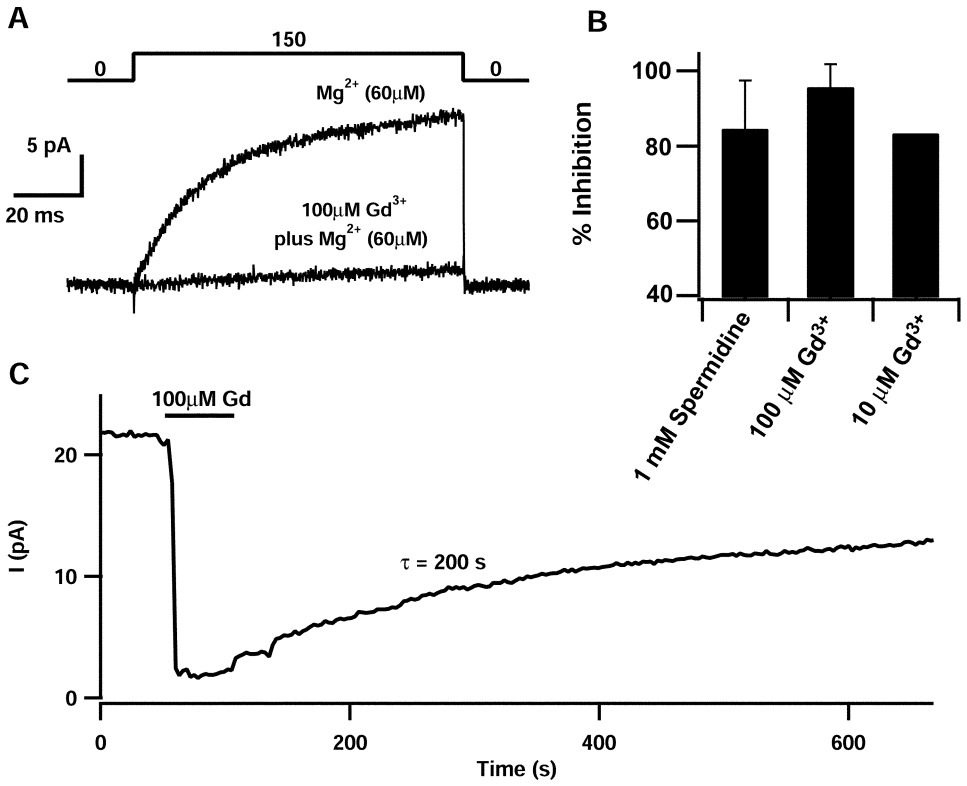

Figure 2-17. Effect of Gd^{3+} and Spermidine on Nerve Terminal Ca^{2+} Sensor

Synaptosome-attached recordings were depolarized repeatedly in the presence of spermidine or Gd^{3+} in low [divalent]$_o$. (A) Exemplar traces showing effect of 100 μM Gd^{3+} on a current present in nominally 0 Ca^{2+} and 60 μM Mg^{2+} and evoked by a depolarization to 150 mV from a holding potential of 0 mV. *Solid line* shows voltage protocol. (B) % inhibition was calculated as the percentage decrease of the current measured in low [divalent]$_o$ caused by the indicated agent. Data represent averages +/- SD of 2 (spermidine), 3 (100 μM Gd^{3+}), and 1 (10 μM Gd^{3+}) experiments. (C) Example experiment showing time course of inhibition and relief from inhibition by Gd^{3+}. Peak amplitude in response to a depolarization every 3 s is plotted against time. 100 μM Gd^{3+} was added during the period indicated by the *horizontal bar*.

for their effect on the current. In synaptosome-attached patches in the presence of 20 μM Mg^{2+} and nominally 0 Ca^{2+}, Gd^{3+} inhibited the currently potently, with a dose of 10 μM resulting in over 80% current reduction (Figure 2-17B). One hundred micromolar Gd^{3+} resulted in almost complete inhibition (Figure 2-17A-C). The onset of inhibition by Gd^{3+} was rapid, like that of Ca^{2+} and Mg^{2+}; however unlike the divalent cations the reversal of inhibition after removal of Gd^{3+} was slow, with a time constant of recovery of 200 s (Figure 2-17B). Spermidine was less potent than Gd^{3+}, inhibiting the current by about 85% at a concentration of 1 mM. Spermidine also exhibited a slow wash off (not shown). EC_{50} values in the literature for activation of the CaR in other systems are 20 μM for Gd^{3+} (Brown et al., 1993) and 4 mM for spermidine (Quinn et al., 1997).

Thus the sequence of relative affinities of four relatively nonselective agents reported here is Gd^{3+}>Ca^{2+}~spermidine>Mg^{2+}, in agreement with that reported for the CaR. While the rank order of affinities appears identical, the EC_{50}s of these agents at the nerve terminal are increased by a factor of 5-10 (see Discussion). In order to test more stringently whether the CaR was responsible for the effect in nerve terminals we tested the putatively specific agent NPS R-467. NPS R-467 is an allosteric activator of the CaR (Hammerland et al., 1998), significantly increasing the potency of Ca^{2+} (and other polyvalent agonists) at the CaR when assayed by measuring the increase in $[Ca^{2+}]_i$ in bovine parathyroid cells exposed to various $[Ca^{2+}]_o$ (an effect mediated by the CaR via G proteins and IP3): a dose of 100 nM NPS R-467 decreased the EC_{50} of $[Ca^{2+}]_o$ from ~1.2 mM to ~0.6 mM and the EC_{50} of NPS R-467 for increasing $[Ca^{2+}]_i$ in the presence of 0.5 mM $Ca^{2+}{}_o$ was 0.5-1 μM (E. Nemeth personal communication). We tested responses to three values of $[Ca^{2+}]_o$ (60 μM, 600 μM, and 6 mM) in the presence and absence of either 0.5 μM (N=2) or 10 μM NPS R-467 (N=3). The response of the CaR to 600 μM $[Ca^{2+}]_o$, and possibly to 60 μM, would be expected to be potentiated by either dose of NPS R-467, however we saw no increase in response to $[Ca^{2+}]_o$ except for a modest increase in one

experiment at 10 μM NPS R-467 and this increase was irreversible (not shown).

2.4 Discussion

2.4.1 Summary of Results

To the best of our knowledge these experiments represent the first electrical recordings of single nerve terminals in the size range typical of the mammalian CNS. Recordings show channels expected to be found in the nerve terminal as well as a novel channel with a small single channel conductance permeable to monovalent cations. This channel is activated by a combination of decreased $[Ca^{2+}]_o$ and depolarization. The channel activates and deactivates slowly compared to Na^+ and Ca^{2+} channels but similarly to some K^+ channels such as the BK channel.

The $[Ca^{2+}]_o$–sensing mechanism is sensitive to various multivalent cations but not the phenylalkylamine NPS R-467. The potencies for the cationic agonists are within approximately one order of magnitude of the those for these agents at the CaR (see below). The $[Ca^{2+}]_o$–sensor in the nerve terminal presumably acts on the NSC channel via an intracellular second messenger based on the time course of the modulation and its ability to inhibit channels in a distant area of membrane. Another possibility is that the regulation of the channel may be via exo/endocytosis (e.g. Yao et al., 1999).

2.4.2 Comparison to Published Reports of Ca^{2+}-sensing—NSC Channel Systems

The pharmacological data indicate that although the nerve terminal Ca^{2+}-sensing mechanism which is the target of polyvalent compounds resembles the CaR in some ways it differs significantly in others. However it is difficult to compare our values and the literature values directly as in both cases a second messenger is involved between the Ca^{2+} sensor and the parameter being measured. In our experiments a significant fraction of the synaptosomal surface—that within the pipette—is continuously exposed to high

[divalent]. A lower [divalent] may be required on the bath-exposed surface in order to compensate for the effect of high divalents within the pipette. In any case the lack of effect of NPS R-467 suggests an important difference between the CaR and the extracellular Ca^{2+} sensor at the nerve terminal. These two Ca^{2+}-sensing entities may either be completely distinct or alternately the nerve terminal receptor may be a previously uncharacterized relative of the CaR.

The NSC channel present at the nerve terminal also appears to be distinct from that activated by the CaR in hippocampal neurons and HEK-293 cells based on two criteria. One channel shown to be activated by the CaR is permeable to Ca^{2+} and has a single channel conductance of 45-60 pS (Ye et al., 1996a; Ye et al., 1996b), another has a single channel conductance of 2.5 nS (Washburn et al., 1999). In contrast the channel in nerve terminals appears to be impermeable to Ca^{2+} and has a much smaller single channel conductance than either of these (we have estimated it to be 30-90 fS by fluctuation analysis, not shown). The NSC channel we have recorded in nerve terminals also differs from a Ca^{2+}-sensing channel recorded in neurons (Xiong et al., 1997) which again had a larger single channel conductance (36 pS) than the synaptic channel and was not voltage dependent. Another difference between the Ca^{2+}-sensing systems which have previously been described and the nerve terminal system described here is the direction of the coupling between the Ca^{2+}-sensing mechanism and the channel. In all published reports increases in $[Ca^{2+}]_o$ were coupled to activation of the channel, whereas here increases in $[Ca^{2+}]_o$ were coupled to inhibition of the channel.

2.4.3 Physiological Relevance

We postulate that the function of the current activated by decreases of $[Ca^{2+}]_o$ is likely to be compensatory. The system revealed by our experiments would be dormant until periods of high activity when the fall in $[Ca^{2+}]_o$ and membrane depolarizations would activate the channel, decreasing the input resistance of the nerve terminal, broad-

ening the action potential, and increasing the duration of the peak period of Ca^{2+} entry. The resulting increase in Ca^{2+} entry might serve to compensate for decreased entry caused by Ca^{2+} channel inactivation and the decreased electrochemical gradient for Ca^{2+} experienced during high activity.

2.5 Materials and Methods

2.5.1 Solutions

Tyrode consisted of (in mM) NaCl, 150; KCl, 4; $CaCl_2$, 2; $MgCl_2$, 2; HEPES, 10; Glucose, 10; pH adjusted with NaOH. High potassium solution was similar with no NaCl and 155 mM KCl, pH adjusted with KOH. In many cases as indicated in the text [Ca^{2+}] and [Mg^{2+}] were changed. 1 mM HEDTA was added to solutions intended to have low [free divalent], with the [total divalent] calculated by Maxchelator software version 6.50 using the Bers constants (Chris Patton, Stanford University, Pacific Grove, CA). Liquid junction potentials between the bath solution and reference electrode were minimized in experiments in which the bath solution was changed by use of a 3 M KCl-containing agar bridge. The maximal change in voltage between bath and agar bridge was 2 mV, measured as described (Hughes et al., 1987). Errors due to these changes were not corrected.

2.5.2 Plating of Synaptosomes

Synaptosomes prepared as described in section 1.6.1 were resuspended in Tyrode at approximately 0.8-1 mg/mL and 150 μL "drops" were placed onto washed 10 mm round coverslips and allowed to settle for 0.5-6 hours in an airtight chamber to reduce evaporation at 4°C before use. Plating in Tyrode caused synaptosomes to clump, however early attempts to plate in sucrose to prevent clumping resulted in a selection for material which did not exhibit active conductances. Precoating the coverslips with poly-L- or poly-R-lysine or Matrigel had no obvious benefit.

2.5.3 FM1-43 Fluorimetry

Synaptosomes were plated as described above except that 400 μL "drops" were placed onto washed 22 X 40 mm coverslips which fit the bath chamber of the Fluoview confocal microscope (Olympus America, Melville, NY). Experiments were conducted at room temperature (23-24°C). Synaptosomes were stained with 3-4 μM FM1-43 in Tyrode where 45 mM NaCl was replaced by 45 mM KCl. This solution was applied to the bath by pipette after the normal gravity-fed bath perfusion was halted. Several bath volumes of dye-containing solution were applied. After 90 s bath perfusion was resumed and this washing continued for at least 15 minutes. Images were acquired and analyzed using the Fluoview software. Excitation of the FM1-43 was by the 488 nm argon laser and emission was monitored above 510 nm.

2.5.4 Electrophysiology

Recordings were made using the cell-attached or inside-out patch-clamp configurations (Hamill et al., 1981) from isolated nerve terminals visualized on an inverted microscope (Axiovert, Zeiss). The coverslip containing the plated synaptosomes was placed in an oval recording chamber (volume ~0.5 ml) to permit continuous perfusion of the preparation. Both bath and "sewer pipe" perfusion were applied by gravity flow. Electrodes were pulled from borosilicate tubing with 1.2 mm outside diameter and 0.69 mm inside diameter (Warner Instrument Corporation) and typical resistances were 20-40 Mohm. Recordings were obtained at room temperature (23-24°C) using an Axopatch 200A amplifier (Axon Instruments). Pulse Control (4.6) and Igor Pro (3.14) were used to manage data acquisition and storage by computer (ITC-16, Instrutech with Quadra 850, Apple or Power Center Pro, Power Computers). Currents were prefiltered by a 2-5 kHz Bessel filter and digitized at 20-100 μs per point. Leak and capacitative currents were subtracted using a P/-4 or P/-8 protocol. Data was analyzed using Igor Pro including macros written by us and other macros kindly provided by Dr. F. Horrigan.

2.5.5 Materials

FM1-43 was from Molecular Probes (Eugene, OR). NPS R-467 was generously donated by NPS pharmaceuticals (Salt Lake City, UT). Other reagents were from Fluka, Aldrich, or Sigma and were of at least ACS grade where applicable.

3 Conclusions

3.1 Summary and Interpretation

Using the synaptosome I have studied two mechanisms of ion channel modulation which may be used by the nerve terminal to accommodate periods of high activity. Synaptosomes are a preparation which allows the bridging of biochemistry and physiology, an attribute which was vital to both projects reported here. By developing the ability to make electrical recordings from synaptosomes I hope my colleague and I have extended the role of the synaptosome in investigating the fascinating and important physiology of the ion channels of the mammalian nerve terminal and the modulatory apparati of those channels.

When BoNtC1 was used to cleave syntaxin, we found an altered pattern of Ca^{2+} entry. Whereas the initial Ca^{2+} rise was unchanged, late Ca^{2+} entry was strongly augmented. Similar results were obtained when Ca^{2+} influx arose from repetitive firing induced by the K^{+}-channel blocker 4-aminopyridine. Cleavage of VAMP with BoNtD or SNAP-25 with BoNtE failed to produce a significant change in Ca^{2+} entry. The BoNtC1-induced alteration in Ca^{2+} signaling was specific to voltage-gated Ca^{2+} channels, not Ca^{2+} extrusion or buffering, and it involved N-, P/Q- and R-type channels, the high voltage-activated channels most intimately associated with presynaptic release machinery. The delay of the development of the BoNtC1 effect, even when Ca^{2+} channels were inactivated before admission of Ca^{2+}, suggested that vesicular turnover may be necessary to make syntaxin available for its stabilizing effect on Ca^{2+} channel inactivation. The requirement for both Ca^{2+} channel inactivation and significant vesicle turnover suggests that this is a mechanism used by the nerve terminal to prevent Ca^{2+} influx in the region of recently released vesicles. This was first proposed (Bezprozvanny et al., 1995) with the thought that such a mechanism might limit what might be considered wasteful Ca^{2+}

influx. Our current theories of synaptic vesicle maturation have a different slant on this idea. If the final zippering of multiple SNARE complexes along the lines proposed by Hanson et al. (1997) is required to cause vesicle fusion, premature Ca^{2+} influx might cause futile zippering of the few matured SNARE complexes on a maturing vesicle before enough have matured to actually drive release. The long time constant for replenishment of the readily releasable pool (~10 s Stevens and Tsujimoto, 1995) supports the idea that such a mechanism could be very useful. Even assuming that only a small fraction of this time is spent assembling the semizippered SNARE complexes, Ca^{2+} influx would reverse the partial maturation achieved by such a vesicle even at moderate firing frequencies.

We have made electrical recordings from synaptosomes and have found that a major component of the membrane current is supported by a novel non-specific cation channel and that this channel is activated by decreases in $[Ca^{2+}]_o$ and membrane depolarization. The responsiveness to $[Ca^{2+}]_o$ is mediated by a distinct receptor that is sensitive to Ca^{2+}, Mg^{2+}, Gd^{3+} and spermidine, but not the phenylalkylamine NPS R-467. This receptor therefore does not appear to be identical to the CaR, however uncertainty about the effect of high $[Ca^{2+}]$ in the recording pipette complicates this conclusion. In any case the receptor may well be related to the CaR, or another mechanism may be involved. This is an area ripe for more experimentation (see below).

Activation of the non-specific cation channel may act to counter the fall in release probability produced by physiological decreases in $[Ca^{2+}]_o$ at the synaptic cleft by broadening subsequent action potentials and countering the decreased electrochemical gradient for Ca^{2+} with an increased duration of Ca^{2+} entry. Other theories are possible however, for example activation of such a channel might significantly outlast the action potential due its slow inactivation and enhance inactivation of Na^+ and Ca^{2+} channels. This would have the opposite effect of the action potential broadening—shutting down

the synapse, possibly allowing it to recover from previous activity.

3.2 Future Directions

3.2.1 Syntaxin Effect on Calcium Channels

3.2.1.1 Corroboration

As with any novel result, corroboration of the effect of syntaxin on nerve terminal VGCCs in another system would be valuable. It is reasonable to believe that the effect may only be seen at the nerve terminal, therefore a nerve terminal which allows the measurement of Ca^{2+} influx is required for such experiments. The imaging methods applied to the synaptosomes might also be applied to cultured neurons or to the cerebellar slice preparation developed by Regehr and colleagues (Sabatini and Regehr, 1995), although concerns about measurement of Ca^{2+} outside of the presynaptic terminal may be a problem. Such concerns might be overcome by attaching proteinaceous Ca^{2+} indicators to presynaptically localized proteins or protein targeting signals such as GAP-43. However an electrophysiological approach would be especially attractive as it would allow for flexible voltage control and better temporal resolution of the early phase of inhibition and its correlation with channel inactivation and possibly even transmitter release. Armed with the detailed kinetic understanding of the syntaxin-Ca^{2+} channel interaction (Degtiar et al., 2000) this might shed light on the fate of syntaxin downstream of vesicle fusion. Any of the large nerve terminals which may be accessed with a recording pipette might be used for such studies. Thus far we have been unable to reliably obtain whole cell or perforated-patch recordings of synaptosomes, but this is also a potential method.

3.2.1.2 $[Ca^{2+}]_i$ dependence

The effect of BoNtC1 was only seen if the synaptosomes were preincubated in nominally zero Ca^{2+} solution, presumably because this preserved a low initial level of $[Ca^{2+}]_i$ (see section 1.6.7). Although we tested for effects of protein kinases it remains unclear

how the basal Ca^{2+} level regulates syntaxin's effects on Ca^{2+} channels, but presumably this result indicates that in higher $[Ca^{2+}]_i$ the syntaxin-channel interaction is prevented. Studies of vesicle trafficking in the nerve terminal have suggested many roles for $[Ca^{2+}]_i$. Unraveling the reason for the change in syntaxin availability may provide important insight into the various roles of Ca^{2+} in the vesicle cycle.

3.2.1.3 Vesicle depletion

Our working hypothesis predicts that depletion of synaptic vesicles would produce excess syntaxin in the state required to inhibit presynaptic Ca^{2+} channels. Indeed, such an effect may have already been demonstrated in *shibire* mutants of *Drosophila,* which undergo a temperature sensitive block of endocytosis due to a defect in dynamin (Kosaka and Ikeda, 1983; Ramaswami et al., 1994). In these experiments Ca^{2+} influx at the fly neuromuscular junction was completely blocked following vesicle depletion (Umbach et al., 1998). However interpretation of these results is complicated by the finding that genetic removal of cysteine string proteins (CSPs) also blocks Ca^{2+} influx (Umbach et al., 1998). CSPs interact with syntaxin (Wu et al., 1999), the II-III loop of P/Q-type Ca^{2+} channels, and VAMP (Leveque et al., 1998), and functionally interact with syntaxin in *Drosophila* (Nie et al., 1999). CSPs have also been shown to have a functional effect on Ca^{2+} channels (Gundersen and Umbach, 1992). These various functional studies are difficult to interpret since they to do not show a direct effect of the protein which is altered. For example removal of CSPs may have a direct inhibitory effect on the Ca^{2+} channel as originally proposed (Gundersen and Umbach, 1992). In contrast if removal of CSPs affects vesicle dynamics or if the CSPs compete with syntaxin for the Ca^{2+} channel synprint site (Wu et al., 1999) then such an intervention may increase the amount of syntaxin available to inhibit the channels. We favor the idea that syntaxin interacts directly with the Ca^{2+} channel because the direct evidence for this functional interaction is the strongest (Bezprozvanny et al., 1995; Wiser et al., 1996; Wiser et al., 1997; Bezprozvanny et al., 2000; Degtiar et al., 2000). While this is not mutually exclusive

prozvanny et al., 2000; Degtiar et al., 2000). While this is not mutually exclusive with a direct effect of CSPs on the Ca^{2+} channel, a more elegant hypothesis would explain the CSP and *shibire* mutants in terms of their effects on syntaxin's interaction with the Ca^{2+} channel.

Unpublished work from co-workers in our laboratory (Erika Piedras-Rentería and Jason Pyle) has recently explored another means of studying Ca^{2+} influx after vesicle depletion. Instead of attempting to deplete all vesicles, they depleted the readily releasable pool of vesicles in cultured neurons by application of hypertonic sucrose (Stevens and Tsujimoto, 1995). This should have the same effect of producing syntaxin in its post-release state. By then challenging the neurons with electrical stimulation they were able to monitor Ca^{2+} influx and assess the effect of vesicle depletion. As predicted from our work, they found that the sucrose prepulse reduces Ca^{2+} influx during the middle of the

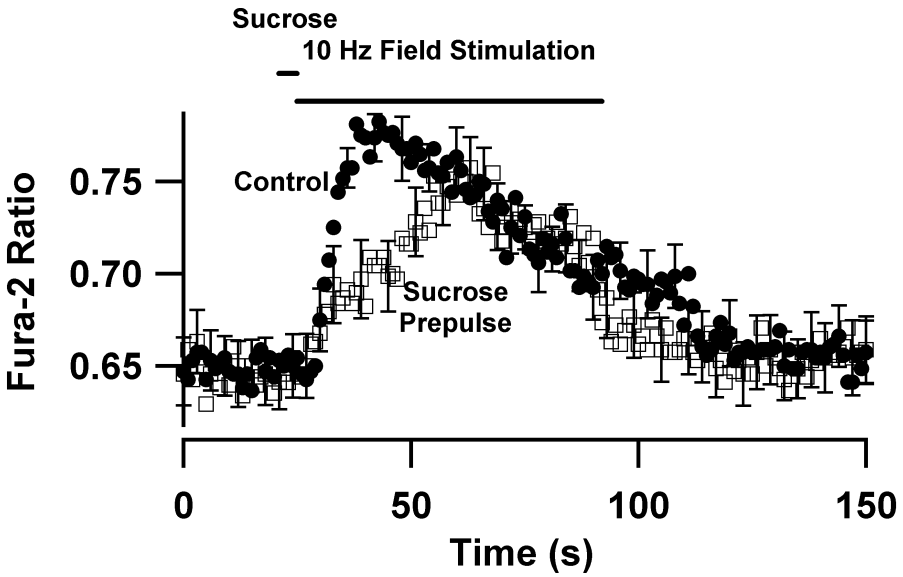

Figure 3-1. Sucrose Prepulse Affects Ca^{2+} Influx

Fura-2 ratio measured at regions on cultured neurons identified as synapses with FM1-43. 10 Hz electrical field stimulation stimulated Ca^{2+} influx and vesicle fusion at the time indicated by the *bar*. In the trace depicted by the *open squares* a 4 s prepulse of hyperosmolar sucrose was given immediately before the field stimulation. *Filled circles* show data without a prepulse. Data are averages +/- SEM from 3 experiments, courtesy of Erika Piedras-Renteria, Jason Pyle, and Richard Tsien.

electrical stimulation (Figure 3-1). We explain their lack of effect early during the stimulation by the lack of inactivated Ca^{2+} channels available to be inhibited, just as in the synaptosomes. Once the channels have inactivated, the channels in the prepulsed terminal are rapidly trapped in this state by the syntaxin made available by the release during sucrose application. Conversely the control terminals must await syntaxin from the only-then-occurring exocytosis. The traces come together late in the stimulation period once both terminals have undergone sufficient exocytosis to produce saturating amounts of syntaxin in the form required to trap the channels.

3.2.2 Recording from Nerve Terminals

3.2.2.1 Extracellular Ca^{2+} sensor and the NSC channel.

We have immediate plans to continue the characterization of the extracellular Ca^{2+} sensor at the nerve terminal. Better control of Ca^{2+} in the pipette should resolve the question of whether the difference in potency of the CaR agonists we have tested is significant. Also the use of pertussis toxin or other G protein-related interventions will establish whether the sensor shares this signaling mechanism with the CaR. One possibility we have considered is that the effect we have seen is mediated by the metabotropic glutamate receptor (mGluR) which is present at the nerve terminal and shares homology with the CaR. Accordingly we plan to test agonists and antagonists of the mGluRs for their effect on the NSC channel.

We also intend to continue to characterize the NSC channel. Establishing with certainty whether it is permeable to Ca^{2+} is our first goal, given the importance of Ca^{2+} influx at the nerve terminal. Additionally we are interested in the method of activation of the channel downstream of the Ca^{2+} sensor. One experiment we will perform in the near future will test for a secretory mode of regulation, similar to that proposed for I_{CRAC} (Yao et al., 1999) by attempting to block their activation with clostridial toxins.

It will be important to test for physiological effects of activation of the NSC. If a specific agent for the Ca^{2+} sensor can be found its effects on release and Ca^{2+} influx during repetitive activity at an intact synapse will help to understand its effect on nerve terminal physiology.

3.2.2.2 Recording other channels

In addition to the NSC channel we have studied, the nerve terminal contains Na^{+}, K^{+}, Ca^{2+}, and other channels. The ability to record these in a functional nerve terminal has already been exploited in large nerve terminals (e.g. Forsythe et al., 1998; Sun et al., 1999), the availability of another preparation with advantages over those currently in use should aid such studies considerably.

4 References

Adams, BA, Tanabe, T, Mikami, A, Numa, S, Beam, KG (1990). Intramembrane charge movement restored in dysgenic skeletal muscle by injection of dihydropyridine receptor cDNAs. Nature 346: 569-572.

Adams, ME, Mintz, IM, Reily, MD, Thanabal, V, Bean, BP (1993). Structure and properties of ω-Agatoxin IVB, a new antagonist of P-type calcium channels. Mol Pharmacol 44: 681-688.

Akaike, N, Kanaide, H, Kuga, T, Nakamura, M, Sadoshima, J, Tomoike, H (1989). Low-voltage-activated calcium current in rat aorta smooth muscle cells in primary culture. J Physiol (Lond) 416: 141-160.

Angelotti, T, Hofmann, F (1996). Tissue-specific expression of splice variants of the mouse voltage-gated calcium channel alpha2/delta subunit. Febs Letters 397: 331-337.

Apparsundaram, S, Sung, U, Kendall, D, Blakely, RD. Regulated association of syntaxin I with norepinephrine transporters. 28th Annual Meeting of the Society for Neuroscience, Vol 1, p113.112, 1998.

Araque, A, Clarac, F, Buno, W (1994). P-type Ca^{2+} channels mediate excitatory and inhibitory synaptic transmitter release in crayfish muscle. Proc Natl Acad Sci USA 91: 4224-4228.

Ashcroft, FM, Proks, P, Smith, PA, Ammala, C, Bokvist, K, Rorsman, P (1994). Stimulus-secretion coupling in pancreatic β cells. J Cell Biochem 55: 54-65.

Assaf, SY, Chung, SH (1984). Release of endogenous Zn^{2+} from brain tissue during activity. Nature 308: 734-736.

Atar, D, Backx, PH, Appel, MM, Gao, WD, Marban, E (1995). Excitation-transcription coupling mediated by zinc influx through voltage-dependent calcium channels. J Biol Chem 270: 2473-2477.

Augustine, GJ, Charlton, MP, Smith, SJ (1985). Calcium entry and transmitter release at voltage-clamped nerve terminals of squid. J Physiol (Lond) 367: 163-181.

Avery, RA, Johnston, D (1996). Multiple channel types contribute to the low-voltage-activated calcium current in hippocampal CA3 pyramidal neurons. J Neurosci 16: 5567-5582.

Bean, BP (1985). Two kinds of calcium channels in canine atrial cells. Differences in kinetics, selectivity, and pharmacology. J Gen Physiol 86: 1-30.

Bech-Hansen, NT, Naylor, MJ, Maybaum, TA, Pearce, WG, Koop, B, Fishman, GA, Mets, M, Musarella, MA, Boycott, KM (1998). Loss-of-function mutations in a calcium-channel alpha1-subunit gene in Xp11.23 cause incomplete X-linked congenital stationary night blindness. Nature Genetics 19: 264-267.

Beckman, ML, Bernstein, EM, Quick, MW (1998). Protein kinase C regulates the interaction between a GABA transporter and syntaxin 1A. J Neurosci 18: 6103-6112.

Benardo, LS, Masukawa, LM, Prince, DA (1982). Electrophysiology of isolated hippocampal pyramidal dendrites. J Neurosci 2: 1614-1622.

Bergsman, JB, Tsien, RW. Testing for botulinum toxin type C1 effect on calcium flux in rat neocortical synaptosomes. J Gen Phys, Vol 108, 1996.

Betz, WJ, Mao, F, Smith, CB (1996). Imaging exocytosis and endocytosis. Curr Opin Neurobiol 6: 365-371.

Bezprozvanny, I, Scheller, RH, Tsien, RW (1995). Functional impact of syntaxin on gating of N-type and Q-type calcium channels. Nature 378: 623-626.

Bezprozvanny, IB, Zhong, P, Scheller, RH, Tsien, RW (2000). Molecular determinants of the functional interaction between syntaxin and N-type Ca^{2+} channel gating. In preparation.

Bindokas, VP, Venema, VJ, Adams, ME (1991). Differential antagonism of transmitter release by subtypes of ω-Agatoxins. J Neurophysiol 66: 590-601.

Birnbaumer, L, Campbell, KP, Catterall, WA, Harpold, MM, Hofmann, F, Horne, WA, Mori, Y, Schwartz, A, Snutch, TP, Tanabe, T, Tsien, RW (1994). The naming of voltage-gated calcium channels. Neuron 13: 505-506.

Black, JL, 3rd, Lennon, VA (1999). Identification and cloning of putative human neuronal voltage-gated calcium channel gamma-2 and gamma-3 subunits: neurologic implications. Mayo Clinic Proceedings 74: 357-361.

Blasi, J, Chapman, ER, Link, E, Binz, T, Yamasaki, S, De Camilli, P, Sudhof, TC, Niemann, H, Jahn, R (1993a). Botulinum neurotoxin A selectively cleaves the synaptic protein SNAP-25 [see comments]. Nature 365: 160-163.

Blasi, J, Chapman, ER, Yamasaki, S, Binz, T, Niemann, H, Jahn, R (1993b). Botulinum neurotoxin C1 blocks neurotransmitter release by means of cleaving HPC-1/syntaxin. EMBO J 12: 4821-4828.

Blaustein, MP (1975). Effects of potassium, veratridine, and scorpion venom on calcium accumulation and transmitter release by nerve terminals in vitro. J Physiol (Lond) 247: 617-655.

Blaustein, MP, Goldring, JM (1975). Membrane potentials in pinched-off presynaptic nerve terminals monitored with a fluorescent probe: evidence that synaptosomes have potassium diffusion potentials. J Physiol (Lond) 247: 589-615.

Blaustein, MP, McGraw, CF, Somlyo, AV, Schweitzer, ES (1980). How is the cytoplasmic calcium concentration controlled in nerve terminals? J Physiol (Paris) 76: 459-470.

Bokvist, K, Eliasson, L, Ammala, C, Renstrom, E, Rorsman, P (1995). Co-localization of L-type Ca^{2+} channels and insulin-containing secretory granules and its significance for the initiation of exocytosis in mouse pancreatic β-cells. EMBO J 14: 50-57.

Bonci, A, Grillner, P, Mercuri, NB, Bernardi, G (1998). L-Type calcium channels mediate a slow excitatory synaptic transmission in rat midbrain dopaminergic neurons. J Neurosci 18: 6693-6703.

Borst, JGG, Sakmann, B (1999). Depletion of calcium in the synaptic cleft of a calyx-type synapse in the rat brainstem. J Physiol 521.1: 123-133.

Bosse, E, Regulla, S, Biel, M, Ruth, P, Meyer, HE, Flockerzi, V, Hofmann, F (1990). The cDNA and deduced amino acid sequence of the γ subunit of the L-type calcium channel from rabbit skeletal muscle. Febs Lett 267: 153-156.

Bourinet, E, Soong, TW, Sutton, K, Slaymaker, S, Mathews, E, Monteil, A, Zamponi, GW, Nargeot, J, Snutch, TP (1999). Splicing of alpha 1A subunit gene generates phenotypic variants of P- and Q-type calcium channels. Nat Neurosci 2: 407-415.

Bourinet, E, Zamponi, GW, Stea, A, Soong, TW, Lewis, BA, Jones, LP, Yue, DT, Snutch, TP (1996). The alpha 1E calcium channel exhibits permeation properties similar to low-voltage-activated calcium channels. J Neurosci 16: 4983-4993.

Bowersox, SS, Miljanich, GP, Sugiura, Y, Li, C, Nadasdi, L, Hoffman, BB, Ramachandran, J, Ko, CP (1995). Differential blockade of voltage-sensitive calcium channels at the mouse neuromuscular junction by novel ω-Conopeptides and ω-Agatoxin-IVA. J Pharmacol Exp Ther 273: 248-256.

Brown, EM (1991). Extracellular Ca^{2}+ sensing, regulation of parathyroid cell function, and role of Ca^{2+} and other ions as extracellular (first) messengers. Physiological Reviews 71: 371-411.

Brown, EM (1999). Physiology and pathophysiology of the extracellular calcium-sensing receptor. American Journal of Medicine 106: 238-253.

Brown, EM, Gamba, G, Riccardi, D, Lombardi, M, Butters, R, Kifor, O, Sun, A, Hediger, MA, Lytton, J, Hebert, SC (1993). Cloning and characterization of an extracellular Ca^{2+}-sensing receptor from bovine parathyroid. Nature 366: 575-580.

Campbell, KP, Leung, AT, Sharp, AH (1988). The biochemistry and molecular biology of the dihydropyridine-sensitive calcium channel. Trends Neurosci 11: 425-430.

Capogna, M, McKinney, RA, O'Connor, V, Gähwiler, BH, Thompson, SM (1997). Ca^{2+} or Sr^{2+} partially rescues synaptic transmission in hippocampal cultures treated with botulinum toxin A and C, but not tetanus toxin. J Neurosci 17: 7190-7202.

Carbone, E, Lux, HD (1984). A low voltage-activated, fully inactivating Ca^{2+} channel in vertebrate sensory neurones. Nature 310: 501-502.

Castillo, PE, Weisskopf, MG, Nicoll, RA (1994). The role of Ca^{2+} channels in hippocampal mossy fiber synaptic transmission and long-term potentiation. Neuron 12: 261-269.

Catterall, WA, Curtis, BM (1987). Molecular properties of voltage-sensitive calcium channels. Soc Gen Physiol Ser 41: 201-213.

Catterall, WA, Seagar, MJ, Takahashi, M (1988). Molecular properties of dihydropyridine-sensitive calcium channels in skeletal muscle. J Biol Chem 263: 3535-3538.

Charton, G, Rovira, C, Ben-Ari, Y, Leviel, V (1985). Spontaneous and evoked release of endogenous Zn^{2+} in the hippocampal mossy fiber zone of the rat *in situ*. Exp Brain Res 58: 202-205.

Charvin, N, L'Eveque, C, Walker, D, Berton, F, Raymond, C, Kataoka, M, Shoji-Kasai, Y, Takahashi, M, De Waard, M, Seagar, MJ (1997). Direct interaction of the calcium sensor protein synaptotagmin I with a cytoplasmic domain of the alpha1A subunit of the P/Q-type calcium channel. EMBO J 16: 4591-4596.

Chen, YA, Scales, SJ, Patel, SM, Doung, YC, Scheller, RH (1999). SNARE complex formation is triggered by Ca2+ and drives membrane fusion. Cell 97: 165-174.

Chuang, RS, Jaffe, H, Cribbs, L, Perez-Reyes, E, Swartz, KJ (1998). Inhibition of T-type voltage-gated calcium channels by a new scorpion toxin. Nat Neurosci 1: 668-674.

Cohen, CJ, McCarthy, RT (1987). Nimodipine block of calcium channels in rat anterior pituitary cells. J Physiol (Lond) 387: 195-225.

Colasante, C, Meunier, FA, Kreger, AS, Molgó, J (1996). Selective depletion of clear synaptic vesicles and enhanced quantal transmitter release at frog motor nerve endings produced by trachynilysin, a protein toxin isolated from stonefish (Synanceia trachynis) venom. Eur J Neurosci 8: 2149-2156.

Cribbs, LL, Lee, JH, Yang, J, Satin, J, Zhang, Y, Daud, A, Barclay, J, Williamson, MP, Fox, M, Rees, M, Perez-Reyes, E (1998). Cloning and characterization of alpha1H from human heart, a member of the T-type Ca2+ channel gene family. Circulation Research 83: 103-109.

De Jongh, KS, Warner, C, Catterall, WA (1990). Subunits of purified calcium channels. α_2 and δ are encoded by the same gene. J Biol Chem 265: 14738-14741.

De Luca, A, Rand, MJ, Reid, JJ, Story, DF (1991). Differential sensitivities of avian and mammalian neuromuscular junctions to inhibition of cholinergic transmission by ω-Conotoxin GVIA. Toxicon 29: 311-320.

De Waard, M, Gurnett, CA, Campbell, KP. (1996). Structural and functional diversity of voltage-activated calcium channels. In Ion Channels, T Narahashi, ed. (New York: Plenum Press), pp. 41-87.

Degtiar, VE, Scheller, RH, Tsien, RW (2000). Syntaxin Modulation of Slow Inactivation Of N-type Calcium Channels. Submitted.

Deisseroth, K, Bito, H, Tsien, RW (1996). Signaling from synapse to nucleus: postsynaptic CREB phosphorylation during multiple forms of hippocampal synaptic plasticity. Neuron 16: 89-101.

Deisseroth, K, Heist, EK, Tsien, RW (1998). Translocation of calmodulin to the nucleus supports CREB phosphorylation in hippocampal neurons. Nature 392: 198-202.

Dippel, WW, Chen, PL, McArthur, NH, Harms, PG (1995). Calcium involvement in luteinizing hormone-releasing hormone release from the bovine infundibulum. Domest Anim Endocrinol 12: 349-354.

Dodge, F, Jr., Rahamimoff, R (1967). Co-operative action a calcium ions in transmitter release at the neuromuscular junction. J Physiol 193: 419-432.

Douglas, WW (1968). Stimulus-secretion coupling: the concept and clues from chromaffin and other cells. Br J Pharmacol 34: 453-474.

Douglas, WW, Rubin, RP (1963). The Mechanism of Catecholamine Release From the Adrenal Medulla and the Role of Calcium in Stimulus-Secretion Coupling. J Physiol 167: 288-310.

Droogmans, G, Nilius, B (1989). Kinetic properties of the cardiac T-type calcium channel in the guinea-pig. J Physiol (Lond) 419: 627-650.

Duarte, CB, Ferreira, IL, Santos, PF, Oliveira, CR, Carvalho, AP (1992). Ca^{2+}-dependent release of [^{3}H]GABA in cultured chick retina cells. Brain Res 591: 27-32.

Dubel, SJ, Starr, TV, Hell, J, Ahlijanian, MK, Enyeart, JJ, Catterall, WA, Snutch, TP (1992). Molecular cloning of the alpha-1 subunit of an omega-conotoxin-sensitive calcium channel. Proc Natl Acad Sci USA 89: 5058-5062.

Dunlap, K, Luebke, JI, Turner, TJ (1995). Exocytotic Ca^{2+} channels in mammalian central neurons. Trends Neurosci 18: 89-98.

Eberst, R, Dai, S, Klugbauer, N, Hofmann, F (1997). Identification and functional characterization of a calcium channel gamma subunit. Pflugers Archiv European Journal of Physiology 433: 633-637.

Edmonds, B, Klein, M, Dale, N, Kandel, ER (1990). Contributions of two types of calcium channels to synaptic transmission and plasticity. Science 250: 1142-1147.

Egelman, DM, Montague, PR (1998). Computational properties of peri-dendritic calcium fluctuations. J Neurosci 18: 8580-8589.

Egelman, DM, Montague, PR (1999). Calcium dynamics in the extracellular space of mammalian neural tissue. Biophys J 76: 1856-1867.

Ehrlich, BE, Jacobson, AR, Hinrichsen, R, Sayre, LM, Forte, MA (1988). Paramecium calcium channels are blocked by a family of calmodulin antagonists. Proc Natl Acad Sci USA 85: 5718-5722.

Eisenberg, RS, McCarthy, RT, Milton, RL (1983). Paralysis of frog skeletal muscle fibres by the calcium antagonist D-600. J Physiol (Lond) 341: 495-505.

el Far, O, Charvin, N, Leveque, C, Martin-Moutot, N, Takahashi, M, Seagar, MJ (1995). Interaction of a synaptobrevin (VAMP)-syntaxin complex with presynaptic calcium channels. Febs Lett 361: 101-105.

el-Hayek, R, Antoniu, B, Wang, J, Hamilton, SL, Ikemoto, N (1995). Identification of calcium release-triggering and blocking regions of the II-III loop of the skeletal muscle dihydropyridine receptor. J Biol Chem 270: 22116-22118.

Ellinor, PT, Zhang, J-F, Randall, AD, Zhou, M, Schwarz, TL, Tsien, RW, Horne, WA (1993). Functional expression of a rapidly inactivating neuronal calcium channel. Nature 363: 455-458.

Ellis, SB, Williams, ME, Ways, NR, Brenner, R, Sharp, AH, Leung, AT, Campbell, KP, McKenna, E, Koch, WJ, Hui, A (1988). Sequence and expression of mRNAs encoding the α_1 and α_2 subunits of a DHP-sensitive calcium channel. Science 241: 1661-1664.

Ertel, SI, Ertel, EA (1997). Low-voltage-activated T-type Ca^{2+} channels. Trend Pharmacol Sci 18: 37-42.

Fabi, F, Chiavarelli, M, Argiolas, L, Chiavarelli, R, del Basso, P (1993). Evidence for sympathetic neurotransmission through presynaptic N-type calcium channels in human saphenous vein. Br J Pharmacol 110: 338-342.

Feng, TP (1936). Studies on the neuromuscular junction II. The universal antagonism between calcium and curarizing agencies. Chin J Physiol 10: 513-528.

Finkelstein, A, Rubin, LL, Tzeng, MC (1976). Black widow spider venom: effect of purified toxin on lipid bilayer membranes. Science 193: 1009-1011.

Fisher, SE, Ciccodicola, A, Tanaka, K, Curci, A, Desicato, S, D'Urso, M, Craig, IW (1997). Sequence-based exon prediction around the synaptophysin locus reveals a gene-rich area containing novel genes in human proximal Xp. Genomics 45: 340-347.

Fisher, TE, Bourque, CW (1995). Distinct omega-agatoxin-sensitive calcium currents in somata and axon terminals of rat supraoptic neurones. Journal of Physiology 489: 383-388.

Florman, HM, Corron, ME, Kim, TD, Babcock, DF (1992). Activation of voltage-dependent calcium channels of mammalian sperm is required for zona pellucida-induced acrosomal exocytosis. Dev Biol 152: 304-314.

Fontana, G, Blaustein, MP (1993). Calcium buffering and free Ca^{2+} in rat brain synaptosomes. J Neurochem 60: 843-850.

Foran, P, Lawrence, GW, Shone, CC, Foster, KA, Dolly, JO (1996). Botulinum neurotoxin C1 cleaves both syntaxin and SNAP-25 in intact and permeabilized chromaffin cells: correlation with its blockade of catecholamine release. Biochemistry 35: 2630-2636.

Forsythe, ID, Tsujimoto, T, Barnes-Davies, M, Cuttle, MF, Takahashi, T (1998). Inactivation of presynaptic calcium current contributes to synaptic depression at a fast central synapse. Neuron 20: 797-807.

Forti, L, Pietrobon, D (1993). Functional diversity of L-type calcium channels in rat cerebellar neurons. Neuron 10: 437-450.

Frankenhaeuser, B, Hodgkin, AL (1957). The Action of Calcium on the Electrical Properties of Squid Axons. J Physiol 137: 218-244.

Frew, R, Lundy, PM (1995). A role for Q type Ca^{2+} channels in neurotransmission in the rat urinary bladder. Br J Pharmacol 116: 1595-1598.

Fried, RC, Blaustein, MP (1978). Retrieval and recycling of synaptic vesicle membrane in pinched-off nerve terminals (synaptosomes). J Cell Biol 78: 685-700.

Fujita, Y, Mynlieff, M, Dirksen, RT, Kim, MS, Niidome, T, Nakai, J, Friedrich, T, Iwabe, N, Miyata, T, Furuichi, T, Furutama, D, Mikoshiab, K, Mori, Y, Beam, KG (1993). Primary structure and functional expression of the omega-Conotoxin-sensitive N-type calcium channel from rabbit brain. Neuron 10: 585-598.

Garcia, J, Tanabe, T, Beam, KG (1994). Relationship of calcium transients to calcium currents and charge movements in myotubes expressing skeletal and cardiac dihydropyridine receptors. J Gen Physiol 103: 125-147.

Garrett, JE, Tamir, H, Kifor, O, Simin, RT, Rogers, KV, Mithal, A, Gagel, RF, Brown, EM (1995). Calcitonin-secreting cells of the thyroid express an extracellular calcium receptor gene. Endocrinology 136: 5202-5211.

Ghosh, A, Ginty, DD, Bading, H, Greenberg, ME (1994). Calcium regulation of gene expression in neuronal cells. J Neurobiol 25: 294-303.

Gillard, SE, Volsen, SG, Smith, W, Beattie, RE, Bleakman, D, Lodge, D (1997). Identification of pore-forming subunit of P-type calcium channels: an antisense study on rat cerebellar Purkinje cells in culture. Neuropharmacology 36: 405-409.

Glossmann, H, Striessnig, J (1990). Molecular properties of calcium channels. Rev Physiol Biochem Pharmacol 114: 1-105.

Glossmann, H, Striessnig, J, Hymel, L, Schindler, H (1987). Purified L-type calcium channels: only one single polypeptide (α_1-subunit) carries the drug receptor domains and is regulated by protein kinases. Biomed Biochim Acta 46: S351-356.

Gonzalez, GA, Montminy, MR (1989). Cyclic AMP stimulates somatostatin gene transcription by phosphorylation of CREB at serine 133. Cell 59: 675-680.

Grabner, M, Bachmann, A, Rosenthal, F, Striessnig, J, Schultz, C, Tautz, D, Glossmann, H (1994). Insect calcium channels. Molecular cloning of an α_1-subunit from housefly (*Musca domestica*) muscle. FEBS Lett 339: 189-194.

Grantham, CJ, Bowman, D, Bath, CP, Bell, DC, Bleakman, D (1994). Omega-conotoxin MVIIC reversibly inhibits a human N-type calcium channel and calcium influx into chick synaptosomes. Neuropharmacology 33: 255-258.

Gray, DB, Bruses, JL, Pilar, GR (1992). Developmental switch in the pharmacology of Ca^{2+} channels coupled to acetylcholine release. Neuron 8: 715-724.

Greenberg, ME, Thompson, MA, Sheng, M (1992). Calcium regulation of immediate early gene transcription. J Physiol (Paris) 86: 99-108.

Grolleau, F, Lapied, B (1996). Two distinct low-voltage-activated Ca^{2+} currents contribute to the pacemaker mechanism in cockroach dorsal unpaired median neurons. Journal of Neurophysiology 76: 963-976.

Grynkiewicz, G, Poenie, M, Tsien, RY (1985). A new generation of Ca^{2+} indicators with greatly improved fluorescence properties. J Biol Chem 260: 3440-3450.

Gundersen, CB, Umbach, JA (1992). Suppression cloning of the cDNA for a candidate subunit of a presynaptic calcium channel. Neuron 9: 527-537.

Hagiwara, N, Irisawa, H, Kameyama, M (1988). Contribution of two types of calcium currents to the pacemaker potentials of rabbit sino-atrial node cells. J Physiol 395: 233-253.

Hamill, OP, Marty, A, Neher, E, Sakmann, B, Sigworth, FJ (1981). Improved patch-clamp techniques for high-resolution current recording from cells and cell-free membrane patches. Pflügers Arch 391: 85-100.

Hammerland, LG, Garrett, JE, Hung, BCP, Levinthal, C, Nemeth, EF (1998). Allosteric activation of the Ca^{2+} receptor expressed in Xenopus laevis oocytes by NPS 467 or NPS 568. Molecular Pharmacology 53: 1083-1088.

Hanson, PI, Heuser, JE, Jahn, R (1997). Neurotransmitter release - four years of SNARE complexes. Current Opinion in Neurobiology 7: 310-315.

Hayashi, T, McMahon, H, Yamasaki, S, Binz, T, Hata, Y, Sudhof, TC, Niemann, H (1994). Synaptic vesicle membrane fusion complex: action of clostridial neurotoxins on assembly. EMBO J 13: 5051-5061.

Hell, JW, Westenbroek, RE, Warner, C, Ahlijanian, MK, Prystay, W, Gilbert, MM, Snutch, TP, Catterall, WA (1993a). Identification and differential subcellular localization of the neuronal class C and class D L-type calcium channel α_1 subunits. J Cell Biol 123: 949-962.

Hell, JW, Yokoyama, CT, Wong, ST, Warner, C, Snutch, TP, Catterall, WA (1993b). Differential phosphorylation of two size forms of the neuronal class C L-type calcium channel α_1 subunit. J Biol Chem 268: 19451-19457.

Hill, CS, Treisman, R (1995). Transcriptional regulation by extracellular signals: mechanisms and specificity. Cell 80: 199-211.

Hille, B (1994). Modulation of ion-channel function by G-protein-coupled receptors. Trends Neurosci 17: 531-536.

Hillyard, DR, Monje, VD, Mintz, IM, Bean, BP, Nadasdi, L, Ramachandran, J, Miljanich, G, Azimi-Zoonooz, A, McIntosh, JM, Cruz, LJ, et, a (1992). A new Conus peptide ligand for mammalian presynaptic Ca^{2+} channels. Neuron 9: 69-77.

Hirning, LD, Fox, AP, McCleskey, EW, Olivera, BM, Thayer, SA, Miller, RJ, Tsien, RW (1988). Dominant role of N-type Ca2+ channels in evoked release of norepinephrine from sympathetic neurons. Science 239: 57-61.

Hoeffler, JP, Meyer, TE, Yun, Y, Jameson, JL, Habener, JF (1988). Cyclic AMP-responsive DNA-binding protein: structure based on a cloned placental cDNA. Science 242: 1430-1433.

Hofmann, F, Biel, M, Flockerzi, V (1994). Molecular basis for Ca^{2+} channel diversity. Annu Rev Neurosci 17: 399-418.

Hofmann, F, Oeken, HJ, Schneider, T, Sieber, M (1988). The biochemical properties of L-type calcium channels. J Cardiovasc Pharmacol 12: S25-30.

Hong, SJ, Chang, CC (1995). Inhibition of acetylcholine release from mouse motor nerve by a P-type calcium channel blocker, ω-Agatoxin IVA. J Physiol (Lond) 482: 283-290.

Horne, WA, Ellinor, PT, Inman, I, Zhou, M, Tsien, RW, Schwarz, TL (1993). Molecular diversity of Ca^{2+} channel α_1 subunits from the marine ray *Discopyge ommata*. Proc Natl Acad Sci USA 90: 3787-3791.

Howell, GA, Welch, MG, Frederickson, CJ (1984). Stimulation-induced uptake and release of zinc in hippocampal slices. Nature 308: 736-738.

Hughes, D, McBurney, RN, Smith, SM, Zorec, R (1987). Caesium ions activate chloride channels in rat cultured spinal cord neurones. Journal of Physiology 392: 231-251.

Huguenard, JR, Prince, DA (1992). A novel T-type current underlies prolonged Ca^{2+}-dependent burst firing in GABAergic neurons of rat thalamic reticular nucleus. J Neurosci 12: 3804-3817.

Isom, LL, De Jongh, KS, Catterall, WA (1994). Auxiliary subunits of voltage-gated ion channels. Neuron 12: 1183-1194.

Jaffe, DB, Johnston, D, Lasser-Ross, N, Lisman, JE, Miyakawa, H, Ross, WN (1992). The spread of Na^+ spikes determines the pattern of dendritic Ca^{2+} entry into hippocampal neurons. Nature 357: 244-246.

Jahnsen, H, Llinás, R (1984). Ionic basis for the electro-responsiveness and oscillatory properties of guinea-pig thalamic neurones *in vitro*. J Physiol 349: 227-247.

Jay, SD, Ellis, SB, McCue, AF, Williams, ME, Vedvick, TS, Harpold, MM, Campbell, KP (1990). Primary structure of the γ subunit of the DHP-sensitive calcium channel from skeletal muscle. Science 248: 490-492.

Jay, SD, Sharp, AH, Kahl, SD, Vedvick, TS, Harpold, MM, Campbell, KP (1991). Structural characterization of the dihydropyridine-sensitive calcium channel α_2-subunit and the associated δ peptides. J Biol Chem 266: 3287-3293.

Jeziorski, MC, Greenberg, RM, Clark, KS, Anderson, PA (1998). Cloning and functional expression of a voltage-gated calcium channel alpha1 subunit from jellyfish. J Biol Chem 273: 22792-22799.

Jun, K-S, Piedras-Rentería, ES, Smith, SM, Wheeler, DB, Lee, SB, Lee, TG, Chin, H, Adams, ME, Scheller, RH, Tsien, RW, Shin, H-S (1999). Ablation of P/Q-type Ca^{2+} channel currents and progressive, fatal ataxia in mice lacking the a1A subunit. Proc Natl Acad Sci USA In Press.

Karst, H, Joëls, M, Wadman, WJ (1993). Low-threshold calcium current in dendrites of the adult rat hippocampus. Neuroscience Letters 164: 154-158.

Katz, B. (1969) The Release of Neural Transmitter Substances (Liverpool: Liverpool University Press).

Katz, B, Miledi, R (1965). The effect of calcium on acetylcholine release from motor nerve terminals. Proc R Soc B 161: 496-503.

Katz, E, Ferro, PA, Cherksey, BD, Sugimori, M, Llinas, R, Uchitel, OD (1995). Effects of Ca^{2+} channel blockers on transmitter release and presynaptic currents at the frog neuromuscular junction. J Physiol (Lond) 486: 695-706.

Kavalali, ET, Plummer, MR (1994). Selective potentiation of a novel calcium channel in rat hippocampal neurones. J Physiol 480: 475-484.

Kavalali, ET, Zhuo, M, Bito, H, Tsien, RW (1997). Dendritic Ca^{2+} channels characterized by recordings from isolated hippocampal dendritic segments. Neuron 18: 651-663.

Kerr, LM, Yoshikami, D (1984). A venom peptide with a novel presynaptic blocking action. Nature 308: 282-284.

Kim, DK, Catterall, WA (1997). Ca^{2+}-dependent and -independent interactions of the isoforms of the alpha1A subunit of brain Ca2+ channels with presynaptic SNARE proteins. Proc Natl Acad Sci USA 94: 14782-14786.

Kleyman, TR, Cragoe, EJ, Jr. (1988). Amiloride and its analogs as tools in the study of ion transport. J Membr Biol 105: 1-21.

Klingauf, J, Kavalali, ET, Tsien, RW (1998). Kinetics and regulation of fast endocytosis at hippocampal synapses. Nature 394: 581-585.

Klugbauer, N, Lacinová, L, Marais, E, Hobom, M, Hofmann, F (1999). Molecular diversity of the calcium channel alpha2delta subunit. J Neurosci 19: 684-691.

Koh, DS, Hille, B (1996). Modulation by neurotransmitters of norepinephrine secretion from sympathetic ganglion neurons detected by amperometry. Soc Neurosci Abstr 22: 507.

Kollmar, R, Fak, J, Montgomery, LG, Hudspeth, AJ (1997). Hair cell-specific splicing of mRNA for the alpha1D subunit of voltage-gated Ca^{2+} channels in the chicken's cochlea. Proc Natl Acad Sci USA 94: 14889-14893.

Kosaka, T, Ikeda, K (1983). Possible temperature-dependent blockage of synaptic vesicle recycling induced by a single gene mutation in Drosophila. Journal of Neurobiology 14: 207-225.

Kostyuk, PG, Shirokov, RE (1989). Deactivation kinetics of different components of calcium inward current in the membrane of mice sensory neurones. J Physiol 409: 343-355.

Kuga, T, Kobayashi, S, Hirakawa, Y, Kanaide, H, Takeshita, A (1996). Cell cycle-dependent expression of L- and T-type Ca^{2+} currents in rat aortic smooth muscle cells in primary culture. Circ Res 79: 14-19.

Lacinová, L, Klugbauer, N, Hofmann, F (1999). Absence of modulation of the expressed calcium channel alpha1G subunit by alpha2delta subunits. Journal of Physiology 516: 639-645.

Lambert, RC, Maulet, Y, Mouton, J, Beattie, R, Volsen, S, De Waard, M, Feltz, A (1997). T-type Ca^{2+} current properties are not modified by Ca^{2+} channel beta subunit depletion in nodosus ganglion neurons. J Neurosci 17: 6621-6628.

Lee, JH, Daud, AN, Cribbs, LL, Lacerda, AE, Pereverzev, A, Klöckner, U, Schneider, T, Perez-Reyes, E (1999). Cloning and expression of a novel member of the low voltage-activated T-type calcium channel family. J Neurosci 19: 1912-1921.

Lei, M, Brown, H, Noble, D. Low-Voltage-Activated T-Type Calcium Channels. International Electrophysiology Meeting, Vol p103-109, 1998.

Lemos, JR, Nowycky, MC (1989). Two types of calcium channels coexist in peptide-releasing vertebrate nerve terminals. Neuron 2: 1419-1426.

Letts, VA, Felix, R, Biddlecome, GH, Arikkath, J, Mahaffey, CL, Valenzuela, A, Bartlett, FS, 2nd, Mori, Y, Campbell, KP, Frankel, WN (1998). The mouse stargazer gene encodes a neuronal Ca^{2+}-channel gamma subunit [see comments]. Nature Genetics 19: 340-347.

Leuranguer, V, Bourinet, E, Lory, P, Nargeot, J (1998). Antisense depletion of beta-subunits fails to affect T-type calcium channels properties in a neuroblastoma cell line. Neuropharmacology 37: 701-708.

Leveque, C, Pupier, S, Marqueze, B, Geslin, L, Kataoka, M, Takahashi, M, De Waard, M, Seagar, M (1998). Interaction of cysteine string proteins with the alpha1A subunit of the P/Q-type calcium channel. J Biol Chem 273: 13488-13492.

Lewis, CA (1979). Ion-concentration dependence of the reversal potential and the single channel conductance of ion channels at the frog neuromuscular junction. Journal of Physiology 286: 417-445.

Lin, Z, Haus, S, Edgerton, J, Lipscombe, D (1997). Identification of functionally distinct isoforms of the N-type Ca channel in rat sympathetic ganglia and brain. J Neurosci in press.

Lin, Z, Lin, Y, Schorge, S, Pan, JQ, Beierlein, M, Lipscombe, D (1999). Alternative splicing of a short cassette exon in alpha1B generates functionally distinct N-type calcium channels in central and peripheral neurons. J Neurosci 19: 5322-5331.

Lindgren, CA, Moore, JW (1989). Identification of ionic currents at presynaptic nerve endings of the lizard. J Physiol (Lond) 414: 201-222.

Liu, H, De Waard, M, Scott, VES, Gurnet, CA, Lennon, VA, Campbell, KP (1996). Indentification of three subnuits of the high affinity omega-conotoxin MVIIC-sensitive Ca^{2+} channel. J Biol Chem 271: 13804-13810.

Llinás, R, Hess, R (1976). Tetrodotoxin-resistant dendritic spikes in avian Purkinje cells. Proc Natl Acad Sci USA 73: 2520-2523.

Llinás, R, Nicholson, C (1971). Electrophysiological properties of dendrites and somata in alligator Purkinje cells. J Neurophysiol 34: 532-551.

Llinás, R, Nicholson, C (1975). Calcium role in depolarization-secretion coupling: an aequorin study in squid giant synapse. Proc Natl Acad Sci USA 72: 187-190.

Llinás, R, Steinberg, IZ, Walton, K (1981). Relationship between presynaptic calcium current and postsynaptic potential in squid giant synapse. Biophys J 33: 323-351.

Llinás, R, Sugimori, M (1980). Electrophysiological properties of *in vitro* Purkinje cell dendrites in mammalian cerebellar slices. J Physiol 305: 197-213.

Llinás, R, Sugimori, M, Hillman, DE, Cherksey, B (1992). Distribution and functional significance of the P-type, voltage-dependent Ca^{2+} channels in the mammalian central nervous system. Trends Neurosci 15: 351-355.

Llinás, RR, Sugimori, M, Cherksey, B (1989). Voltage-dependent calcium conductances in mammalian neurons: the P channel. Ann N Y Acad Sci 560: 103-111.

Lopez, MG, Albillos, A, de la Fuente, MT, Borges, R, Gandia, L, Carbone, E, Garcia, AG, Artalejo, AR (1994). Localized L-type calcium channels control exocytosis in cat chromaffin cells. Pflügers Arch 427: 348-354.

Lu, J, Dalton, JFt, Stokes, DR, Calabrese, RL (1997). Functional role of Ca^{2+} currents in graded and spike-mediated synaptic transmission between leech heart interneurons. Journal of Neurophysiology 77: 1779-1794.

Lu, X, Xu, L, Meissner, G (1994). Activation of the skeletal muscle calcium release channel by a cytoplasmic loop of the dihydropyridine receptor. J Biol Chem 269: 6511-6516.

Lu, X, Xu, L, Meissner, G (1995). Phosphorylation of dihydropyridine receptor II-III loop peptide regulates skeletal muscle calcium release channel function. Evidence for an essential role of the β-OH group of Ser687. J Biol Chem 270: 18459-18464.

Luebke, JI, Dunlap, K, Turner, TJ (1993). Multiple calcium channel types control glutamatergic synaptic transmission in the hippocampus. Neuron 11: 895-902.

Lundy, PM, Hamilton, MG, Frew, R (1994). Pharmacological identification of a novel Ca^{2+} channel in chicken brain synaptosomes. Brain Research 643: 204-210.

Magee, JC, Christofi, G, Miyakawa, H, Christie, B, Lasser-Ross, N, Johnston, D (1995). Subthreshold synaptic activation of voltage-gated Ca^{2+} channels mediates a localized Ca^{2+} influx into the dendrites of hippocampal pyramidal neurons. J Neurophysiol 74: 1335-1342.

Magee, JC, Johnston, D (1995). Characterization of single voltage-gated Na^{+} and Ca^{2+} channels in apical dendrites of rat CA1 pyramidal neurons. J Physiol 487: 67-90.

Maguire, G, Maple, B, Lukasiewicz, P, Werblin, F (1989). γ-Aminobutyrate type B receptor modulation of L-type calcium channel current at bipolar cell terminals in the retina of the tiger salamander. Proc Natl Acad Sci USA 86: 10144-10147.

Markram, H, Helm, PJ, Sakmann, B (1995). Dendritic calcium transients evoked by single back-propagating action potentials in rat neocortical pyramidal neurons. J Physiol (Lond) 485: 1-20.

Markram, H, Sakmann, B (1994). Calcium transients in dendrites of neocortical neurons evoked by single subthreshold excitatory postsynaptic potentials via low-voltage-activated calcium channels. Proc Natl Acad Sci USA 91: 5207-5211.

Marsal, J, Ruiz-Montasell, B, Blasi, J, Moreira, JE, Contreras, D, Sugimori, M, Llinás, R (1997). Block of transmitter release by botulinum C1 action on syntaxin at the squid giant synapse. Proc Natl Acad Sci USA 94: 14871-14876.

Martin-Moutot, N, Charvin, N, Leveque, C, Sato, K, Nishiki, T, Kozaki, S, Takahashi, M, Seagar, M (1996). Interaction of SNARE complexes with P/Q-type calcium channels in rat cerebellar synaptosomes. J Biol Chem 271: 6567-6570.

Mastrogiacomo, A, Parsons, SM, Zampighi, GA, Jenden, DJ, Umbach, JA, Gundersen, CB (1994). Cysteine string proteins: a potential link between synaptic vesicles and presynaptic Ca^{2+} channels. Science 263: 981-982.

Masukawa, LM, Prince, DA (1984). Synaptic control of excitability in isolated dendrites of hippocampal neurons. J Neurosci 4: 217-227.

Matteson, DR, Armstrong, CM (1986). Properties of two types of calcium channels in clonal pituitary cells. J Gen Physiol 87: 161-182.

McCormick, DA, Bal, T (1997). Sleep and arousal: thalamocortical mechanisms. Annual Review of Neuroscience 20: 185-215.

McMahon, HT, Foran, P, Dolly, JO, Verhage, M, Wiegant, VM, Nicholls, DG (1992). Tetanus toxin and botulinum toxins type A and B inhibit glutamate, gamma-aminobutyric acid, aspartate, and met-enkephalin release from synaptosomes. Clues to the locus of action. J Biol Chem 267: 21338-21343.

McMahon, HT, Nicholls, DG (1991). Transmitter glutamate release from isolated nerve terminals: evidence for biphasic release and triggering by localized Ca^{2+}. J Neurochem 56: 86-94.

Meder, W, Fink, K, Göthert, M (1997). Involvement of different calcium channels in K^+- and veratridine-induced increases of cytosolic calcium concentration in rat cerebral cortical synaptosomes. Naunyn-Schmiedebergs Arch Pharmacol 356: 797-805.

Meir, A, Dolphin, AC (1998). Known calcium channel alpha1 subunits can form low threshold small conductance channels with similarities to native T-type channels. Neuron 20: 341-351.

Mermelstein, P, Foehring, R, Tkatch, T, Song, W-J, Baranauskas, G, Surmeier, D (1999). Properties of Q-Type Calcium Channels in Neostriatal and Cortical Neurons are Correlated with Beta Subunit Expression. J Neurosci 19: 7268-7277.

Mermelstein, PG, Surmeier, DJ (1997). A calcium channel reversibly blocked by omega-conotoxin GVIA lacking the class D alpha 1 subunit. Neuroreport 8: 485-489.

Mikami, A, Imoto, K, Tanabe, T, Niidome, T, Mori, Y, Takeshima, H, Narumiya, S, Numa, S (1989). Primary structure and functional expression of the cardiac dihydropyridine-sensitive calcium channel. Nature 340: 230-233.

Miledi, R (1973). Transmitter release induced by injection of calcium ions into nerve terminals. Proc R Soc Lond (Biol) 183: 421-425.

Miller, RJ, Freedman, SB (1984). Are dihydropyridine binding sites voltage sensitive calcium channels? Life Sci 34: 1205-1221.

Mintz, IM, Adams, ME, Bean, BP (1992a). P-type calcium channels in rat central and peripheral neurons. Neuron 9: 85-95.

Mintz, IM, Bean, BP (1993). Block of calcium channels in rat neurons by synthetic ω-Aga-IVA. Neuropharmacology 32: 1161-1169.

Mintz, IM, Sabatini, BL, Regehr, WG (1995). Calcium control of transmitter release at a cerebellar synapse. Neuron 15: 675-688.

Mintz, IM, Venema, VJ, Swiderek, KM, Lee, TD, Bean, BP, Adams, ME (1992b). P-type calcium channels blocked by the spider toxin omega-Aga-IVA. Nature 355: 827-829.

Mochida, S, Saisu, H, Kobayashi, H, Abe, T (1995). Impairment of syntaxin by botulinum neurotoxin C1 or antibodies inhibits acetylcholine release but not Ca^{2+} channel activity. Neuroscience 65: 905-915.

Mochida, S, Sheng, ZH, Baker, C, Kobayashi, H, Catterall, WA (1996). Inhibition of neurotransmission by peptides containing the synaptic protein interaction site of N-type Ca^{2+} channels. Neuron 17: 781-788.

Mogul, DJ, Adams, ME, Fox, AP (1993). Differential activation of adenosine receptors decreases N-type but potentiates P-type Ca^{2+} current in hippocampal CA3 neurons. Neuron 10: 327-334.

Montecucco, C, Schiavo, G (1995). Structure and function of tetanus and botulinum neurotoxins. Q Rev Biophys 28: 423-472.

Montminy, MR, Bilezikjian, LM (1987). Binding of a nuclear protein to the cyclic-AMP response element of the somatostatin gene. Nature 328: 175-178.

Morgan, JI, Curran, T (1988). Calcium as a modulator of the immediate-early gene cascade in neurons. Cell Calcium 9: 303-311.

Morgan, JI, Curran, T (1989). Stimulus-transcription coupling in neurons: role of cellular immediate-early genes. Trends Neurosci 12: 459-462.

Mori, Y, Friedrich, T, Kim, MS, Mikami, A, Nakai, J, Ruth, P, Bosse, E, Hofmann, F, Flockerzi, V, Furuichi, T, Mikoshiba, K, Imoto, K, Tanabe, T, Numa, S (1991). Primary structure and functional expression from complementary DNA of a brain calcium channel. Nature 350: 398-402.

Mouginot, D, Bossu, JL, Gähwiler, BH (1997). Low-threshold Ca^{2+} currents in dendritic recordings from Purkinje cells in rat cerebellar slice cultures. J Neurosci 17: 160-170.

Mynlieff, M, Beam, KG (1994). Adenosine acting at an A_1 receptor decreases N-type calcium current in mouse motoneurons. J Neurosci 14: 3628-3634.

Näbauer, M, Callewaert, G, Cleemann, L, Morad, M (1989). Regulation of calcium release is gated by calcium current, not gating charge, in cardiac myocytes. Science 244: 800-803.

Naito, T, Saito, Y, Yamamoto, J, Nozaki, Y, Tomura, K, Hazama, M, Nakanishi, S, Brenner, S (1998). Putative pheromone receptors related to the Ca^{2+}-sensing receptor in Fugu. Proc Natl Acad Sci USA 95: 5178-5181.

Namkung, Y, Smith, SM, Lee, SB, Skrypnyk, NV, Kim, HL, Chin, H, Scheller, RH, Tsien, RW, Shin, HS (1998). Targeted disruption of the Ca^{2+} channel beta3 subunit reduces N- and L-type Ca^{2+} channel activity and alters the voltage-dependent activation of P/Q-type Ca^{2+} channels in neurons. Proc Natl Acad Sci USA 95: 12010-12015.

Naren, AP, Nelson, DJ, Xie, W, Jovov, B, Pevsner, J, Bennett, MK, Benos, DJ, Quick, MW, Kirk, KL (1997). Regulation of CFTR chloride channels by syntaxin and Munc18 isoforms. Nature 390: 302-305.

Naren, AP, Quick, MW, Collawn, JF, Nelson, DJ, Kirk, KL (1998). Syntaxin 1A inhibits CFTR chloride channels by means of domain-specific protein-protein interactions. Proc Natl Acad Sci USA 95: 10972-10977.

Neher, E (1995). The use of fura-2 for estimating Ca buffers and Ca fluxes. Neuropharmacology 34: 1423-1442.

Neher, E (1998). Vesicle pools and Ca^{2+} microdomains: new tools for understanding their roles in neurotransmitter release. Neuron 20: 389-399.

Neher, E, Augustine, GJ (1992). Calcium gradients and buffers in bovine chromaffin cells. J Physiol 450: 273-301.

Newcomb, R, Szoke, B, Palma, A, Wang, G, Chen, X, Hopkins, W, Cong, R, Miller, J, Urge, L, Tarczy-Hornoch, K, Loo, JA, Dooley, DJ, Nadasdi, L, Tsien, RW, Lemos, J, Miljanich, G (1998). Selective peptide antagonist of the class E calcium channel from the venom of the tarantula Hysterocrates gigas. Biochemistry 37: 15353-15362.

Nicholls, DG, Rugolo, M, Scott, IG, Meldolesi, J (1982). alpha-latrotoxin of black widow spider venom depolarizes the plasma membrane, induces massive calcium influx, and stimulates transmitter release in guinea pig brain synaptosomes. Proc Natl Acad Sci USA 79: 7924-7928.

Nicholls, DG, Sihra, TS (1986). Synaptosomes possess an exocytotic pool of glutamate. Nature 321: 772-773.

Nicholls, DG, Sihra, TS, Sanchez-Prieto, J (1987). Calcium-dependent and -independent release of glutamate from synaptosomes monitored by continuous fluorometry. J Neurochem 49: 50-57.

Nicholson, C, Bruggencate, GT, Steinberg, R, Stöckle, H (1977). Calcium modulation in brain extracellular microenvironment demonstrated with ion-selective micropipette. Proc Natl Acad Sci USA 74: 1287-1290.

Nicholson, C, ten Bruggencate, G, Stöckle, H, Steinberg, R (1978). Calcium and potassium changes in extracellular microenvironment of cat cerebellar cortex. Journal of Neurophysiology 41: 1026-1039.

Nie, Z, Ranjan, R, Wenniger, JJ, Hong, SN, Bronk, P, Zinsmaier, KE (1999). Overexpression of Cysteine-String Proteins in Drosophila Reveals Interactions with Syntaxin. J Neurosci 19: 10270-10279.

Niemann, h, Blasi, J, Jahn, R (1994). Clostridial neurotoxins: new tools for dissecting exocytosis. Trends Cell Biol 4: 179-185.

Niidome, T, Teramoto, T, Murata, Y, Tanaka, I, Seto, T, Sawada, K, Mori, Y, Katayama, K (1994). Stable expression of the neuronal BI (class A) calcium channel in baby hamster kidney cells. Biochem Biophys Res Commun 203: 1821-1827.

Nilius, B, Hess, P, Lansman, JB, Tsien, RW (1985). A novel type of cardiac calcium channel in ventricular cells. Nature 316: 443-446.

Nowycky, MC, Fox, AP, Tsien, RW (1985). Three types of neuronal calcium channel with different calcium agonist sensitivity. Nature 316: 440-443.

O'Connor, V, Heuss, C, De Bello, WM, Dresbach, T, Charlton, MP, Hunt, JH, Pellegrini, LL, Hodel, A, Burger, MM, Betz, H, Augustine, GJ, Schäfer, T (1997). Disruption of syntaxin-mediated protein interactions blocks neurotransmitter secretion. Proc Natl Acad Sci USA 94: 12186-12191.

Olivera, BM, Miljanich, GP, Ramachandran, J, Adams, ME (1994). Calcium channel diversity and neurotransmitter release: the ω-Conotoxins and ω-Agatoxins. Annu Rev Biochem 63: 823-867.

Patil, PG, Brody, DL, Yue, DT (1998). Preferential closed-state inactivation of neuronal calcium channels. Neuron 20: 1027-1038.

Perez-Reyes, E, Cribbs, LL, Daud, A, Lacerda, AE, Barclay, J, Williamson, MP, Fox, M, Rees, M, Lee, JH (1998). Molecular characterization of a neuronal low-voltage-activated T-type calcium channel [see comments]. Nature 391: 896-900.

Perney, TM, Hirning, LD, Leeman, SE, Miller, RJ (1986). Multiple calcium channels mediate neurotransmitter release from peripheral neurons. Proc Natl Acad Sci USA 83: 6656-6659.

Piedras-Renteria, ES, Chen, CC, Best, PM (1997). Antisense oligonucleotides against rat brain alpha1E DNA and its atrial homologue decrease T-type calcium current in atrial myocytes. Proc Natl Acad Sci USA 94: 14936-14941.

Piedras-Rentería, ES, Tsien, RW (1998). Antisense oligonucleotides against alpha1E reduce R-type calcium currents in cerebellar granule cells. Proc Natl Acad Sci USA 95: 7760-7765.

Pinto, A, Gillard, S, Moss, F, Whyte, K, Brust, P, Williams, M, Stauderman, K, Harpold, M, Lang, B, Newsom-Davis, J, Bleakman, D, Lodge, D, Boot, J (1998). Human autoantibodies specific for the alpha1A calcium channel subunit reduce both P-type and Q-type calcium currents in cerebellar neurons. Proc Natl Acad Sci USA 95: 8328-8333.

Poncer, JC, McKinney, RA, Gähwiler, BH, Thompson, SM (1997). Either N- or P-type calcium channels mediate GABA release at distinct hippocampal inhibitory synapses. Neuron 18: 463-472.

Protti, DA, Reisin, R, Mackinley, TA, Uchitel, OD (1996). Calcium channel blockers and transmitter release at the normal human neuromuscular junction. Neurology 46: 1391-1396.

Protti, DA, Szczupak, L, Scornik, FS, Uchitel, OD (1991). Effect of ω-Conotoxin GVIA on neurotransmitter release at the mouse neuromuscular junction. Brain Res 557: 336-339.

Protti, DA, Uchitel, OD (1993). Transmitter release and presynaptic Ca^{2+} currents blocked by the spider toxin ω-Aga-IVA. Neuroreport 5: 333-336.

Pupier, S, Leveque, C, Marqueze, B, Kataoka, M, Takahashi, M, Seagar, MJ (1997). Cysteine string proteins associated with secretory granules of the rat neurohypophysis. J Neurosci 17: 2722-2727.

Putney, JW. (1997) Capacitative Calcium Entry (Austin, TX: R.G. Landes Company).

Quinn, SJ, Ye, CP, Diaz, R, Kifor, O, Bai, M, Vassilev, P, Brown, E (1997). The Ca^{2+}-sensing receptor: a target for polyamines. American Journal of Physiology 273: C1315-1323.

Raciborska, DA, Trimble, WS, Charlton, MP (1998). Presynaptic protein interactions in vivo: evidence from botulinum A, C, D and E action at frog neuromuscular junction. Eur J Neurosci 10: 2617-2628.

Rajadhyaksha, A, Barczak, A, Macías, W, Leveque, JC, Lewis, SE, Konradi, C (1999). L-Type Ca^{2+} channels are essential for glutamate-mediated CREB phosphorylation and c-fos gene expression in striatal neurons. J Neurosci 19: 6348-6359.

Ramaswami, M, Krishnan, KS, Kelly, RB (1994). Intermediates in synaptic vesicle recycling revealed by optical imaging of Drosophila neuromuscular junctions. Neuron 13: 363-375.

Randall, A, Tsien, RW (1995). Pharmacological dissection of multiple types of Ca^{2+} channel currents in rat cerebellar granule neurons. J Neurosci 15: 2995-3012.

Randall, A, Tsien, RW. (1998). Distinctive Biophysical and Pharmacological Features of T-Type Calcium Channels. In Low-Voltage-Activated T-Type Calcium Channels, RW Tsien, J-P Clozel J Nargeot, eds. (Basel, Switzerland: Adis International), pp. 29-43.

Regehr, WG, Mintz, IM (1994). Participation of multiple calcium channel types in transmission at single climbing fiber to Purkinje cell synapses. Neuron 12: 605-613.

Reid, CA, Clements, JD, Bekkers, JM (1997). Nonuniform distribution of Ca^{2+} channel subtypes on presynaptic terminals of excitatory synapses in hippocampal cultures. J Neurosci 17: 2738-2745.

Rettig, J, Heinemann, C, Ashery, U, Sheng, ZH, Yokoyama, CT, Catterall, WA, Neher, E (1997). Alteration of Ca^{2+} dependence of neurotransmitter release by disruption of Ca^{2+} channel/syntaxin interaction. J Neurosci 17: 6647-6656.

Rettig, J, Sheng, ZH, Kim, DK, Hodson, CD, Snutch, TP, Catterall, WA (1996). Isoform-specific interaction of the alpha1A subunits of brain Ca^{2+} channels with the presynaptic proteins syntaxin and SNAP-25. Proc Natl Acad Sci USA 93: 7363-7368.

Reuter, H (1995). Measurements of exocytosis from single presynaptic nerve terminals reveal heterogeneous inhibition by Ca^{2+} channel blockers. Neuron 14: 773-779.

Reuter, H (1996). Diversity and function of presynaptic calcium channels in the brain. Curr Opin Neurobiol 6: 331-337.

Riccardi, D, Park, J, Lee, WS, Gamba, G, Brown, EM, Hebert, SC (1995). Cloning and functional expression of a rat kidney extracellular calcium/polyvalent cation-sensing receptor. Proc Natl Acad Sci USA 92: 131-135.

Ríos, E, Brum, G (1987). Involvement of dihydropyridine receptors in excitation-contraction coupling in skeletal muscle. Nature 325: 717-720.

Rock, DM, Horne, WA, Stoehr, SJ, Hashimoto, C, Cong, RZ, M., Palma, A, Hidayetoglu, D, Offord, J. (1998). Does α_{1E} code for T-type Ca^{2+} channels? A comparison of recombinant α_{1E} Ca^{2+} channels with GH3 pituitary T-type and recombinant α_{1B} Ca^{2+} channels. In Low-Voltage-Activated T-type Calcium Channels, J Nargeot, JP Clozel RW Tsien, eds. (Chester, England: Aidis Press), pp. 279-289.

Rosen, LB, Greenberg, ME (1994). Regulation of c-*fos* and other immediate-early genes in PC12 cells as a model for studying specificity in neuronal signaling. Molec Neurobiol 7: 203-216.

Rosenberg, RL, Hess, P, Reeves, JP, Smilowitz, H, Tsien, RW (1986). Calcium channels in planar lipid bilayers: insights into mechanisms of ion permeation and gating. Science 231: 1564-1566.

Ruat, M, Molliver, ME, Snowman, AM, Snyder, SH (1995). Calcium sensing receptor: molecular cloning in rat and localization to nerve terminals. Proc Natl Acad Sci USA 92: 3161-3165.

Sabatini, BL, Regehr, WG (1995). Detecting changes in calcium influx which contribute to synaptic modulation in mammalian brain slice. Neuropharmacology 34: 1453-1467.

Sabria, J, Pastor, C, Clos, MV, Garcia, A, Badia, A (1995). Involvement of different types of voltage-sensitive calcium channels in the presynaptic regulation of noradrenaline release in rat brain cortex and hippocampus. J Neurochem 64: 2567-2571.

Sano, K, Enomoto, K, Maeno, T (1987). Effects of synthetic ω-Conotoxin, a new type Ca^{2+} antagonist, on frog and mouse neuromuscular transmission. Eur J Pharmacol 141: 235-241.

Sather, WA, Tanabe, T, Zhang, J-F, Mori, Y, Adams, ME, Tsien, RW (1993). Distinctive biophysical and pharmacological properties of class A (BI) calcium channel α_1 subunits. Neuron 11: 291-303.

Schafer, WR, Kenyon, CJ (1995). A calcium-channel homologue required for adaptation to dopamine and serotonin in *Caenorhabditis elegans*. Nature 375: 73-78.

Schiavo, G, Benfenati, F, Poulain, B, Rossetto, O, Polverino de Laureto, P, DasGupta, BR, Montecucco, C (1992). Tetanus and botulinum-B neurotoxins block neurotransmitter release by proteolytic cleavage of synaptobrevin [see comments]. Nature 359: 832-835.

Schiavo, G, Shone, CC, Bennett, MK, Scheller, RH, Montecucco, C (1995). Botulinum neurotoxin type C cleaves a single Lys-Ala bond within the carboxyl-terminal region of syntaxins. J Biol Chem 270: 10566-10570.

Schiller, J, Helmchen, F, Sakmann, B (1995). Spatial profile of dendritic calcium transients evoked by action potentials in rat neocortical pyramidal neurones. J Physiol (Lond) 487: 583-600.

Schmitt, R, Clozel, JP, Iberg, N, Buhler, FR (1995). Mibefradil prevents neointima formation after vascular injury in rats. Possible role of the blockade of the T-type voltage-operated calcium channel. Arterioscler Thromb Vasc Biol 15: 1161-1165.

Schmitz, Y, Witkovsky, P (1997). Dependence of photoreceptor glutamate release on a dihydropyridine-sensitive calcium channel. Neuroscience 78: 1209-1216.

Schneider, MF, Chandler, WK (1973). Voltage dependent charge movement of skeletal muscle: a possible step in excitation-contraction coupling. Nature 242: 244-246.

Schneider, T, Wei, X, Olcese, R, Costantin, JL, Neely, A, Palade, P, Perez-Reyes, E, Qin, N, Zhou, J, Crawford, GD, et, a (1994). Molecular analysis and functional expression of the human type E neuronal Ca^{2+} channel alpha 1 subunit. Receptors and Channels: 255-270.

Schultz, LM, Christie, RB, Sejnowski, TJ. Distribution of T-Type Calcium Channels in CA1 Stratum Oriens Interneurons. Society for Neuroscience, Vol 1, p79.79, 1999.

Scott, VE, De Waard, M, Liu, H, Gurnett, CA, Venzke, DP, Lennon, VA, Campbell, KP (1996). β Subunit heterogeneity in N-type Ca^{2+} channels. J Biol Chem 271: 3207-3212.

Sheng, ZH, Rettig, J, Cook, T, Catterall, WA (1996). Calcium-dependent interaction of N-type calcium channels with the synaptic core complex. Nature 379: 451-454.

Sheng, ZH, Rettig, J, Takahashi, M, Catterall, WA (1994). Identification of a syntaxin-binding site on N-type calcium channels. Neuron 13: 1303-1313.

Sheng, ZH, Yokoyama, CT, Catterall, WA (1997). Interaction of the synprint site of N-type Ca^{2+} channels with the C2B domain of synaptotagmin I. Proc Natl Acad Sci USA 94: 5405-5410.

Simmons, ML, Terman, GW, Gibbs, SM, Chavkin, C (1995). L-type calcium channels mediate dynorphin neuropeptide release from dendrites but not axons of hippocampal granule cells. Neuron 14: 1265-1272.

Smart, TG, Xie, X, Krishek, BJ (1994). Modulation of inhibitory and excitatory amino acid receptor ion channels by zinc. Prog Neurobiol 42: 393-341.

Smirnova, T, Fossier, P, Stinnakre, J, Mallet, J, Baux, G (1995). A syntaxin-related protein controls acetylcholine release by different mechanisms in *Aplysia*. Neuroscience 68: 125-133.

Smith, LA, Wang, XJ, Peixoto, AA, Neumann, EK, Hall, LM, Hall, JC (1996). A drosophila calcium channel α_1 subunit gene maps to a genetic locus associated with behavioral and visual defects. J Neurosci 16: 7868-7879.

Smith, SJ (1992). Do astrocytes process neural information? Progress in Brain Research 94: 119-136.

Snutch, TP, Leonard, JP, Gilbert, MM, Lester, HA, Davidson, N (1990). Rat brain expresses a heterogeneous family of calcium channels. Proc Natl Acad Sci USA 87: 3391-3395.

Snutch, TP, Reiner, PB (1992). Ca^{2+} channels: diversity of form and function. Curr Opin Neurobiol 2: 247-253.

Soldatov, NM (1994). Genomic structure of human L-type Ca^{2+} channel. Genomics 22: 77-87.

Soldatov, NM, Bouron, A, Reuter, H (1995). Different voltage-dependent inhibition by dihydropyridines of human Ca^{2+} channel splice variants. J Biol Chem 270: 10540-10543.

Soong, TW, Stea, A, Hodson, CD, Dubel, SJ, Vincent, SR, Snutch, TP (1993). Structure and functional expression of a member of the low voltage-activated calcium channel family. Science 260: 1133-1136.

Spencer, WA, Kandel, ER (1961). Electrophysiology of hippocampal neurons IV: fast potentials. J Neurophysiol 24: 272-285.

Spruston, N, Schiller, Y, Stuart, G, Sakmann, B (1995). Activity-dependent action potential invasion and calcium influx into hippocampal CA1 dendrites. Science 268: 297-300.

Stanley, EF (2000). Presynaptic Calcium Channels and the Depletion of Synaptic Cleft Calcium Ions. J Neurophysiol 83: 477-482.

Stanley, EF, Mirotznik, RR (1997). Cleavage of syntaxin prevents G-protein regulation of presynaptic calcium channels. Nature 385: 340-343.

Starr, TV, Prystay, W, Snutch, TP (1991). Primary structure of a calcium channel that is highly expressed in the rat cerebellum. Proc Natl Acad Sci USA 88: 5621-5625.

Stea, A, Tomlinson, WJ, Soong, TW, Bourinet, E, Dubel, SJ, Vincent, SR, Snutch, TP (1994). Localization and functional properties of a rat brain α_{1A} calcium channel reflect similarities to neuronal Q- and P-type channels. Proc Natl Acad Sci USA 91: 10576-10580.

Stevens, CF, Tsujimoto, T (1995). Estimates for the pool size of releasable quanta at a single central synapse and for the time required to refill the pool. Proc Natl Acad Sci USA 92: 846-849.

Strom, TM, Nyakatura, G, Apfelstedt-Sylla, E, Hellebrand, H, Lorenz, B, Weber, BH, Wutz, K, Gutwillinger, N, Rüther, K, Drescher, B, Sauer, C, Zrenner, E, Meitinger, T, Rosenthal, A, Meindl, A (1998). An L-type calcium-channel gene mutated in incomplete X-linked congenital stationary night blindness. Nature Genetics 19: 260-263.

Stuart, GJ, Dodt, HU, Sakmann, B (1993). Patch-clamp recordings from the soma and dendrites of neurons in brain slices using infrared video microscopy. Pflügers Arch 423: 511-518.

Stuart, GJ, Sakmann, B (1994). Active propagation of somatic action potentials into neocortical pyramidal cell dendrites. Nature 367: 69-72.

Sugimori, M, Tong, CK, Fukuda, M, Moreira, JE, Kojima, T, Mikoshiba, K, Llinás, R (1998). Presynaptic injection of syntaxin-specific antibodies blocks transmission in the squid giant synapse. Neuroscience 86: 39-51.

Sun, XP, Schlichter, LC, Stanley, EF (1999). Single-channel properties of BK-type calcium-activated potassium channels at a cholinergic presynaptic nerve terminal. Journal of Physiology 518: 639-651.

Sutton, RB, Fasshauer, D, Jahn, R, Brunger, AT (1998). Crystal structure of a SNARE complex involved in synaptic exocytosis at 2.4 A resolution [see comments]. Nature 395: 347-353.

Swartz, KJ, Merritt, A, Bean, BP, Lovinger, DM (1993). Protein kinase C modulates glutamate receptor inhibition of Ca^{2+} channels and synaptic transmission. Nature 361: 165-168.

Takahashi, M, Seagar, MJ, Jones, JF, Reber, BF, Catterall, WA (1987). Subunit structure of dihydropyridine-sensitive calcium channels from skeletal muscle. Proc Natl Acad Sci USA 84: 5478-5482.

Takahashi, T, Momiyama, A (1993). Different types of calcium channels mediate central synaptic transmission. Nature 366: 156-158.

Talley, EM, Cribbs, LL, Lee, JH, Daud, A, Perez-Reyes, E, Bayliss, DA (1999). Differential distribution of three members of a gene family encoding low voltage-activated (T-type) calcium channels. J Neurosci 19: 1895-1911.

Tanabe, T, Beam, KG, Adams, BA, Niidome, T, Numa, S (1990). Regions of the skeletal muscle dihydropyridine receptor critical for excitation-contraction coupling. Nature 346: 567-569.

Tanabe, T, Beam, KG, Powell, JA, Numa, S (1988). Restoration of excitation-contraction coupling and slow calcium current in dysgenic muscle by dihydropyridine receptor complementary DNA. Nature 336: 134-139.

Tanabe, T, Takeshima, H, Mikami, A, Flockerzi, V, Takahashi, H, Kangawa, K, Kojima, M, Matsuo, H, Hirose, T, Numa, S (1987). Primary structure of the receptor for calcium channel blockers from skeletal muscle. Nature 328: 313-318.

Teramoto, T, Kuwada, M, Niidome, T, Sawada, K, Nishizawa, Y, Katayama, K (1993). A novel peptide from funnel web spider venom, omega-Aga-TK, selectively blocks, P-type calcium channels. Biochem Biophys Res Commun 196: 134-140.

Tibbs, GR, Barrie, AP, Van Mieghem, FJ, McMahon, HT, Nicholls, DG (1989). Repetitive action potentials in isolated nerve terminals in the presence of 4-aminopyridine: effects on cytosolic free Ca^{2+} and glutamate release. J Neurochem 53: 1693-1699.

Tibbs, GR, Dolly, JO, Nicholls, DG (1996). Evidence for the induction of repetitive action potentials in synaptosomes by K^+-channel inhibitors: an analysis of plasma membrane ion fluxes. J Neurochem 67: 389-397.

Toth, PT, Bindokas, VP, Bleakman, D, Colmers, WF, Miller, RJ (1993). Mechanism of presynaptic inhibition by neuropeptide Y at sympathetic nerve terminals. Nature 364: 635-639.

Tottene, A, Moretti, A, Pietrobon, D (1996). Functional diversity of P-type and R-type calcium channels in rat cerebellar neurons. J Neurosci 16: 6353-6363.

Tottene, A, Volsen, S, Pietrobon, D. The R-Type Calcium Current of Rat Cerebellar Granule Cells Comprises Three Components With Distinct Biophysical and Pharmacological Properties. Society for Neuroscience, Vol 1, p431.433, 1999.

Trudeau, LE, Fang, Y, Haydon, PG (1998). Modulation of an early step in the secretory machinery in hippocampal nerve terminals. Proc Natl Acad Sci USA 95: 7163-7168.

Tsien, RW, Fox, AP, Hess, P, McCleskey, EW, Nilius, B, Nowycky, MC, Rosenberg, RL (1987). Multiple types of calcium channel in excitable cells. Soc Gen Physiol Ser 41: 167-187.

Tsien, RW, Lipscombe, D, Madison, DV, Bley, KR, Fox, AP (1988). Multiple types of neuronal calcium channels and their selective modulation. Trends Neurosci 11: 431-438.

Tsien, RW, Wheeler, DB. (1999). Voltage-gated calcium channels. In Calcium as a Cellular Regulator, E Carafoli CB Klee, eds. (New York: Oxford University Press), pp. 171-199.

Turner, TJ, Adams, ME, Dunlap, K (1993). Multiple Ca^{2+} channel types coexist to regulate synaptosomal neurotransmitter release. Proc Natl Acad Sci USA 90: 9518-9522.

Turner, TJ, Lampe, RA, Dunlap, K (1995). Characterization of presynaptic calcium channels with omega-Conotoxin MVIIC and omega-grammotoxin SIA: role for a resistant calcium channel type in neurosecretion. Mol Pharmacol 47: 348-353.

Umbach, JA, Saitoe, M, Kidokoro, Y, Gundersen, CB (1998). Attenuated influx of calcium ions at nerve endings of csp and shibire mutant Drosophila. J Neurosci 18: 3233-3240.

Usowicz, MM, Sugimori, M, Cherksey, B, Llinás, R (1992). P-type calcium channels in the somata and dendrites of adult cerebellar Purkinje cells. Neuron 9: 1185-1199.

Vance, CL, Begg, CM, Lee, WL, Dubel, SJ, Copeland, TD, Sönnichsen, FD, McEnery, MW (1999). N-type calcium channel/syntaxin/SNAP-25 complex probed by antibodies to II-III intracellular loop of the alpha1B subunit. Neuroscience 90: 665-676.

Vassilev, PM, Mitchel, J, Vassilev, M, Kanazirska, M, Brown, EM (1997). Assessment of frequency-dependent alterations in the level of extracellular Ca^{2+} in the synaptic cleft. Biophys J 72: 2103-2116.

Vázquez, E, Sánchez-Prieto, J (1997). Presynaptic modulation of glutamate release targets different calcium channels in rat cerebrocortical nerve terminals. Eur J Neurosci 9: 2009-2018.

Vergara, C, Latorre, R, Marrion, NV, Adelman, JP (1998). Calcium-activated potassium channels. Current Opinion in Neurobiology 8: 321-329.

Verhage, M, Ghijsen, WE, Nicholls, DG, Wiegant, VM (1991). Characterization of the release of cholecystokinin-8 from isolated nerve terminals and comparison with exocytosis of classical transmitters. J Neurochem 56: 1394-1400.

Verhage, M, Hens, JJ, De Grann, PN, Boomsma, F, Wiegant, VM, da Silva, FH, Gispen, WH, Ghijsen, WE (1995). Ba2+ replaces Ca2+/calmodulin in the activation of protein phosphatases and in exocytosis of all major transmitters. European Journal of Pharmacology 291: 387-398.

Wakamori, M, Niidome, T, Furutama, D, Furuichi, T, Mikoshiba, K, Fujita, Y, Tanaka, I, Katayama, K, Yatani, A, Schwartz, A (1994). Distinctive functional properties of the neuronal BII (class E) calcium channel. Receptors Channels 2: 303-314.

Walker, D, De Waard, M (1998). Subunit interaction sites in voltage-dependent Ca^{2+} channels: role in channel function. Trends in Neurosciences 21: 148-154.

Washburn, DL, Smith, PM, Ferguson, AV (1999). Control of neuronal excitability by anion-sensing receptor. Eur J Neurosci 11: 1947-1954.

Watanabe, S, Takagi, H, Miyasho, T, Inoue, M, Kirino, Y, Kudo, Y, Miyakawa, H (1998). Differential roles of two types of voltage-gated Ca^{2+} channels in the dendrites of rat cerebellar Purkinje neurons. Brain Research 791: 43-55.

Waterman, SA (1996). Multiple subtypes of voltage-gated calcium channel mediate transmitter release from parasympathetic neurons in the mouse bladder. J Neurosci 16: 4155-4161.

Waterman, SA (1997). Role of N-, P- and Q-type voltage-gated calcium channels in transmitter release from sympathetic neurones in the mouse isolated vas deferens. Br J Pharmacol 120: 393-398.

Waterman, SA, Lang, B, Newsom-Davis, J (1997). Effect of Lambert-Eaton myasthenic syndrome antibodies on autonomic neurons in the mouse. Annals of Neurology 42: 147-156.

Welling, A, Kwan, YW, Bosse, E, Flockerzi, V, Hofmann, F, Kass, RS (1993). Subunit-dependent modulation of recombinant L-type calcium channels. Molecular basis for dihydropyridine tissue selectivity. Circ Res 73: 974-980.

Wessler, I, Dooley, DJ, Osswald, H, Schlemmer, F (1990). Differential blockade by nifedipine and ω-Conotoxin GVIA of α_1- and β_1-adrenoceptor-controlled calcium channels on motor nerve terminals of the rat. Neurosci Lett 108: 173-178.

Westenbroek, RE, Ahlijanian, MK, Catterall, WA (1990). Clustering of L-type Ca^{2+} channels at the base of major dendrites in hippocampal pyramidal neurons. Nature 347: 281-284.

Westenbroek, RE, Hell, JW, Warner, C, Dubel, SJ, Snutch, TP, Catterall, WA (1992). Biochemical properties and subcellular distribution of an N-type calcium channel α_1 subunit. Neuron 9: 1099-1115.

Westenbroek, RE, Sakurai, T, Elliott, EM, Hell, JW, Starr, TV, Snutch, TP, Catterall, WA (1995). Immunochemical identification and subcellular distribution of the α_{1A} subunits of brain calcium channels. J Neurosci 15: 6403-6418.

Wheeler, DB, Randall, A, Tsien, RW (1994). Roles of N-type and Q-type Ca^{2+} channels in supporting hippocampal synaptic transmission. Science 264: 107-111.

Wheeler, DB, Randall, A, Tsien, RW (1996). Changes in action potential duration alter reliance of excitatory synaptic transmission on multiple types of Ca^{2+} channels in rat hippocampus. J Neurosci 16: 2226-2237.

Whittaker, VP (1993). Thirty years of synaptosome research. J Neurocytol 22: 735-742.

Williams, ME, Brust, PF, Feldman, DH, Patthi, S, Simerson, S, Maroufi, A, McCue, AF, Velicelebi, G, Ellis, SB, Harpold, MM (1992a). Structure and functional expression of an omega-conotoxin-sensitive human N-type calcium channel. Science 257: 389-395.

Williams, ME, Feldman, DH, McCue, AF, Brenner, R, Veliçelebi, G, Ellis, SB, Harpold, MM (1992b). Structure and functional expression of α_1, α_2, and β subunits of a novel human neuronal calcium channel subtype. Neuron 8: 71-84.

Williams, ME, Marubio, LM, Deal, CR, Hans, M, Brust, PF, Philipson, LH, Miller, RJ, Johnson, EC, Harpold, MM, Ellis, SB (1994). Structure and functional characterization of neuronal α_{1E} calcium channel subtypes. J Biol Chem 269: 22347-22357.

Williamson, LC, Halpern, JL, Montecucco, C, Brown, JE, Neale, EA (1996). Clostridial neurotoxins and substrate proteolysis in intact neurons: botulinum neurotoxin C acts on synaptosomal-associated protein of 25 kDa. J Biol Chem 271: 7694-7699.

Wiser, O, Bennett, MK, Atlas, D (1996). Functional interaction of syntaxin and SNAP-25 with voltage-sensitive L- and N-type Ca^{2+} channels. EMBO J 15: 4100-4110.

Wiser, O, Tobi, D, Trus, M, Atlas, D (1997). Synaptotagmin restores kinetic properties of a syntaxin-associated N-type voltage sensitive calcium channel. FEBS Lett 404: 203-207.

Wiser, O, Trus, M, Hernandez, A, Renstrom, E, Barg, S, Rorsman, P, Atlas, D (1999). The voltage sensitive Lc-type Ca^{2+} channel is functionally coupled to the exocytotic machinery. Proc Natl Acad Sci USA 96: 248-253.

Wong, RK, Prince, DA, Basbaum, AI (1979). Intradendritic recordings from hippocampal neurons. Proc Natl Acad Sci USA 76: 986-990.

Wu, LG, Borst, JG, Sakmann, B (1998). R-type Ca^{2+} currents evoke transmitter release at a rat central synapse. Proc Natl Acad Sci USA 95: 4720-4725.

Wu, MN, Fergestad, T, Lloyd, TE, He, Y, Broadie, K, Bellen, HJ (1999). Syntaxin 1A interacts with multiple exocytic proteins to regulate neurotransmitter release in vivo. Neuron 23: 593-605.

Wyatt, CN, Page, KM, Berrow, NS, Brice, NL, Dolphin, AC (1998). The effect of overexpression of auxiliary Ca^{2+} channel subunits on native Ca2+ channel currents in undifferentiated mammalian NG108-15 cells. Journal of Physiology 510: 347-360.

Xiong, Z, Lu, W, MacDonald, JF (1997). Extracellular calcium sensed by a novel cation channel in hippocampal neurons. Proc Natl Acad Sci USA 94: 7012-7017.

Yao, Y, Ferrer-Montiel, AV, Montal, M, Tsien, RY (1999). Activation of store-operated Ca^{2+} current in Xenopus oocytes requires SNAP-25 but not a diffusible messenger. Cell 98: 475-485.

Ye, C, Kanazirska, M, Quinn, S, Brown, EM, Vassilev, PM (1996a). Modulation by polycationic Ca^{2+}-sensing receptor agonists of nonselective cation channels in rat hippocampal neurons. Biochemical and Biophysical Research Communications 224: 271-280.

Ye, C, Rogers, K, Bai, M, Quinn, SJ, Brown, EM, Vassilev, PM (1996b). Agonists of the Ca^{2+}-sensing receptor (CaR) activate nonselective cation channels in HEK293 cells stably transfected with the human CaR. Biochemical and Biophysical Research Communications 226: 572-579.

Yokoyama, CT, Sheng, ZH, Catterall, WA (1997). Phosphorylation of the synaptic protein interaction site on N-type calcium channels inhibits interactions with SNARE proteins. J Neurosci 17: 6929-6938.

Yokoyama, CT, Westenbroek, RE, Hell, JW, Soong, TW, Snutch, TP, Catterall, WA (1995). Biochemical properties and subcellular distribution of the neuronal class E calcium channel α_1 subunit. J Neurosci 15: 6419-6432.

Yoshida, K, Imaki, J, Matsuda, H, Hagiwara, M (1995). Light-induced CREB phosphorylation and gene expression in rat retinal cells. J Neurochem 65: 1499-1504.

Yuste, R, Gutnick, MJ, Saar, D, Delaney, KR, Tank, DW (1994). Ca^{2+} accumulations in dendrites of neocortical pyramidal neurons: an apical band and evidence for two functional compartments. Neuron 13: 23-43.

Zhang, J-F, Randall, AD, Ellinor, PT, Horne, WA, Sather, WA, Tanabe, T, Schwarz, TL, Tsien, RW (1993). Distinctive pharmacology and kinetics of cloned neuronal Ca^{2+} channels and their possible counterparts in mammalian CNS neurons. Neuropharmacology 32: 1075-1088.

Zhong, H, Yohoyama, CT, Scheuer, T, Catterall, WA (1999). Reciprocal regulation of P/Q-type Ca^{2+} channels by SNAP-25, syntaxin and synaptotagmin. Nature 2: 939-941.

Zhou, Z, January, CT (1998). Both T- and L-type Ca^{2+} channels can contribute to excitation-contraction coupling in cardiac Purkinje cells. Biophys J 74: 1830-1839.

Zhu, Y, Ikeda, SR (1993). Adenosine modulates voltage-gated Ca^{2+} channels in adult rat sympathetic neurons. J Neurophysiol 70: 610-620.